NBSIR 80-2162

Technical Activities 1980 Office of Nondestructive Evaluation

World Bureau Assessment Mention, Estato

Office of Nondestructive Evaluation
National Measurement Laboratory
National Bureau of Standards
U.S. Department of Commerce
Washington, DC 20234

September 1980

NBSIR 80-2162

TECHNICAL ACTIVITIES 1980 OFFICE OF NONDESTRUCTIVE EVALUATION

Harold Berger and Leonard Mordfin, Editors

Office of Nondestructive Evaluation
National Measurement Laboratory
National Bureau of Standards
U.S. Department of Commerce
Washington, DC 20234

November 1980

Prepared for:
National Bureau of Standards
Department of Commerce
Washington, DC 20234

U.S. DEPARTMENT OF COMMERCE, Philip M. Klutznick, *Secretary*

Jordan J. Baruch, *Assistant Secretary for Productivity, Technology, and Innovation*
NATIONAL BUREAU OF STANDARDS, Ernest Ambler, *Director*

TECHNICAL ACTIVITIES

Table of Contents

Introduction

Nondestructive evaluation (NDE) involves many measurement methods that are used to examine materials or assemblies in such a way that the tested object can be used after the test is finished. This is in contrast to destructive tests in which the tested object is destroyed in order to obtain the required information, e.g., a tensile test in which the object is pulled apart. NDE methods vary from straightforward visual inspection to sophisticated approaches in which three-dimensional images of the interior of objects are reconstructed from x-ray, ultrasonic or neutron measurements. These kinds of tests, involving optical, radiographic, magnetic, electrical, ultrasonic and other similar phenomena, are chosen and used so as not to impair the usefulness of the tested object. A comparison of the common methods for NDE is given in Table I.

The traditional reason for the use of NDE in industry has been to assure safety. Therefore, NDE is particularly well used in critical industries such as aerospace, nuclear and military. In recent years, a greater appreciation for the value of NDE in consumer industries has also become apparent. In addition to providing improved safety, NDE, as part of an improved quality assurance activity, offers potential for improved productivity, conservation of both energy and materials and better quality products.

Despite the increasing use of NDE methods for practical purposes, there are needs to improve NDE measurement methods and to relate measurements to the actual performance of the material. The Office of Nondestructive Evaluation was established by the National Bureau of Standards to assist industry and government agencies in improving the reliability of materials and structures; NBS is working to help industry develop methods for accurate and reproducible NDE measurements. This includes technical investigations, development of standards (both measurement standards and procedural documents), characterization of instruments, and assessments of the meaning of NDE measurements in relation to material performance. The main emphasis of the NBS program is on the needs for improved measurements, calibration standards and procedures for many of the NDE methods commonly used in industry.

At the Bureau the NDE program is coordinated by the National Measurement Laboratory. Strong interactions with industry, technical societies, and government agencies have been established in order to solicit their advice on needs and to aid in technology transfer for developed methods and standards.

An overview of the NBS technical program in NDE follows. More detailed reports of recent progress in selected areas of the program are provided in the next section of this report.

Work reported in the Technical Progress section includes several NDE-related programs not funded directly by the Office of NDE.

1

Table I

COMPARISON OF COMMON NONDESTRUCTIVE EVALUATION METHODS

Method	Characteristics Detected	Advantages	Limitations	Example of Use
Ultrasonics	Changes in acoustic impedance caused by cracks, nonbonds, inclusions, or interfaces.	Can penetrate thick materials; excellent for crack detection; can be automated.	Normally requires coupling to material either by contact to surface or immersion in a fluid such as water.	Adhesive assemblies for bond integrity.
Radiography	Changes in density from voids, inclusions, material variations; placement of internal parts.	Can be used to inspect wide range of materials and thicknesses; versatile; film provides record of inspection.	Radiation safety requires precautions; expensive; detection of cracks can be difficult.	Pipeline welds for penetration, inclusions, voids.
Visual-Optical	Surface characteristics such as finish, scratches, cracks, or color; strain in transparent materials.	Often convenient; can be automated.	Can be applied only to surfaces, through surface openings, or to transparent material.	Paper, wood, or metal for surface finish and uniformity.
Eddy Currents	Changes in electrical conductivity caused by material variations, cracks, voids, or inclusions.	Readily automated; moderate cost.	Limited to electrically conducting materials; limited penetration depth.	Heat exchanger tubes for wall thinning and cracks.
Liquid Penetrant	Surface openings due to cracks, porosity, seams, or folds.	Inexpensive, easy to use, readily portable, sensitive to small surface flaws.	Flaw must be open to surface. Not useful on porous materials.	Turbine blades for surface cracks or porosity.
Magnetic Particles	Leakage magnetic flux caused by surface or near-surface cracks, voids, inclusions, material or geometry changes.	Inexpensive, sensitive both to surface and near-surface flaws.	Limited to ferromagnetic material; surface preparation and post-inspection demagnetization may be required.	Railroad wheels for cracks.

2

Acoustic-Ultrasonic Programs:

Work is in progress to develop and improve methods for calibration of ultrasonic and acoustic emission transducers. Spectral characteristics, beam profile, and total sound power measurements are being studied. Several transducer calibration services, both in ultrasonics and acoustic emission, are available.

NBS Researchers are investigating ultrasonic test blocks to improve the measurement reproducibility of these metal calibration blocks. A calibration service for aluminum and steel ultrasonic reference blocks is available. Further directions for this effort include the development of material-independent test blocks and the development of well-characterized fatigue cracks that could serve as a calibration artifact for may NDE tests.

Electromagnetic Methods:

NBS Scientists are examining methods for the measurement of visual acuity under typical NDE inspection conditions. This includes the effects of subdued lighting common in radiographic reading rooms and of the dark booth situations typically used in fluorescent penetrant and magnetic particle inspection. The program will characterize test methods used in NDE where the human eye is an integral part of the system. Visual parameters critical to the ability of people to detect and judge visual indications of defects will be identified. These accomplishments will lead to recommendations for improved visual acuity measurement methods.

Optical methods utilizing reflected and scattered light are being investigated for the characterization of surface defects and for the measurement of surface roughness. A review of optical NDE methods is in preparation. Consideration is being given to the need for standards in holographic NDE.

Facilities for dc and ac electrical conductivity measurements have been completed. Procedures have been established for the measurement of conductivity over the range of 1-100 percent of the International Annealed Copper Standard (IACS). Methods for the calibration of eddy-current test equipment are under investigation. Conductivity standards for the range from 30 to 60% IACS are available as an SRM.

The magnetics program is particularly concerned with improving measurements for magnetic particle testing. The work includes efforts to determine the uniformity of magnetization within the inspected part, measurements of magnetic leakage flux and determination of the leakage flux needed for detection of subsurface defects.

Leakage Testing:

Reference standards for leakage rate are being developed to improve leak rate measurements.

Penetrant Testing:

NBS scientists have developed a crack calibration plate for the evaluation of penetrant sensitivity; this is now available as an SRM. The fluids and particles used for penetrant testing are also of interest. Brightness measurements of fluorescent penetrants are planned, along with work on measurements of key properties of the fluids.

Radiography:

Current programs involve work in both neutron and x-radiography. The x-ray program includes investigations of standards for the measurement of spatial resolution in radiographic systems, for the determination of response of x-ray film and for the characterization of real-time fluoroscopic systems. Developments in progress include work on improved x-ray screens and determination of scattered radiation content and its effect on radiographic detectors and systems.

The neutron radiographic studies are made primarily at the NBS research reactor and the 100 MeV linear accelerator. Work has also been carried out with a 3 MeV Van de Graaff accelerator. A recommended practice for thermal neutron radiography has been developed in collaboration with the American Society for Testing and Materials. Standards for characterizing neutron beams for radiography and gaging are under investigation. NBS scientists have investigated the use of three-dimensional thermal neutron radiography and have shown the application of this inspection procedure to nuclear fuel subassemblies, batteries, and art objects. Work has been done with resonance neutrons and plans include radiographic studies with cold neutrons.

Thermal-Infrared:

A recently completed program resulted in the development of a method for the nondestructive evaluation of batteries used in critical assemblies such as cardiac pacemakers. A microcalorimeter capable of measurements in the 0.2 to 1000 microwatt range is used to measure heat generated in batteries and, in some cases, pacemakers under a variety of conditions. Heat generation by new and partially discharged batteries is measured under no-load conditions as a measure of self-discharge. The work has resulted in a nondestructive method to determine power cell quality. Additional work on infrared NDE systems is being considered.

4

Wear Debris Analysis:

Detection of worn metal in lubricants in mechanical machinery is now
used in both military and civilian programs to determine the proper time for
engine, bearing, and transmission overhaul. This method is now being expanded
in a current NBS program, in which the wear debris particles in the lubricant
are detected, sized, and examined in order to determine where and by what
mechanism wear is occurring. X-ray microanalysis techniques have been developed
for particles in the micrometer range. The techniques offer increased sensi-
tivity for engine condition monitoring compared to conventional SOAP methods.

1. Absolute Acoustic Emission Sensor Calibration
   F. Breckenridge
   Mechanical Production Metrology Division
   National Engineering Laboratory

Acoustic emission (AE) techniques are widely used for inspection and monitoring of high performance structures such as large pressure vessels (steam boilers, nuclear reactors, etc.), piping, and aircraft and for control of manufacturing processes. Central to all such work is the necessity to be able to standardize and intercompare the equipment used and the results obtained. All acoustic emission systems use transducers to convert the structure-borne sound waves to electrical signals. System characterization, therefore, depends on being able to characterize and understand the action of the transducers. The need for a standard method of calibrating transducers has been stressed by the ASNT,[a] the ASTM,[b] the ASME,[c] and other technical organizations concerned with using acoustic emission techniques. It is the fervent hope of many that the calibration be in terms of absolute physical quantities such as open circuit volts of output per meter of surface displacement as the transducer face. We have made a major step in this direction by offering a calibration service for AE transducers using an absolute surface-pulse method.

Results of any acoustic emission test, such as an event count or a ring-down count depend very much upon the sensitivities and frequency responses of the transducers used. If the transducers of a source-locating array are of unequal sensitivity or respond differently to a particular kind of wave motion, then the results may be in error. By providing a standard basis on which transducers can be compared we have made it possible to compare results of one test with those of another. It is now possible for a manufacturer or a user to set up acceptance-rejection criteria for transducers so that repeatable results can be approached.

We have developed and implemented a calibration scheme, which we feel is suitable for the purpose, and which yields the frequency response of a transducer to structure-borne waves at a surface of the type that are normally encountered in acoustic emission work. Furthermore, the calibration is absolute in the sense that the transducer output voltage response is measured for a given well-established, dynamic input displacement. This displacement is determined by two independent methods, both of which are absolute and which agree with each other within a few percent. The calibration results can be given either as a transducer impulse response, or as a frequency response to a constant displacement (or velocity or acceleration) input. In any case, the units are output volts per meter (or meter per second or per meter per second squared).

---

[a] American Society for Nondestructive Testing

[b] American Society for Testing and Materials

[c] American Society for Mechanical Engineers

The basic principles that make the calibration possible were described by Breckenridge, Tschiegg, and Greenspan[1] in 1975. These principles have been applied by us in the calibration system we have constructed. A calibration system[2,3] patterned after ours, but with some modifications, has been built and is in use now by one major manufacturer of acoustic emission systems and transducers. Another manufacturer is actively developing a system also based on the research of this project.

We expect that most of the transducers submitted to us for calibration will be used as secondary standards against which other transducers will be calibrated. The techniques used to transfer the calibration to other transducers will, in most cases, be similar to that which we use in our primary calibration. Furthermore, using the techniques that we have developed, it is possible for any laboratory desiring calibrated transducers to design and build a system which could calibrate transducers directly against measureable physical quantities without reference to any secondary-standard transducer.

This calibration service (formally announced in SP 250 addendum dated December 1979) has been received with considerable interest. Between January and September 1980, 50 calibration events have been processed. Clients include AET,[d] B&K,[e] Battelle, Dunnegan/Endevco, Rockwell as well as ASTM and the other NBS units. While the now existing calibration service provides a basis for traceability and some very important information, the service has a number of caveats which we hope to eliminate. Provision of an epicenter calibration capability will significantly enhance our ability to provide the required information.

References

1. F. R. Breckenridge, C. E. Tschiegg, and M. Greenspan, "Acoustic Emission: Some Applications of Lamb's Problem," J. Acoust. Soc. Am. 57, 627-631 (1975).

2. Ching Feng and R. M. Whittier, "Acoustic Emission Transducer Calibration Using Transient Surface Waves and Signal Analysis," paper presented at the International Conference on Acoustic Emission, September 1979.

3. "Now Hear This," September 1979, Dunegan/Endevco, San Juan Capistrano, CA.

---

d Acoustic Emission Technology

e Brvel and Kjaer (Denmark)

2. Standard Transducer for the Acoustic Emission Calibration Service
   F. Breckenridge
   Mechanical Production Metrology Division
   National Engineering Laboratory

A critical part of the recently announced (Dec. 1979) calibration capability for acoustic emission (AE) sensors is the standard transducer against which a sensor under test is compared. A complete analysis of the standard transducer has just been completed.[1]

The standard transducer, shown in Figure 1, is a capacitive line sensitive device which makes an absolute measurement of the normal component of dynamic surface displacement on a flat solid. It is used to measure the normal component of surface-wave motion, the direction of travel of the wave being known. This is accomplished with a very high sensitivity and without loading the surface which is measured.

The transducer consists mainly of a cylinder of brass supported above the horizontal surface whose vertical motion is to be measured. The brass cylinder, which is the charged electrode of the variable capacitor, has its axis horizontal and is separated from the steel surface by an air gap of about 4 µm. Thus the active area is a narrow strip approximating a line segment. The line segment is oriented so as to be tangent at its midpoint to the advancing circular wavefronts from the point source used in the calibration. This is accomplished with the help of a small mirror attached parallel to the transducer axis.

Calculation of the capacitance between a cylinder of finite length and a parallel plane, as well as calculation of the sensitivity of such a transducer, is difficult. The problem is simple, however, for an infinite cylinder. Accordingly, the transducer consists of three cylindrical parts, end to end, with insulators in between, as shown in Fig. 2. The center part is the active electrode and the two ends are electrical guards, which, when in use, are driven by a unity gain amplifier whose input is connected to the center part. The center part may be considered as part of an infinitely long cylinder.

The transducer rests on very thin polycarbonate shims which determine the air gap between the brass back plate and the flat surface. The supports are remote from the sensing portion and are compliant so that the measured surface is practically not loaded at least over the range of 10 kHz to 1 MHz.

The sensitivity has been calculated starting with the known sensitivity of an infinitely long cylinder parallel to a plane. Effects due to the motion not all being in phase under the transducer have been analyzed. For example, at 1 MHz this effect decreases the amplitude by about 0.71 dB and does not shift the phase. Effects due to the line reception of a circular wave front have also been analyzed and, for example, at 1 MHz this effect reduces the amplitude by less than 1 percent and retards the phase by about 8 percent. Transducer resonances have also been analyzed and measured and occur mostly below 1 kHz.

Examining true errors (those for which corrections cannot be made) results in an estimate of an uncertainty of about 3 percent. To test this uncertainty, experimental results were compared to theory with an agreement of 2 to 4 percent.

In summary, a capacitive, line-sensitive, displacement transducer has been constructed for measuring the surface-wave displacement of a surface without loading it. The transducer has a bandwidth of better than 10 kHz to 1 MHz, and a displacement threshold of about 10^{-12} m rms. It has been demonstrated that the output from the transducer can be calculated within a few percent. The transducer is expected to be used in the calibration of acoustic emission sensors.

References

1. F. R. Breckenridge and M. Greenspan, "Surface-Wave Displacement: Absolute Measurements Using a Capacitive Transducer," to be published in the Journal of the Acoustical Society of America.
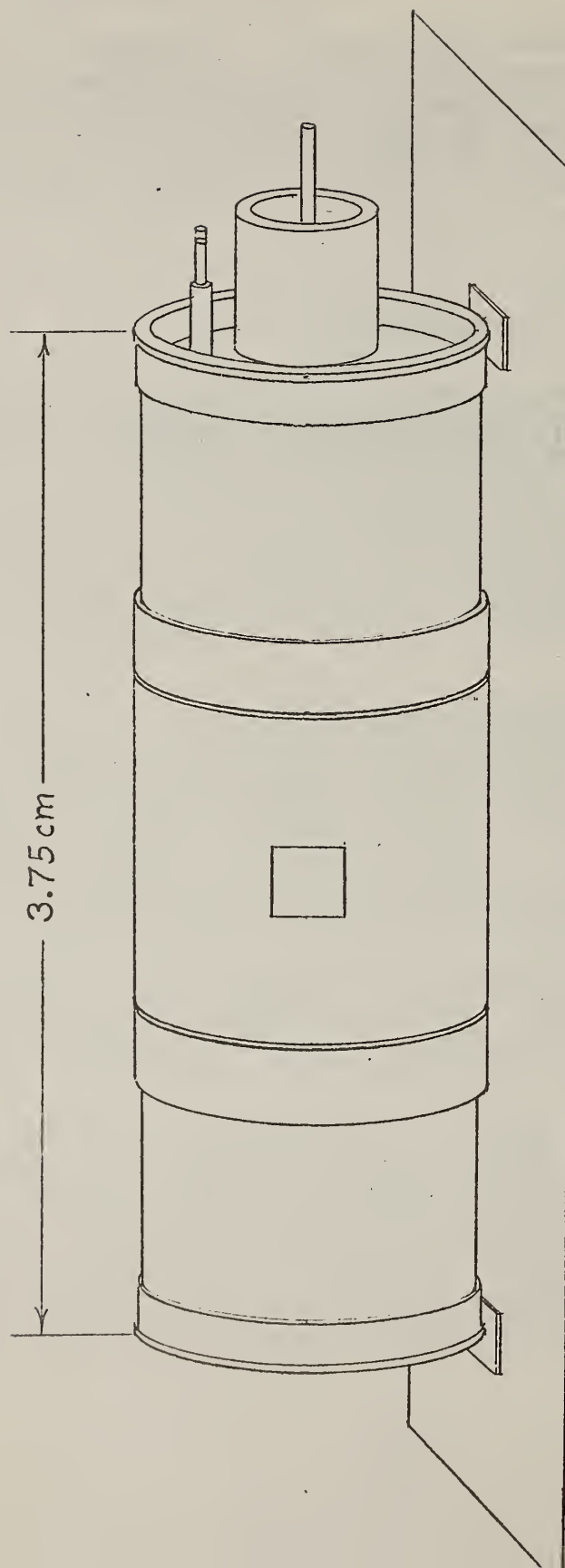
Figure 1. Sketch of cylindrical, capacitance transducer shown in relation to a rectangular portion of the mounting surface. The two square shims under the ends determine the air dielectric gap.
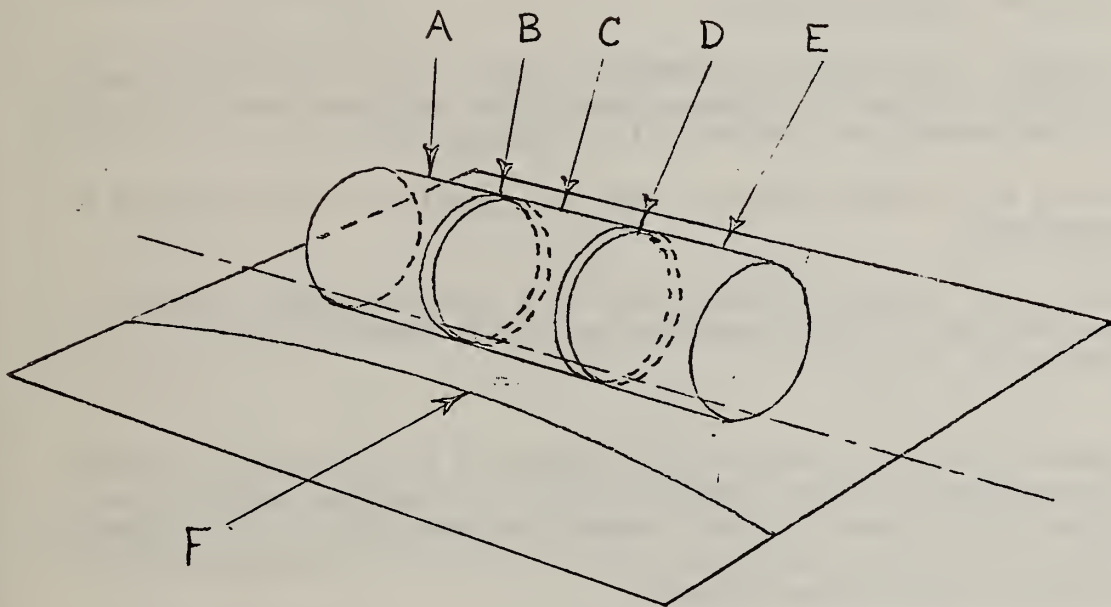
Figure 2. The basic functional parts of the capacitive transducer. A and E are the electrical guards, C is the active part of the transducer, B and D are insulators, and F is the advancing wavefront.

3.   Acoustic Emission Source Characterization--Laboratory Controlled
         Experimental Study of the Physical Processes of AE
      N. Hsu
      Mechanical Production Metrology Division
      National Engineering Laboratory

      The ultimate goal of AE signal analysis is to determine the exact nature
of the AE source from detected signals so that the source mechanism can be
quantified and the reliability of AE technology can be assured. To achieve
such a goal, we studied the details of the physical processes of AE, from the
generation of the stress wave at the source to the detection of the electrical
voltage signals, through the combination of analysis, design, and conducting
of controlled experiments in our laboratory. The steps are:

      1.   Analyze the AE signal evolution process and break down the problem
           into three separable parts.

      2.   Construct a laboratory experimental system with an analytical basis
           such that the coupling between theoretical and experimental results
           provides unambiguous and definitive interpretation.

      3.   Resolve the forward problem - make the signature of the detected AE
           predictable.

      4.   Resolve the inverse problem - develop a signal analysis technique
           to derive the AE source waveform explicitly from the remotely-
           detected AE signals.

      Some relevant laboratory test results concerning the detected AE signals
and how they relate to the source waveforms have been reported and they are
summarized below. While these findings showed the complexities of AE signals
and the difficulties of their analysis, these definitive findings did point
out the direction for future developments.

      1.   The detected AE signals have little resemblance to the original
           source waveforms.

      2.   Given a well-defined simulated source, the detected signals have
           reproducible features which depend on (a) sensor characteristics,
           (b) relative location between sensor and source, and (c) geometry
           of the structure.

      3.   The initial part of the detected signal carries the essential in-
           formation about the source when the sensor is close to the source.
           Furthermore the detected signal can be predicted by theory if the
           source waveform is known.

4.   Under laboratory-controlled conditions the inverse problem, to
     compute the source waveform explicitly from the detected signal,
     can be solved.

     Specific applications of sensor characterization, structure calibration,
and AE source quantification based upon the understanding of the physical
processes of AE are being developed.   Source deconvolution techniques for
complex structures based upon experimentally determined impulse response
functions are also being developed.

4.   Acoustic Emission Flaw Location

N. Hsu
Mechanical Production Metrology Division
National Engineering Laboratory

The detection of the differences in time of arrival of Acoustic Emission (AE) from an active flaw to strategically placed sensors provides a unique technique for determining the location of the active flaw. In this technique the location of the AE source is computed by the triangulation method. The technique has the advantage of being passive and is capable of monitoring a relatively large area in situ and in real time. Since 1979 we have initiated a systematic study of the problems and possible solutions associated with AE flaw location. The objectives of the study are to devise system calibration techniques to ensure reproducibility and reliability and to define limitations and optimization procedures through error analysis. Included in the study are the characterization of the various modules of a triangulation system and the development of laboratory experiments and theory to analyze transient wave propagation in structures. The system characterization and the transient wave analysis are essentially an extension of the study of a well-characterized AE system developed and reported previously.

Characterization of flaw location systems using triangulation involves both instrumentation hardware and computer software. Methods are being developed for calibration of sensors, amplifiers, filters and switching pulsers, and time coincidence counters. A time coincidence counter module has been designed and constructed. The module is interfaced to a minicomputer through direct memory access. Time of arrivals in modular units of 8 channels each can be acquired and a self-test scheme is incorporated in the construction. Triangulation algorithms are classified into four groups: 1) over determined linearization; 2) direct computation based upon polar coordinates; 3) iteration schemes, and; 4) sorting against pre-computed grids. These algorithms have been programmed in FORTRAN. Detailed comparison of these programs with regard to their speed, versatility, accuracy and limitation are being made.

5.   Improved Acoustic Emission Transducers*
     T. Proctor
     Mechanical Production Metrology Division
     National Engineering Laboratory

     With the increased need for better signal interpretation in the Acoustic
Emission field, high quality mechanical to electrical signal reproduction is
of great importance to improvements in the acoustic emission NDE method of
determining and monitoring structural integrity. The importance of using trans-
ducers that are truly hi-fi cannot be overstated. Identification and charac-
terization of AE events from signature information will only be possible through
the use of hi-fi transducers. Such useful schemes as deconvolution and coinci-
dence techniques will only be put to full use for eliminating random and coherent
noise problems when hi-fi transducers are available. As a result, there exists
a need for a transducer which has very good response, and which is also conve-
nient to use and which has good sensitivity. The capacitance transducer does
have very good frequency and phase response for vertical motion but it is deli-
cate and somewhat difficult to use because of high surface finish requirements
and it has low sensitivity. We have been working on a series of improved piezo-
electric transducers which have good frequency and phase response while being
much more convenient to use than the capacitance transducer and also having a
much higher sensitivity.

     Basically these improved piezoelectric transducers have been designed so
as to avoid any physical mechanism which would cause resonant conditions or
coherent interference to occur in the frequency range of interest. This has
been accomplished by (1) reducing the reflection of the back wave in the trans-
ducer through the use of a matched backing (2) reducing the contact area of the
transducer such that its dimension is small compared to the smallest wavelength
of interest, (3) eliminating of extraneous parts of the transducer such as case,
connector, etc. in an effort to avoid coupled resonance conditions and (4)
eliminating the usual wear plate which often produced coherent interference in
the signal received.

     A family of transducers which embody the four notions mentioned has been
constructed to establish feasibility. These transducers are primarily vertical
displacement sensors. Their performance is remarkably good. Over the band of
10 KHz to 1 MHz these transducers have a displacement spectra which is essentially
flat and is free of any resonant conditions. The phase response is also very well
controlled. Figures 3 and 4 display the amplitude response and the phase response
as determined by the NBS acoustic emission transducer calibration procedure.

     A third way of examining transducer response for faithful reproduction is
to compare the time waveform with the actual displacement-time history. Fig. 5
is the response of the standard capacitance transducer to a step force function.
It reproduces the surface vertical displacement due to this driving function

_____
* Publication subject to patent disclosure.

almost perfectly. Figure 6 is the response of one improved piezoelectric transducer. Fig. 7 is a typical response of a commercially available transducer to the same step force signal. When comparing this response with the response of most of the commercially available transducers, it is apparent that its response is much better while its sensitivity is comparable.

The surface and through-pulses produced by a step force are good signals with which to test transducer responses and performance. This is primarily because the wave solutions are known. Presently, we are working on through-pulse method for calibrating transducers. In particular, through-pulse comparisions have been made using the improved piezoelectric transducer. The results although not final, are very encouraging. Some of these results will be available for reporting in a talk before the Acoustical Society in November.

In addition to the on-going research on transducers for vertical motion, the same techniques will be applied to horizontal-motion sensors. We have every reason to believe that this will produce a good hi-fi, horizontal motion detector for use in acoustic emission NDE.

SPECTRUM MAGNITUDE: DIV: 101

DISPLACEMENT RESPONSE

Figure 3
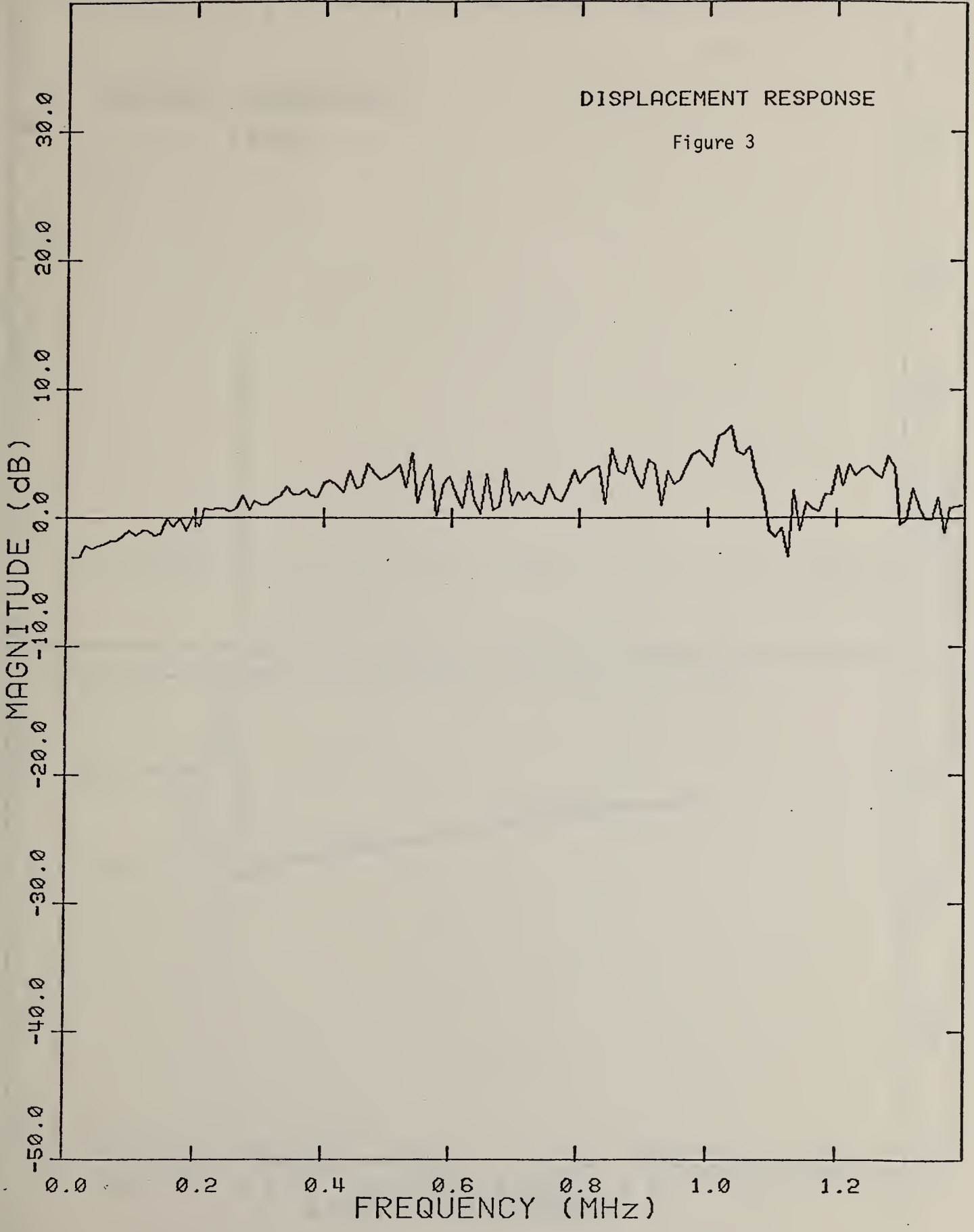
SPECTRUM PHASE: DIV: 101

DISPLACEMENT RESPONSE

Figure 4
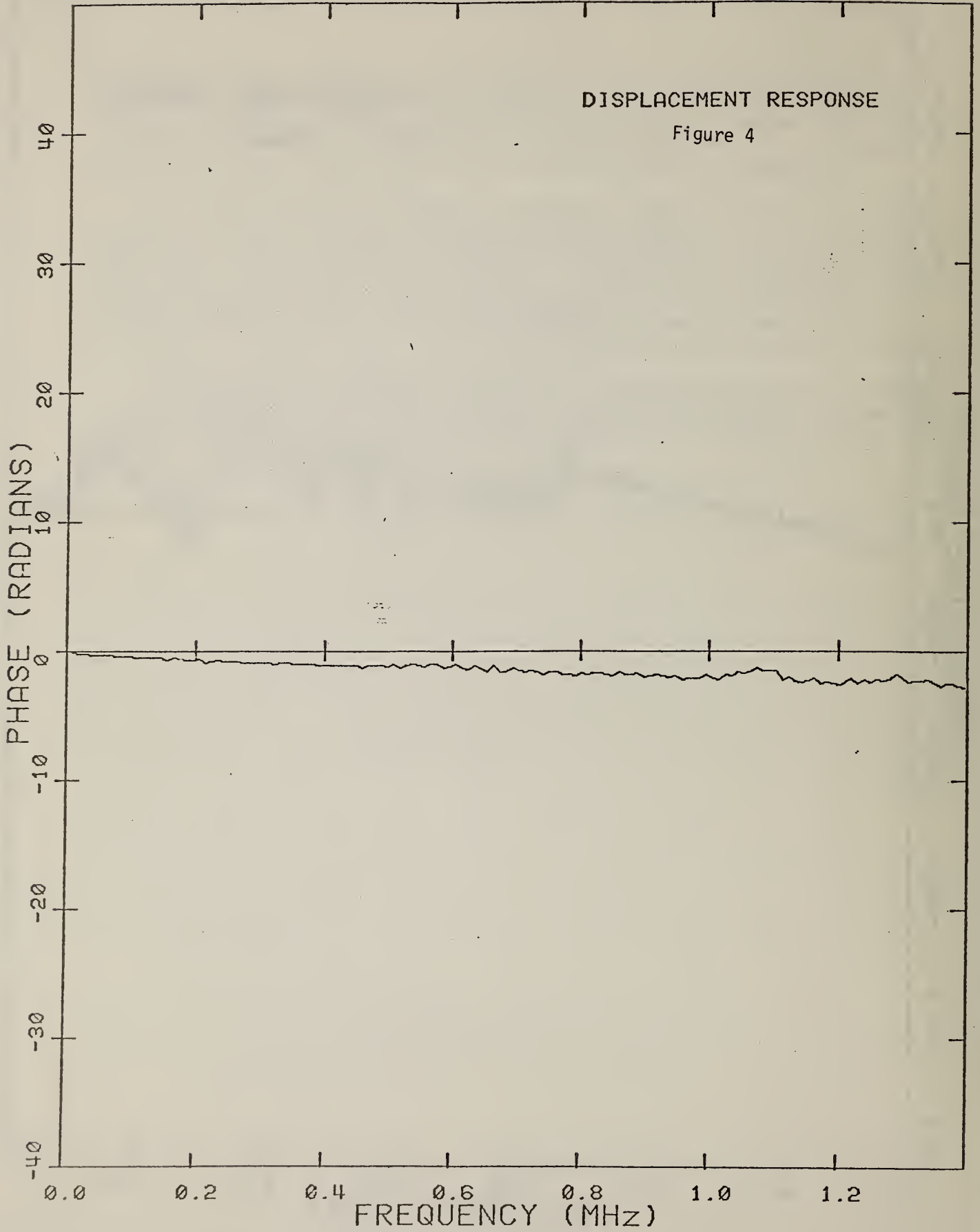
TRANSDUCER OUTPUT: STD: 101

Figure 5

TRANSDUCER OUTPUT: UNK: 101

Figure 6

TRANSDUCER OUTPUT: UNK: 110
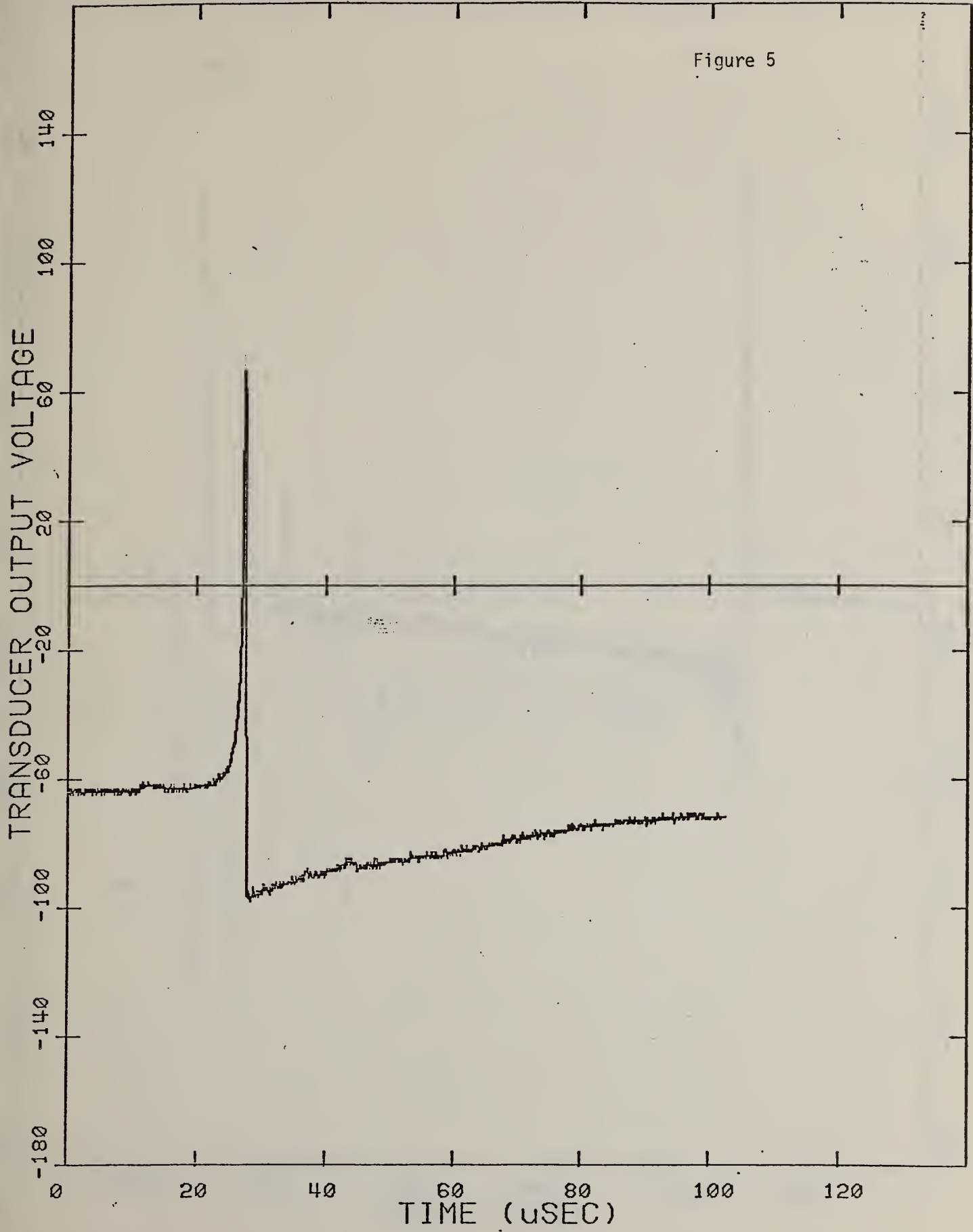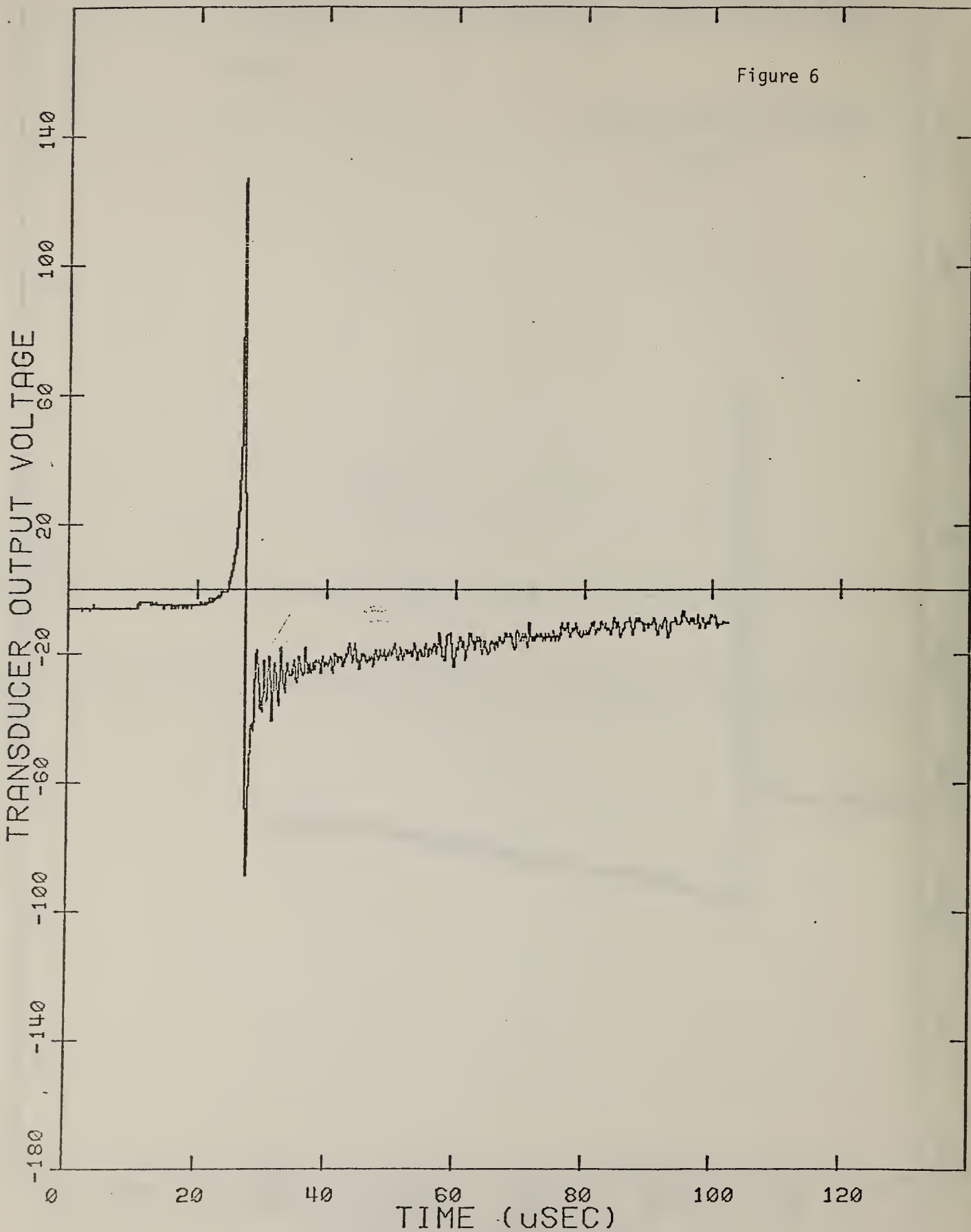
Figure 7
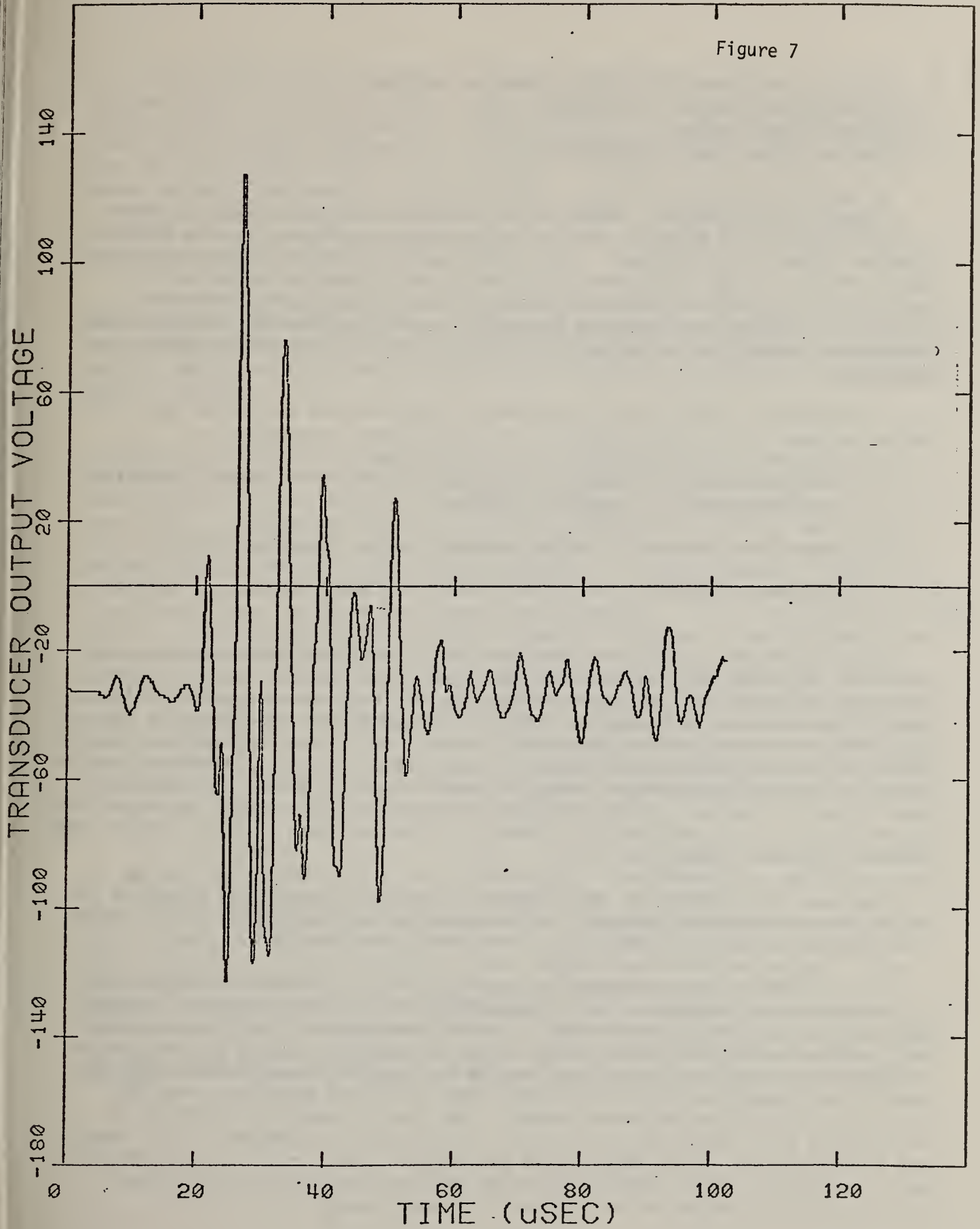
6. Acoustic Emission - Materials Characterization
   J. A. Simmons and R. B. Clough
   Metallurgy Division
   National Measurement Laboratory

Acoustic emission (AE) relies on the detection of stress waves emitted during the motion of flaws or from other microstructural changes in a highly stressed region of a structure. This technique has been applied to aerospace, petrochemical, bridge, and power plant structures to monitor structural integrity. It has also been used to detect faulty welds in production lines. In addition, AE has been used for materials research studies on microstructure related properties such as deformation mechanisms, phase transformations, and fracture.

Highlights in the AE area in the Metallurgy Division during the past year are:

1) Development of Indentation Techniques for the experimental production of AE signals from material defects;

2) Experiment design for multichannel AE source characterization;

3) Progress on acoustic emission theory and signal processing techniques.

1) Indentation techniques have been highly developed for use with ceramic materials for studying crack growth under controlled loading. We have therefore begun to adapt the technique to use with metals as a new type of controllable acoustic emission source. Besides the control possible on the growth of defects, this method also ensures that the source location is fixed, an essential feature for AE signal analysis and microstructure correlation. Such a technique provides, under the proper conditions, a means of generating reproducible AE signals from known types of sources, having predicable signatures. This allows one to actively control AE and thus constitutes an advance in the technique from its present mode of merely passive listening.

We have been developing the indentation method in metals and alloys so far using three new types of methods: (a) indentation brittle fracture; (b) indentation fatigue; and (c) indentation stress corrosion cracking.

The brittle fracture method has been successful on steels which have been hardened by heat treatment. It has been found that if the surface is hardened to greater than 45±5 on the Rockwell C scale, indentation by a diamond pyramid will produce subsurface penny-shaped median plane cracks generally less than a millimeter in size. By controlled loading it is possible to produce identical repetitive signatures, typically on the order of 10 but sometimes over 100. Comparison with SEM micrographs suggests that these signals are produced by incremental crack growth along carbides and martensitic platelets. This idea has been exploited in the design of a portable "acoustic embrittlement detector" which can detect locally embrittled areas of structures such as in the heat affected zones of welds or on critically stressed areas.

22

This technique has also been studied as a means of producing localized fatigue cracks in 2024 and 7075 aluminum where, after sufficient load cycling, reproducible signals are emitted. Comparison of AE signals and SEM micrographs shows characteristic differences in signals in these alloys which are explainable in terms of the defect microstructure. Finally, fatigue cracks can be generated and after removal of the indentor a drop of corrosive medium is placed over the indentation. The residual stress is sufficient to generate numerous stress corrosion signals which are also being studied in relation to microstructure.

Interactive experiments with Dr. Wadley of AERE, Harwell, have also begun using a plate indented with a bias stress to give further control on the defect morphology. There are in fact a number of interesting experiments suggested by this newly available research tool which cannot be summarized now but appear quite fruitful.

2) A high speed interface has been designed and is being constructed for monitoring up to 16 AE channels using 20 MHz transient A to D recorders with variable timescale for synchronization, up to 100 dB dynamic range, and less than 100 millisecond dead time to dump all channels. This interface will be connected to our new Perkin-Elmer 3220 microcomputer and will be operated remotely in the laboratory under computer control. Monitoring of experimental parameters will also be under computer control. A loading machine capable of producing bias stresses in large metal plates is being designed to permit creating defects under variable but controlled conditions. This instrumentation will permit us to simultaneously monitor at several transducer sites AE from defect sources produced on a plate by indentation or other directed energy loading. Using the theory developed at NBS we will then be able to calculate the stress drop history characterizing the source. Knowledge of the stress drop history gives information on the defect orientation and geometry, the dynamics of the emission process, and the local stress conditions. This information will be used interactively with metallurgical examination and defect mechanism modeling to enhance our understanding of defect dynamics and to develop critical AE indicators to signal critical feature events.

3) The theory of acoustic emission from defect sources has been extended to include inhomogeneities such as martensitic transformations and micro-cracks. In addition, an extensive series of computations of waveforms to be expected in steel and glass plates have been carried out. These calculations have graphically demonstrated the great directionality of acoustic emission signals as well as pointing to the potential of new signal processing techniques. The plate code is currently under revision to allow more accurate Fourier transforms of the plate solutions to be computed, thus permitting more reliable inversion methods. Finally, the theory of noise propagation has been carefully studied using quadratic noise statistics and criteria have been developed for optimal noise filtering to use in conjunction with deconvolution techniques.

7. Electric Power Research Institute/National Bureau of Standards
        Joint Acoustic Emission Program
    D. G. Eitzen
    Mechanical Production Metrology Division
    National Engineering Laboratory

The acoustic emission technique has great potential for determining and monitoring structural integrity. Acoustic emission (AE) signals contain potentially useful information about the location and identity of defects and about the criticality of the defects in a structure under load. However, current signal processing techniques such as threshold counting, RMS recording, energy measurement, peak detection, and spectral analysis often fail to extract the remaining information unambiguously. The difficulty lies in the inherent complexity of the generating mechanism, the transient wave propagation details and the physics of the sensor's mechanical-to-electrical conversion process.

The objective of the EPRI/NBS Joint Program on Acoustic Emission is to develop certain of the information needed to form a basis for the AE monitoring of nuclear reactor structures and to establish the feasibility of AE monitoring in a simple structure. The achievements of this program include:

1. Contributions to data interchangeability for laboratory and field measurements through the development of a transducer calibration service.

2. Contributions to the reliability of AE field data through the development of calibrated sources.

3. A better understanding of AE source behavior through theoretical predictions of the behaviour of AE sources.

4. A better understanding of the limitations of conventional AE methods through a critical analysis.

5. A framework for understanding the AE process from source to measured voltage.

6. An analysis of the potential information in AE signals, an understanding of the modification to signals by wave propagation, experimentally verified theoretical predictions of remote displacement due to an AE source, and part of the basis for secondary sensor calibrations, all through the theoretical solution for wave propagation in a plate.

7. Demonstration of the feasibility of determining the actual AE source function by making remote measurements based on having performed this in glass and in steel using time domain deconvolution.

8. Development of a methodology for determining the significance of received AE signals.

9. Development of several additional very promising signal processing techniques.

Some of these developments are being used in industrial applications and others are being used by other AE researchers. While these applications and others are consistent with the technical plan, it appears that additional information must be developed before power producers can obtain all the information from AE that is desired. An extension of the agreement has been negotiated and will result in further improvements in the transducer calibration capability, in deconvolution of complex structures and in information about the significance of AE sources.

8. Polymer Sensors for NDE

S. Edelman and S. C. Roth
Polymer Science and Standards Division
National Measurement Laboratory

Our recent work involved the use of polymer sensors to measure dynamic elastic moduli and to detect wear in airplane control cables.

Making use of the sensitivity, low density, and flexibility of piezo-electric polymer strain gauges, we have worked out a non-resonant method for measuring both the real and imaginary parts of both the dynamic Young's modulus and the dynamic shear modulus of structural materials in the form of long, thin rods. All four quantities can be obtained as continuous functions of both frequency and static load. The frequency can be varied over a wide range, and the static load can be varied from a large compressive value through zero to a large tensile value.

The method can be used to study the basic dynamic properties of materials. It should be especially useful in studying composite materials and polymers, materials whose dynamic properties are likely to vary with static load. In the case of composite materials, variation of damping characteristics with static load can be expected to be a sensitive test of the quality of the bonding between components. The method can be used to provide basic engineering data needed for designing structures which are to be subjected to dynamic stresses or for which particular levels of internal damping must be obtained.

Since all measurements are made on a single specimen under identical conditions (except for the type of excitation) any deductions about the internal structure are free of the uncertainties introduced where measurements at different frequencies require different specimens and where measurements of the different moduli require different apparatus. The method can be used for non-destructive evaluation of structural elements either for compliance with design specifications or for monitoring a change in properties during service. A paper describing the method was presented at the April 1980 meeting of the Acoustical Society of America. Support for a laboratory installation to apply the method is being sought.

The study of airplane control cables is performed on an apparatus in which the cable, under tension, is pulled around a small pulley by a cam which converts the rotation of an electric motor to reciprocating motion. A polymer sensor, attached to the cable near the pulley, detects the noise of the motion of the strands as they deform on the pulley. The sensor can be removed from the cable and reattached readily so that the same sensor can be used to compare different cables or different conditions. An elaborate mechanical filter eliminates motor noise from the signal. A spectrum analyzer operates on the sensor signal, and changes in the spectrum are monitored to detect the effects of fatigue and wear.

9. Strength Development of Concrete
   J. R. Clifton
   Structures and Materials Division
   Center for Building Technology
   National Measurement Laboratory

The maturity concept is considered to be a promising NDE method for estimating the compressive strength of inplace concrete at early ages. This concept is based on the premise that the combined effects of curing time and temperature can be mathematically related. Maturity (M) is defined by the equation:

$$M = \int (T-T_o)\, dt$$

where T is the temperature of concrete at time t, and To is the datum temperature. The datum temperature is the temperature at which the strength of immature concrete remains constant. Several relationships have been empirically developed based on empirical considerations, e.g.,

$$c' = A+B \log M$$

Where c' is the compressive strength of concrete and A and B are regression coefficients.

The development of mathematical models relating the development of strength of concrete to maturity has been undertaken. In the first phase of this work, a mathematical model developed at NBS for the hydration of tricalcium silicate has been used to derive maturity relationships. Comparison of model output and experimental data is shown in Fig. 8. The fit is believed to be reasonable considering that concrete contains several cementitious constituents in addition to tricalcium silicate and it also contains fine and coarse aggregates.

This work is contributing to the development of a more fundamental basis for maturity-strength relationships which will ultimately facilitate the acceptance of the maturity concept.
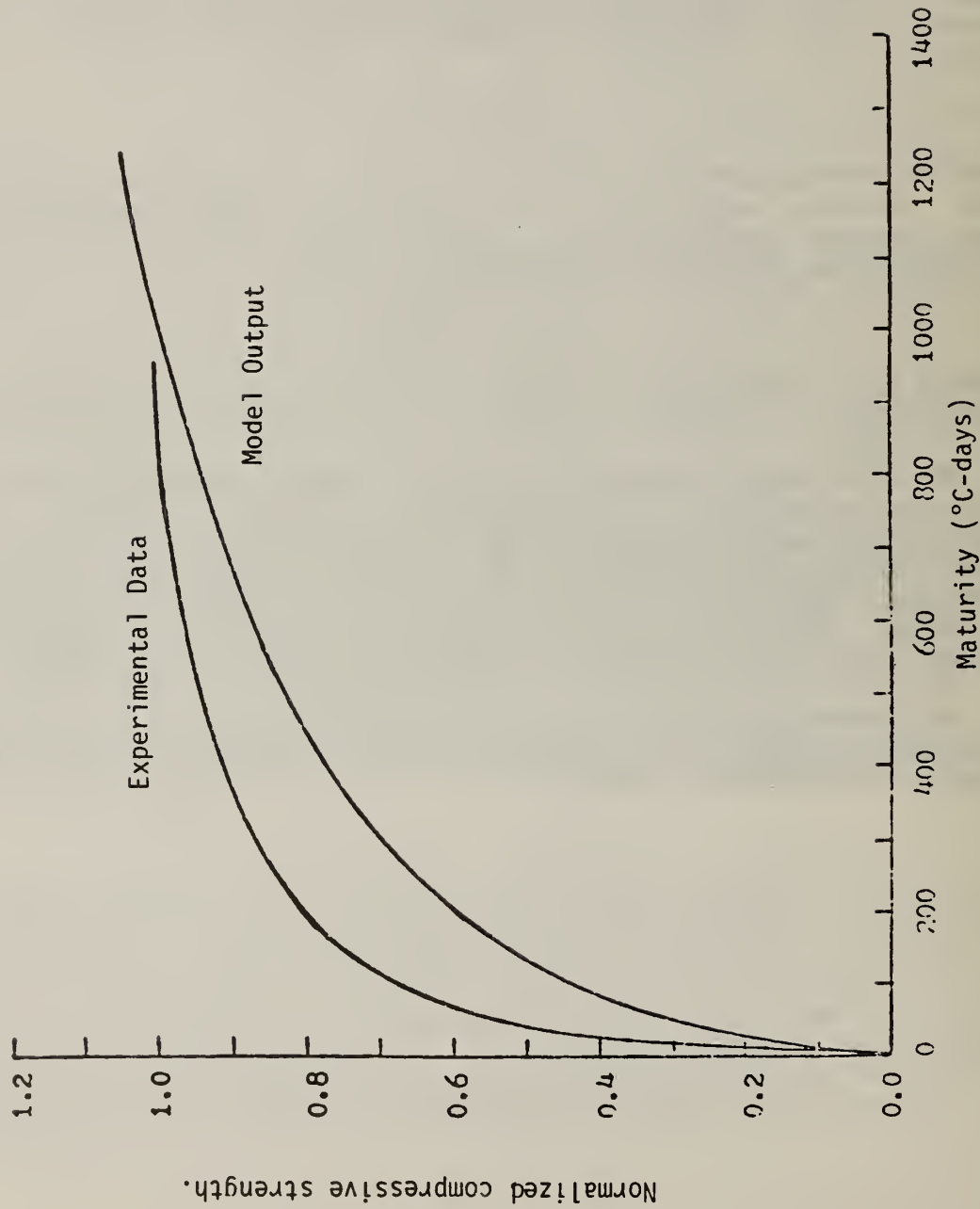
Figure 8.   Normalized compressive strength as a function of maturity. Normalized strength is ratio of strength at given maturity to ultimate strength.

10. Application of NDE to Construction/Army

J. R. Clifton and L. Knab
Structures and Materials Division
Center for Building Technology
National Engineering Laboratory

The use of NDE methods in quality acceptance of buildings is being studied for the U.S. Army Construction Engineering Research Laboratory. At present, when the military has a building constructed, it depends largely on construction inspectors to determine if design specifications and acceptable construction practices are being followed. However, often these inspectors do not have the necessary skills and experience to be effective. Therefore, the military is seeking alternative approaches. An approach being considered is the incorporation of quality acceptance testing of the installed building materials prior to acceptance of the completed building. This quality acceptance testing approach is based upon the use of NDE techniques.

NDE techniques applicable to concrete quality acceptance were first identified and assessed. The important properties and factors of concrete which often need to be characterized and appropriate NDE methods are listed in Table 2. These techniques were assessed based on consideration of usefulness of information obtained, reliability, level of expertise required to use the equipment and to interpret the results, and cost effectiveness. The results of the assessments are given in the paper "Nondestructive Evaluation Methods for Quality Acceptance of Hardened Concrete in Structures," NBS Technical Note (in press).

The use of NDE for the inspections of other building materials and building components is currently being addressed. The building materials and components which are being covered in the current phase of the work are listed in Table 3.

Field demonstrations of selected NDE techniques are an important part of this project. Purpose of these demonstrations is to convey to military personnel responsible for design and construction of military facilities, the usefulness of NDE in quality control and quality acceptance programs.

TABLE 2. NDE METHODS FOR QUALITY ASSURANCE TESTING OF HARDENED CONCRETE

CONCRETE PROPERTIES	RECOMMENDED TEST METHODS	POSSIBLE TEST METHODS
Strength	Windsor Probe Schmidt Rebound Hammer Cast-In-Place Pullouts Maturity Concept Cores	
General Quality and Uniformity	Windsor Probe Schmidt Rebound Hammer Ultrasonic Pulse Gamma Radiography Cores	Ultrasonic Pulse Echo Microwaves
Thickness	Covermeter Microwaves (Radar) Cores	Gamma Radiography Ultrasonic Pulse
Air Content	Cores	Neutron Density Gage
Moduli of elasticity		Dead Weight Loading with Acoustic Emission
Surface Properties	Visual Schmidt Rebound Hammer Cores	Microwaves Ultrasonic Pulse Echo
Density	Gamma Radiography Cores	Neutron Density Gage
Rebar Size and Location	Covermeter Gamma Radiography	Microwaves (Radar) Ultrasonic Pulse Echo
Corrosion State of Reinforcing Steel	Visual Electrical Potential Measurement	

TABLE 3. FACTORS CONSIDERED IN QUALITY ACCEPTANCE OF BUILDINGS

MATERIAL OR COMPONENT	DESIGN FACTORS OR PROPERTIES
1. BRICK AND MORTAR UNITS	INTEGRITY, THICKNESS, REINFORCING STEEL, PRESENCE OF INNER GROUT
2. WOOD AND LUMBER	INTEGRITY AND GENERAL QUALITY, DENSITY, MOISTURE CONTENT, ADHESIVE BOND FOR LAMINATED WOOD
3. METALS	
A. STRUCTURAL	LOCATION, TYPE OF METAL, CRACKS, CORROSION CONDITION, LOOSE CONNECTORS
B. WELDS	WELD DEFECTS
C. PIPES AND TANKS	WALL THICKNESS, LEAKS AND CONTINUITY, CORROSION CONDITION
D. ELECTRICAL WIRING	WIRE SIZE, TYPE OF METAL, CONDITION OF ELECTRICAL INSULATION
4. ROOFING SYSTEMS	COMPOSITION, MOISTURE CONTENT, PERMEABILITY, SLOPES, SELF SUPPORTING
5. PAINTS AND COATINGS	NUMBER OF LAYERS, FILM THICKNESS, INTEGRITY, ADHESION, QUALITY
6. SOILS	PERMEABILITY, PROPER BACKFILL
7. SEALANTS	ADHESION
8. PIPE AND DRAINAGE SYSTEMS	FLOW RATE AND PRESSURE, NO LEAKS, PRESENCE OF DIELECTRIC JOINTS, NO BACK FLOW OF WATER
9. ELECTRICAL WIRING SYSTEMS	CARRIES DESIGN LOAD, FUNCTIONS PROPERLY, CIRCUIT BREAKERS OPERATE
10. HVAC	PROPER FLOW RATE
11 BUILDING COMPONENTS	DESIGN FACTORS OR PROPERTIES OF WALLS AND CEILINGS, FOUNDATION AND BASEMENT, ROOF, BUILDING ENVELOPE AND FLOOR.

JC/KLB

11. NDE of Moisture in Roofing Systems/Air Force
     L. I. Knab and R. G. Mathey
     Structures and Materials Division
     Center for Building Technology
     National Engineering Laboratory

     The purpose of the NDE of moisture in roofing project, funded by the
Air Force was to investigate commercially available NDE methods for:

     1. Their ability to quantitatively detect the minimum moisture
         content, and

     2. Their ability to quantitatively detect moisture beyond the
         minimum amount.

     During FY 78 and 79, a state-of-the-art report was prepared on the NDE
methods and a controlled laboratory study was conducted.

     During FY80 a large amount of NDE data from the laboratory study was
reduced and analyzed. The data represented three NDE methods (electrical
capacitance (three instruments), nuclear backscatter (two instruments), and
an infrared thermography instrument), two roof decks (concrete and steel),
two asphalt thicknesses, and five insulation types (fiberglass, perlite board,
fiberboard, polystyrene, and polyurethane) in one and two inch nominal thick-
nesses. The data, in the form of NDE response versus the moisture content of
roofing specimens, was computerized and analyzed. A technique was developed
for assessing the performance of the NDE methods on a quantitative basis.

     An NBS Technical Note report on the state-of-the-art of NDE methods to
detect moisture in built-up roofing is currently in editorial and technical
review and will be published in 1980. A draft of the results of the laboratory
study has been completed and the paper, an NBS Building Science Series report,
will be submitted to editorial and technical review in October 1980.

12. Eddy Current Imaging System
     B. Field
     Electrical Measurements and Standards Division
     Center for Absolute Physical Quantities
     National Measurement Laboratory

     The initial concept for a real-time eddy current flaw detection and
characterization system presented in last year's report has been proven
feasible this year. The system uses a relatively large-sized array of pick-
up coils surrounded by four separate exciting coils. This arrangement will
be used to determine the shape, location, size, and orientation of disconti-
ties in flat non-ferrous metal plates, and display this information in real
time on a video display. Presentation of the information is to be in a format
similar to a radiograph which should provide increased operator confidence in
the measurements.

     The measurement configuration was described and a drawing of a prototype
probe system was included in the 1979 NDE Annual Report (NBSIR 80-2007). The
probe consists of a square array of pickup coils surrounded by four vertical
exciting coils that are energized in opposite pairs. The symmetry in two di-
mensions allows the system to be equally sensitive to discontinuities regard-
less of their orientation in the metal. We expect to energize one pair of
coils at a time with currents 180 degrees out-of-phase, thus creating a two
dimensional plane, perpendicular to the surface of the metal, where the com-
ponent of magnetic field is zero in the direction parallel to the metal surface
(zero horizontal field). By varying the intensity of the current in the two
driving coils the plane of zero horizontal field may be moved across the surface
of the plate performing an electronic eddy current scanning of the plate. The
advantage of this method is the ability to accurately locate small defects with
a few relatively large area pickup coils.

     To test the theory, the problem was reduced to a one dimensional experiment.
A slot type defect in an aluminum plate was mechanically scanned at several dif-
ferent field orientations using a single pickup coil. These data are plotted
in Fig. 9.

     The output of the pickup coil (the voltage component in phase with the
driving coil voltage) is plotted in the vertical direction, and each of the
nine traces represent a different field orientation. The mechanical scanning
was used for convenience only and for this case is equivalent to a row of
closely spaced pickup coils. As can be seen from the figure, the magnitude
of the signal due to the defect changes with field orientation, and appears
to go to zero somewhere between trace 5 and 6. Thus if the relationship be-
tween the coil excitation currents and the field orientation (i.e., the posi-
tion of the zero horizontal field plane) is known, the location of the defect
may be calculated based on measurements from sensors nearby, but not neces-
sarily exactly at, the location of the defect. To do this the response pat-
tern of the sensors must be known, and the sensors must be adequately sensitive
to respond to small defects. The latter attribute is a function of sensor
geometry and the signal-to-noise ratio of the instrumentation.

Thus pickup sensors must be chosen with regard to the following requirements.

1. High sensitivity to magnetic field perpendicular to the surface of the plate. The horizontal component conveys no significant information in this configuration.

2. Spatial response of the sensor must be known, preferably uniform sensitivity over the surface of the device.

3. The sensors must be matched in output response to permit sensitive differential measurements to be made to improve the signal-to-noise ratio. This also implies that a simple manufacturing technique is needed for production of matched devices.

Candidates for sensors include printed-circuit type coils, wire-wound coils, and Hall effect magnetic sensors.

Hall devices were investigated initially as they were known to be easily mass produced and have a uniform response to magnetic field over the surface of the device. Although the devices exhibit low sensitivity to magnetic field it was thought that this could be improved with sophisticated instrumentation.

Low sensitivity of Hall devices to magnetic fields not only requires more sensitivity in the measuring instrumentation but also increases the problem of stray field pickup in the leads of the device. In general it is not practical to use Hall devices at frequencies much above 500 Hz unless special precautions are taken to reduce pickup to an absolute minimum. For our system extensive shielding is not possible and tightly twisting the leads did not provide sufficient rejection of the stray field. To eliminate the effect of stray field the Hall device was excited using ac (rather than dc as is usual) and the device was then used as a non-linear mixer of the ac excitation and ac magnetic field. The output of the device was filtered and synchronously detected to eliminate unwanted signals due to stray field pickup and residual voltage. This procedure is explained by the short derivation given below.

In an alternating magnetic field the Hall voltage can be expressed by:

$$V_H = K_1 \frac{dB}{dt} I + RI$$

where B is the magnetic field orthogonal to the device, K_1 is the sensitivity constant, R is the residual resistive component, and I is the Hall device exciting current.

In addition there is pickup of stray field from the leads, thus

$$V_H = K_1 \frac{dB}{dt} + RI + K_2 B'$$

34

where B' is the same frequency as B but of different magnitude and phase.

If
$$B = \frac{B_o}{w_1} \sin w_1 t, \quad I = I_o \sin w_2 t$$

and
$$B' = B_o' \sin(w_1 t + \emptyset)$$

then
$$\frac{dB}{dt} = B_o \cos w_1 t$$

and
$$V_H = K_1 B_o I_o (\cos w_1 t)(\sin w_2 t) + R I_o \sin w_2 t + K_2 B_o \sin(w_1 t + \emptyset).$$

The product term can be expanded into an upper and lower sideband, thus for $w_2 > w_1$,

$$V_H = \frac{K_1 B_o I_o}{2} [\sin(w_1 + w_2)t + \sin(w_2 - w_1)t] + R I_o \sin w_2 t + K_2 B_o \sin (w_1 t + \emptyset).$$

If a high pass filter is used to eliminate all the frequency components at w_2 and below, we are left with a signal at a frequency of $w_1 + w_2$ that is a function of only the magnetic field strength and the Hall exciting current (which is known).

At this time we had only one frequency synthesizer available so a special purpose single-frequency synthesizer was built to excite the Hall device and provide a reference for a lock-in analyzer. As a result of measurements made using this system two problems were identified. Unless the Hall device is used with exciting currents substantially below the nominal magnitude, significant self-heating of the device occurs, which may locally alter the conductivity of the metal being measured. Also, large amounts of noise prevented sensitive measurements from being made at the required microgauss level. Thus it appears that Hall devices are not suitable for this application due to an insufficient signal-to-noise ratio, irrespective of the measuring instrumentation that is used.

A parallel investigation of the printed-circuit type coils shown in Fig. 10 was also performed. This type of coil has the advantage of being easily produced with close matching of the individual coils. The arrangement shown in the figure consists of four coils electrically connected in a "star" configuration for differential voltage measurements. Measurements of the coil output voltages in a uniform magnetic field in air showed excellent matching

of coil properties. Placing the coils on a metal surface however produced widely varying outputs among the simlar coils. These changes were found to be due to the design of the coil which requires the connecting leads be separated. This introduces a loop in the circuit that is sensitive to the horizontally oriented field and which in this case contributes a significant error to the coil signal. Different manufacturing techniques capable of producing finer line-widths and thus coils with a greater number of turns, or the use of thinner backing materials will help reduce this problem.

Rather than go to complicated manufacturing techniques for a small number of research devices, we decided to use carefully fabricated wire-wound coils to simulate devices with a large number of turns. The coil dimensions were determined by Computer-Aided-Design (CAD) using several programs published by C. V. Dodd[1] for analyzing the defect sensitivity of reflection-type coils. These new designs reduced the effect of stray field pickup by a factor of more than 100. Careful manufacturing techniques yielded coils with outputs that are matched to within 0.1% air. Unfortunately, the coils exhibit very poor matching when placed in a uniform field on a metal surface. We speculate that the problem may be due to small differences in interwinding capacitance which cause changes in the resonant frequencies of the different coils. More work in this area is planned.

We are satisfied with the design concept, however, further work is required to develop a pickup sensor capable of meeting the requirements of the proposed probe.

---

[1] Dodd, C. V., Cheng, D. C., Simpson, W. A., Deeds, D. A., Smith J. H., Oak Ridge National Laboratory Report ORNL-TM-4107, April 1973.
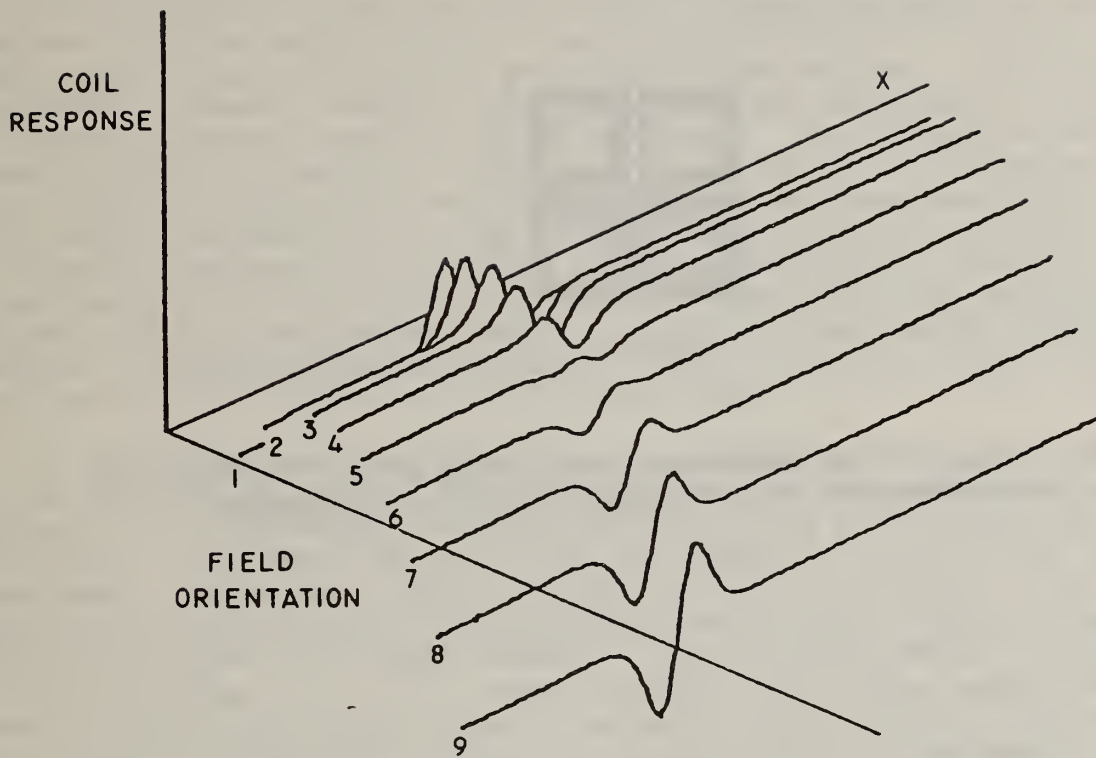
Fig. 9   Response of a pickup coil mechanically scanned over an aluminum plate, containing a slot type defect, at different magnetic field orientations.
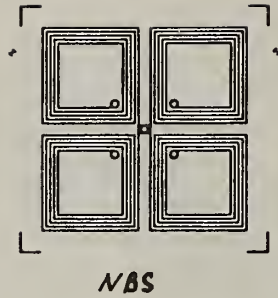
Fig. 10   Pattern of the printed-circuit pickup coil. The four coils are connected for differential voltage measurements.

13. Eddy Current Conductivity
    G. Free
    Electrical Measurements and Standards Division
    Center for Absolute Physical Quantities
    National Measurement Laboratory

The variable frequency eddy current bridge that had been developed[1] is extremely accurate but requires much time to balance the bridge on each test specimen. Various modifications of the bridge were tried. The latest measurement scheme is now being tested for accuracy and precision. The bridge is essentially a Maxwell bridge so that inductance and resistance of the test coil are known in terms of capacitance and resistance. The arms of the bridge which usually contain a capacitor and resistor in parallel, a single resistor and the Wien grounding network have been replaced by an operational amplifier network (Fig. 11). This configuration has the advantage of requiring a single balance of network components and places the input impedance of the voltage dividers in a position where they have no effect on the bridge balance as frequency is varied. Errors in measurement are due primarily to the leakage current. With the use of a high performance operational amplifier and the proper choice of resistance values this error should be quite small.

A second method of measuring electrical conductivity has also been developed during the past year and may make it possible to measure conductivty with an accuracy in the ppm range. This new method is based on an entirely different coil design. The theory related to the performance of this coil design is well developed[2]. The output voltage of a coil constructed as shown in Fig. 12 is a function of coil dimensions, frequency and conductivity of the test sample. By making the length of the lower inner coil (l_B) slightly greater than the length of the upper inner coil (l_T) a unique frequency for a given conductivity can be found at which the output voltage is in-phase with the current driving the primary coil. A bridge shown in Fig. 13 is used to make the measurement. The equation at balance is BR=V where V is the output voltage, R is the value of the resistor and B is the setting of the inductive divider. The output voltage of the coil is characterized in terms of a single resistor. The measurement can be made with extreme accuracy and precision due to this dependence on only one standard. Although other bridge components are necessary for the bridge balance their values do not have to be known exactly.

A somewhat less accurate bridge is also being tested (Fig. 14). The simplicity of the bridge and speed with which measurements can be made makes it one of great promise. Measurements are done quickly with only a single balance. Further, when measurements are made at low frequencies, i.e., 1-10 kHz, the bridge has only a slight sensitivity to lift-off in the 0.0 - 0.5 mm range.

Since many commercial coils which have been used in the NBS bridge were extremely non-linear, it was decided that experimental coils using computer aided design[3] should be constructed. The coils were designed to have maximum sensitivity to conductivity change in the NBS bridge network. The agreement between the theoretical calculations and actual coil performance was in the 1-5% range. It was found that coils could be made which are linear to about 0.4% over a measurement range of 10% IACS. A number of coils (6) were made for use in the eddy current program.

Work is in progress to determine electrical conductivity in an absolute manner using eddy currents. If successful this work would determine any difference that exists between the ac and dc determination of conductivity. Theoretical studies and computer analysis are being used to determine the accuracy that can be expected in the measurement. The major problem in designing an absolute experiment is that test coil dimensions must be known with a high degree of accuracy and the coil must be geometrically uniform. Both the construction and measurement of a coil to small tolerances is very difficult. Thus, an experiment must be developed which is either independent of the coil dimensions or must contain two measurements in which the dimensions of the coil enter the coil equations in a different way. The approach being considered uses a coil with an intermeshed secondary. The coil will have an inner diameter of approximately 2.5 cm so that the coil can be used on a flat surface or with a metal rod inserted through the coil normal to the coil axis. The driving voltage will have a triangular shaped waveform. With this type of waveform the output voltage of the secondary will be a constant voltage except when the slope of the waveform changes sign. At this point an exponential decay takes place which is a function of the conductivity of the test piece. Several rough experiments indicated the feasibility of relating the decay rate to the conductivity with sufficient accuracy.

References

1. Free, G. M., "High Accuracy Conductivity Measurements in Non-ferrous Metals," ASTM (STP) to be published in 1980.

2. Dodd, C. V., Deeds, W. E., Luquirre, J. W., "Integral Solutions to Some Eddy Current Problems," International Journal of Nondestructive Testing, Vol. 1, pp. 29-90, 1969.

3. Swartzendruber, Free, Mordfin, et al., "Nondestructive Evaluation of Nonuniformities in 2219 Aluminum Alloy Plate-Relationship to Processing," Technical Report for NASA, April 1980.
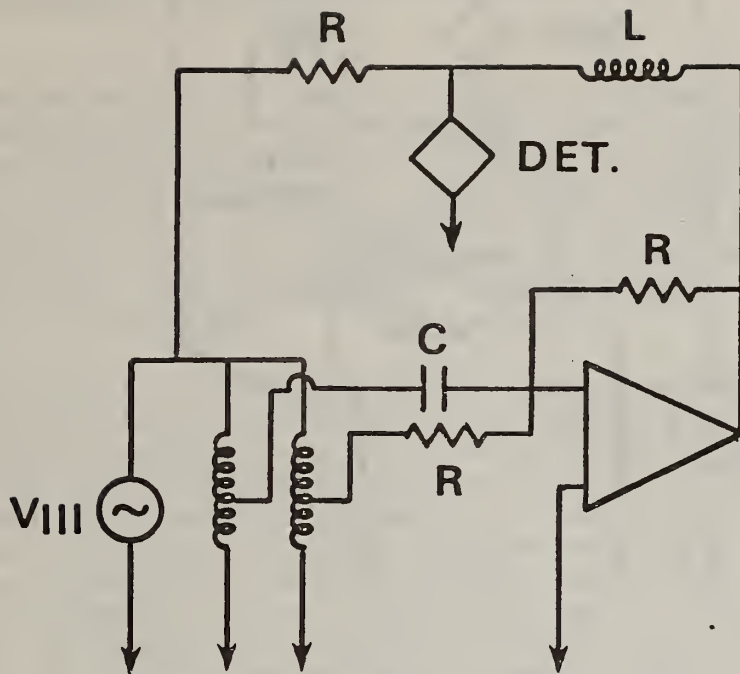
Fig. 11
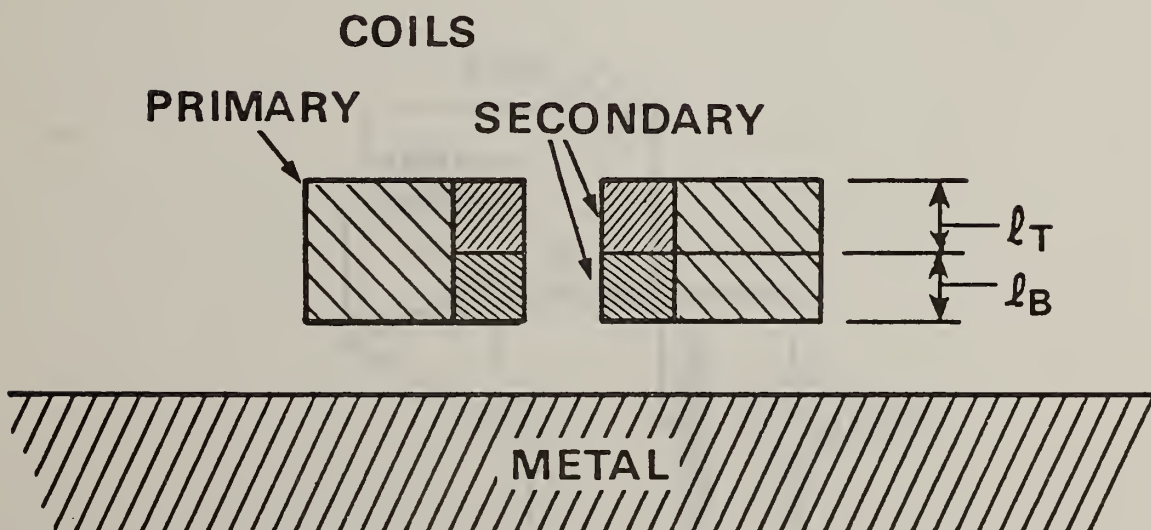
Fig. 12
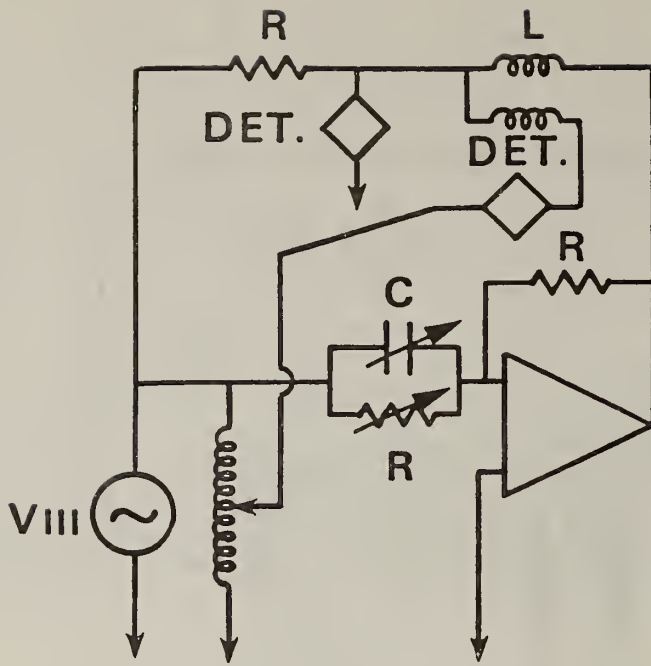
Fig. 13
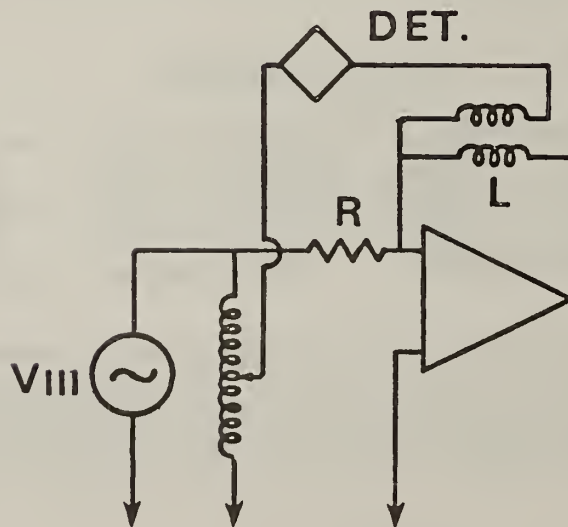
Fig. 14

14. Theoretical Modeling in Eddy Current NDE
    A. Kahn
    Ceramics, Glass and Solid State Science Division
    National Measurement Laboratory

We have examined methods for solving inversion problems by the analysis of
eddy current experimental data. If we limit the investigation to simple geometries,
such as a slab or a cylinder, it should be possible to use impedance measurement
as a function of frequency to construct a resistivity profile of the material by
examination. This inversion can be performed by a method of integral equations
(known as the Gelfand-Levitan and Marchenko methods in quantum theory) and by
another method of direct Fourier analysis. Both methods are now being explored
for computational practicability.

In the problem of crack diagnosis by eddy current methods, there have been
reports of wide variability in the signals from real and artificially produced
crack or other defect specimens. Part of this variability may arise from the
zone of plastic deformation in the vicinity of the crack. This plastic zone may
vary in dimensions and in material parameters, according to its method of pro-
duction. Initial calculations show that expected resistivity variations in the
plastic zone have little effect on eddy current signals, but that possible vari-
ations in magnetic permeability, as in stainless steels, could produce a sig-
nificant effect. A computational appraoch, based on the finite element method,
is being prepared for finding the eddy current distribution in the vicinity of a
crack with allowance for the variation of material parameters in the plastic zone.

15. Eddy Current Standards
    L. H. Bennett, J. R. Cuthill and L. J. Swartzendruber
    Metallurgy Division
    Center for Materials Science
    National Measurement Laboratory

    The specifications for a set of aluminum conductivity standards were
established. Four alloys were chosen to cover the conductivity range of 30
to 60 %IACS; 2024-T351 for a standard with nominal conductivity of 30 %IACS,
6061-T6 for a standard with nominal conductivity 40 %IACS, 2024-O for a stan-
dard with a nominal conductivity of 50 %IACS, and 1100-F for a standard with
a nominal conductivity of 60 %IACS. These alloys are to be milled into coupons
44.5mm x 44.5mm x 9.5mm from a plate 12.7mm thick. The surface finish on both
sides is specified to be better than 1 um RMS and each alloy is to be anodized
in a distinctive color. A set of 100 of each of these standards has been ordered
and received and turned over the the Electrical Measurements and Standards
Division for calibration. Work has been initiated on finding a suitable alloy
and specifications to cover conductivity standards in the range of 1 %IACS which
are required for use with titanium alloys, and to determine what standards would
be desirable for use with eddy current measurements on steel.

16. Development/Application of Deep Penetration Eddy Current Techniques
    J. B. Beal (Research Associate - Martin Marietta Aerospace Corp.)
    Electrical Measurements and Standards Division
    Center for Absolute Physical Quantities
    National Measurement Laboratory

     Material characteristics, weight savings, life-cycle requirements, improved
welding methods and cost controls make it imperative that latest advances in
nondestructive evaluation (NDE) be explored and implemented for examination of
the welds on the External Propellant Tank of the Space Shuttle Program (900 meters
total). Objective of the eight month assignment to NBS was to evaluate eddy
current techniques to detect and characterize surface and internal flaws within
constant thickness and tapered welds of 2219-T87 aluminum alloy (3.65 to 5.59 mm
thickness range). Welded, tapered test panels were prepared with simulated
flaws (slots and holes) of various dimensions and orientations. These panels
(and other aluminum plates with simulated flaws) were evaluated, with available
off-the-shelf low frequency eddy current equipment, to determine flaw detection
capabilities at various depths. Frequency, probe diameter, scan speed, lift-
off and sensitivity were evaluated to determine optimum factors for maximum
penetration.

     An ongoing effort during this assignment has been document retrieval from
the NBS Library on multifrequency and pulsed deep penetration eddy current
techniques. Document review and discussion with investigators indicates that
pulsed deep penetration methods offer promise. Eventual application of eddy
current deep penetration techniques of flaw detection will substantially simplify
and reduce the current material and labor-intensive NDE method of radiography
and penetrants.

     Results of equipment evaluations and recommendations for applications will
be published at the end of this year.

17. Nondestructive Evaluation of Nonuniformities in 2219 Aluminum Alloy
        Plate - Relationship to Processing/NASA
    L. J. Swartzendruber, L. K. Ives, W. J. Boettinger, S. R. Coriell,
    D. B. Ballard, D. E. Laughlin, R. B. Clough, F. S. Biancaniello,
    P. J. Blau, J. W. Cahn, and R. Mehrabian
    Metallurgy Division
    Center for Materials Science
    National Measurement Laboratory

    G. M. Free
    Electrical Measurements and Standards Division
    Center for Absolute Physical Quantities
    National Measurement Laboratory

The work was initiated at the National Bureau of Standards at the request
of the National Aeronautics and Space Administration. It was motivated by
serious government and aerospace industry concerns on the possibility that
substrength aluminum alloys may have been used in aircraft and space vehicle
structures. These concerns originated from the discovery of "soft" spots in
an anodized 2024-T851 aluminum alloy machined part in June 1979. The part
was machined from a $\sim$ 14 cm (5.5 inch) thick plate of the alloy produced at a
particular manufacturing plant. It was postulated that the "soft" spots were
due to improper processing of the plate. Furthermore, it was established that
the same plant was producing a variety of other aluminum alloy plates including
the 2219 aluminum alloy which was the subject of this investigation.

The aim of this work was to develop specific relationships between pro-
cessing variables used during ingot casting, working and heat treatment of the
alloy, and the resulting microstructures, properties and NDE responses. This
detailed blend of metallurgical examination of the alloy with its NDE response
is necessary not only to attack the specific problem at hand but also to gain a
fundamental knowledge of the features of metallurgical microstructures which
cause changes in NDE parameters. We have focused primarily on eddy current
testing (conductivity) for the present but initial explorations into the use of
ultrasonic measurements (wave speed; attenuation) have also been conducted.
Work in this program is divided into five areas:

1. Studies on as-received plate of 2219 aluminum alloy - This is motivated
by the realization that the properties vary across plate thickness. These vari-
ations can have different effects on various NDE techniques.

2. Solidification-Segregation Studies - Part of the variation in
properties across finished alloy plate is caused by segregation of the alloy
components (Cu, Mn) during ingot casting.

3. Determination of time-temperature transformation diagrams (C-curves)
and the relationship between mechanical properties and conductivity - Samples
produced during various thermomechanical treatment have a wide range of mechan-
ical properties (hardness, yield strength, tensile strength) and conductivity.

4.   Electron microscopy studies done on the wide range of metallurgical microstructures produced - Extremely fine scale (<100 A) particles are responsible for the strength of aluminum alloys and contribute to associated changes in conductivity.

5.   Predictions of heat flow conditions during malfunctions of the commercial process, namely slow quenching from the solutionizing temperature; and predictions using experimentally determined C-curves of the resultant mechanical property degradations.

Conclusions reached in the study are listed below:

1.   As-received Plate

°   Moderate variations in composition, hardness, electrical conductivity and mechanical properties were noted across the thickness of a 12.7 cm (5 inch) thick 2219 aluminum alloy plate. Composition variations, which influence measured conductivities, can be traced to the original ingot. The variations in hardness and tensile properties are mainly due to changes in cooling rate across the plate during the quench and are probably influenced by inhomogeneous mechanical deformation during processing.

2.   Solidification Segregation Studies

°   Macrosegregation of copper in Direct Chill (DC) cast ingots of 2219 aluminum alloy cannot be completely eliminated by chill face scalping and subsequent thermomechanical treatment. Macrosegregation does remain in the finished plate product. However, good scalping practice should limit copper content to above the solid solubility limit with no deterioration in mechanical properties.

°   Elements with equilibrium partition coefficients less than unity exhibit macrosegregation similar to copper while those with coefficients greater than unity are opposite to copper. The magnitude of deviations from the nominal are related to the deviation of the coefficient from unity.

°   The major phases present in cast 2219 aluminum alloy in this study have been determined by electron microprobe analysis and electron diffraction. They are α-aluminum solid solution, θ-$CuAl_2$ and Cu_2FeAl_7. These phases are also present in the heat treated finished plate product.

°   Predictable macrosegregation has been obtained in laboratory ingots of 2219 aluminum alloy. Both positive and negative segregation similar to DC cast ingots are observed and are caused by the flow of segregated inter-dendritic liquid (Fig. 15).

°   Electrical conductivity determined by eddy current measurements of cast 2219 aluminum alloy is inversely related to copper content. This fact complicates the relationship of conductivity to mechanical properties used for nondestructive evaluation of the finished plate product. (Fig. 15)

47

° Surface hardness and eddy current measurements may be very sensitive to scalping depth in their ability to evaluate the condition of finished alloy plate.

° Hardness, yield strength and ultimate tensile strength of heat treated 2219 aluminum alloys decrease significantly when the average copper content drops below approximately 5.5 wt%.

3. C-Curve Determination and Relationship between Mechanical Properties and Conductivity

° No significant difference in either strength or hardness was detected between alloys stretched between 5 and 7% permanent strain during the thermomechanical processing of 2219 aluminum alloy.

° The functional form developed by Cahn and used previously by Staley for 7075-T6 and 6061-T6 aluminum alloy was found to give an adequate representation of the C curves for 2219-T87* if the form was modified to include a minimum value for each property in question. Some deficiency in this form at the highest and lowest temperatures was noted.

° An efficient computer program was developed for using time-temperature and property measurement data to establish C curve parameters.

° For each heat treatment sequence, C curves were determined for hardness, yield strength, tensile strength and electrical conductivity. These C curves can be used to determine the correlations between these properties. C curves could not be developed for elongation, probably because this property is more sensitive to grain size and other factors.

° A small but significant difference was found between the C curves for sequence A (direct transfer to salt bath) and sequence B (water quench and reheat in salt bath) type quenches. For a given salt bath time and temperature, sequence B quenches resulted in a greater degradation of mechanical properties.

° The scatter in hardness and conductivity was found to be large. This scatter can be expected to complicate NDE measurements and should be properly taken into account when establishing NDE procedures and specifications (Figs.16 and 17).

° There is a great need for standardizing conductivity measurements in order to bring about better inter-laboratory agreement.

° 2219 aluminum alloy is not as quench sensitive as some of the other high strength aluminum alloys such as 7050.

4.   Electron Microscopy Studies

°   The age-hardening response of 2219-T87* and T851 is determined princi-
    pally by the formation of θ' precipitates with some contribution by θ''
    precipitates.

°   An abnormal quench treatment which results in dwell times significant
    with respect to the C curves leads to the heterogeneous nucleation and
    rapid growth of θ and θ'' precipitates.

°   The nucleation and growth behavior of the θ and θ' precipitates formed
    during an abnormal quench depend on the pre-existing microstructural
    state of the material and on the thermal "path."

°   The large incoherent θ and θ' precipitates formed during an abnormal
    quench consume copper available from the matrix and thereby reduce the
    concentration of θ' and θ'' precipitates that contribute to precipitation
    hardening during subsequent aging.

°   The C curves are a measure of the concentration of large θ and θ'
    precipitates formed during the quench treatment.

5.   Heat Flow Calculations - Property Predictions

°   Calculated plate properties, e.g., yield strength and hardness, decrease
    monotonically with increasing distance from surface to centerline of a
    plate for fixed heat transfer conditions.

°   For symmetric cooling and sequence (a) C curves, the calculated minimum
    yield strength (at the center of the plate) is 54.9, 53.7, and 51.8 ksi
    for 2.54, 7.62 and 12.7 cm (1, 3, and 5 inch) thick plates, respectively.

°   For asymmetric cooling and sequence (A) C curves, the calculated minimum
    yield strength (at the botton surface of the plate) is 54.4, 50.7 and
    45.9 ksi for 2.54, 7.62 and 12.7 cm (1, 3, and 5 inch) thick plates,
    respectively.

°   For plate thicknesses greater than 2.54 cm, sequence (b) C curves yield
    lower properties values than sequence (A) C curves. For example, for
    asymmetric cooling and sequence (B) C curves the calculated minimum yield
    strength is 54.6, 48.0, and 41.5 ksi for 2.54, 7.62 and 12.7 cm (1, 3, and
    5 inch) thick plates, respectively.

°   Interrupted (abnormal) cooling, in which the heat transfer coefficient at
    the bottom surface changes from the same value as at the top surface to a
    zero value, can result in lower property values than found for asymmetric
    cooling. For example, for a 12.7 cm (5 inch) thick plate and sequence (B)
    C curves interrupted cooling yields a minimum yield strength of 39.0 ksi
    compared with 41.5 ksi for asymmetric cooling.

49

Work in this program will continue in three general areas. A round robin of conductivity measurements at various laboratories has been conducted on NBS prepared 2219 aluminum alloys in various heat-treated conditions. This work will lead to a set of aluminum alloy conductivity standards. Second, controlled ultrasonic measurements are being planned for pure Al-Cu precipitation hardened alloys. Thirdly, a program has been initiated to investigate the relationship of processing to NDE response of 2024 aluminum alloy. This alloy appears to be more sensitive to heat-treating practice than 2219 aluminum alloy.
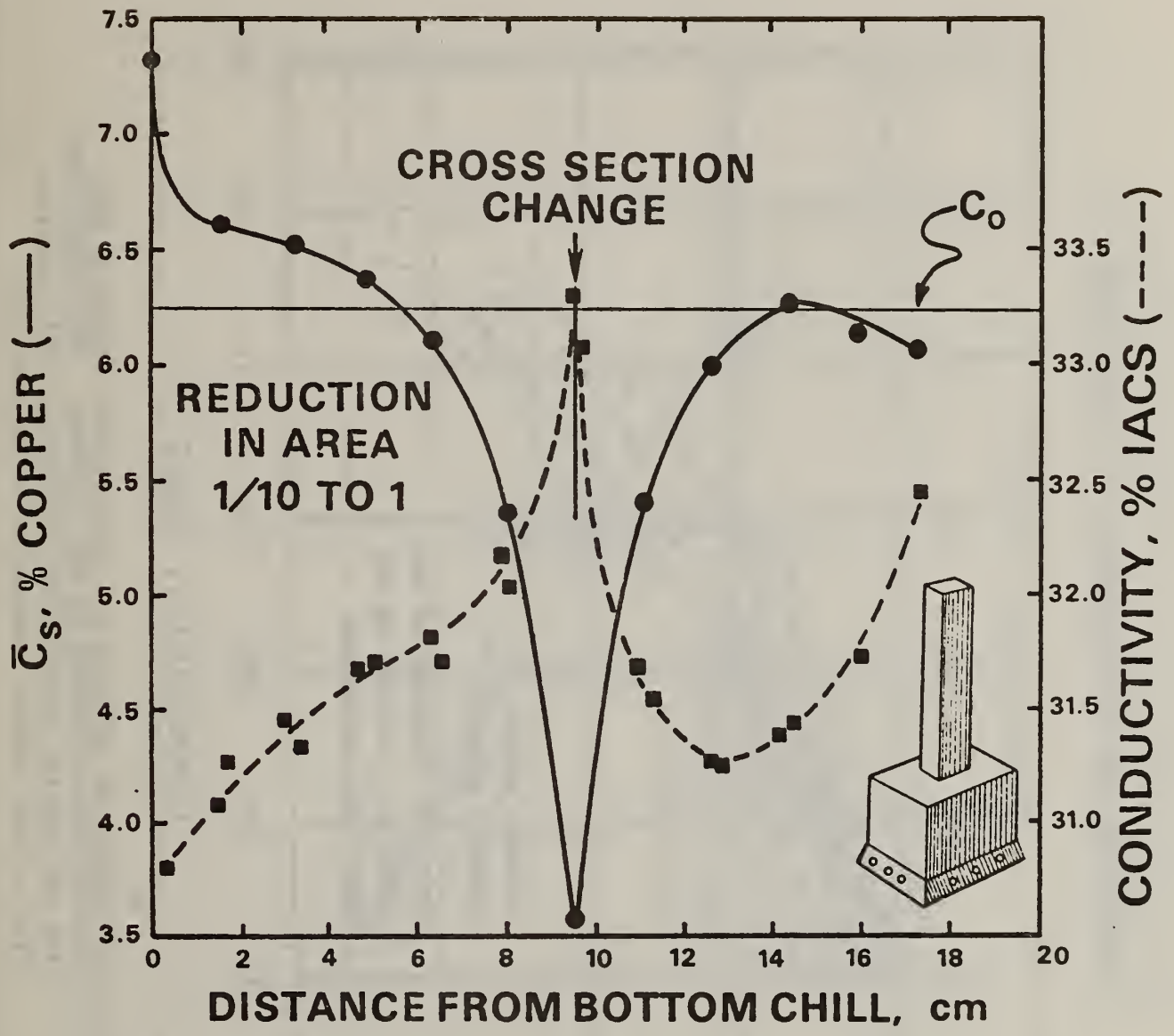
Figure 15   Average copper content and electrical conductivity versus distance from the bottom chill, in a unidirectionally solidified reduced cross section laboratory ingot of 2219 aluminum alloy.

Figure 16   Comparison of hardness vs. conductivity data with the correlations predicted by the C curves. The dashed lines are the scatter band ($\sim$ 95% confidence level) obtained from a least squares quadratic fit to the data.

Figure 17 Comparison of tensile strength vs. conductivity data with the correlations predicted by the C curves. The dashed lines are the scatter band (∿ 95% confidence level) obtained from a least squares quadratic fit to the data.

18. Electrochemical Noise
J. Kruger
Chemical Stability and Corrosion Division
National Measurement Laboratory

Measurements on two electrochemical systems, copper in copper sulfate and aluminum in boric acid/tetraborate buffer, have been carried out by recording the amplitude spectrum of the fluctuations in the current density. For these measurements, a low-noise potentiostat developed and built at NBS was employed. In the case of copper, the current spectra are found to be the deterministic response of the electrode to the noise voltage generated by the potentiostat. The electrode characteristics for charge-transfer and for diffusion could be obtained from the impedance plots derived from the measurements when the level of the applied signal was of the order of $10^{-7}V$. In the case of aluminum, the deterministic response observed in the absence of pitting gave way to random flucuations in the current in conditions leading to pitting. It is shown that the onset of pit information can be detected from noise measurements.

Random fluctuations in the passive current of electrodes under potentiostatic conditions have been measured also on a Fe-Cr-Ni alloy, both in the amorphous and in the crystalline state, in sulfuric acid. The onset of pitting can be detected by the large increase in current noise. The noise level is different in the amorphous and crystalline Fe-Cr-Ni alloy, indicating that the breakdown of the passive film differs in the two conditions.

The difference in behavior upon anodic polarization is shown in Fig. 18. Spectra 1 and 2 were taken on the amorphous alloy. Even polarizing at 1.59 V, where transpassive dissolution begins to occur and the dc current density increases more than 20 times the fluctuations are small. The crystalline alloy, on the contrary, shows the characteristics of localized attack: an increase in potential of 70 mV from 1.37 V to 1.44 V causes only a modest increase in the dc current density, from 130 to 200 $\mu A/cm^2$, but has a spectacular effect in the noise level as shown by spectra 3 and 4 of Fig. 18.

The remarkable difference in the noise spectra of the amorphous and crystallized alloy clearly show that the latter has a much greater tendency to localized attack, no doubt because of structural inhomogenity of the passive film. Moreover, the noise measurements have revealed that the superior resistance to breakdown of the passive film in the amorphous alloy is not a result of the static properties of this film because the overall current densities observed did not differ greatly wehn comparing the crystallized and amorphous alloys.
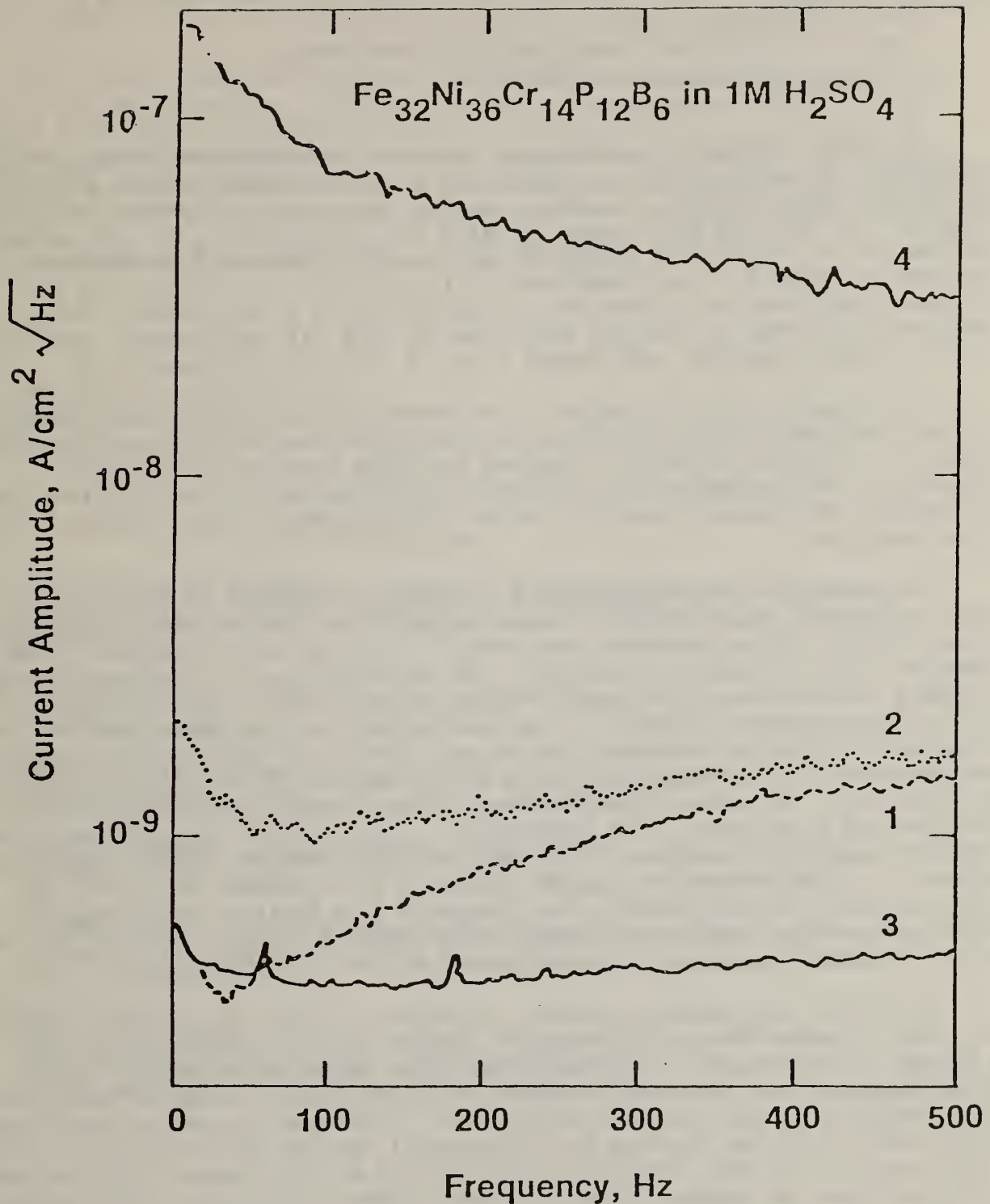
Fig. 18 Current spectra for amorphous and crystalline $Fe_{32}Ni_{36}Cr_{14}P_{12}B_6$ in 1 M H_2SO_4. Amorphous: 1) E=1.14 V; i_{dc}=1.5 · 10^{-4} A/cm²; 2) E=1.59; i_{dc}=3.5 · 10^{-3} A/cm². Crystalline: 3) E=1.37 V; i_{dc}-1.3 · 10^{-4} A/cm²; 4) E=1.44 V; i_{dc}=2.0 · 10^{-4} A/cm².
Reference: NHE. Averages over 256 spectra.

19. Leak Rate Reference Standards
    S. Ruthberg
    Electron Devices Division
    Center for Electronics and Electrical Engineering
    National Engineering Laboratory

Leak rate reference standards are used for the calibration of measurement apparatus, for determining the sensitivity of a measurement procedure as applied to a given system, and for providing precise flow-rates for control purposes. Commercially supplied units range in value from approximately 10^{-2} atm·cm^3/s to 10^{-9} atm·cm^3/s* with stated accuracies of 10 - 20%, although interlaboratory comparison has shown a three sigma uncertainty of $\pm$ 0.33 in the logarithm of standard leak rate so that measured values differ by up to a factor of four.[1] Yet some standards for critical usage specify leak rate measurement uncertainty of not greater than 20%, and leakage rates of $<10^{-10}$ are now specified.

The objective of this project is to improve the uniformity and agreement in leak rate measurements through more accurate reference standards. The first phase of the effort is for the standard leak rate range of 1 to 1 x 10^{-5} atm·cm^3/s. Within-laboratory precision is under evaluation for capillary leaks as measured by pressure rate-of-rise (or fall) apparatus, and uncertainties are being analyzed.

The principle of the measurement procedure is embodied in Figure 19. A leak specimen is inserted into a vacuum connector within the small chamber LC. A gas pressure of one standard atmosphere ** is established in chamber I and admitted into LC around the specimen. The resultant gas flow through the leak causes a pressure rise in chamber II which is initially at zero pressure. If the upstream pressure (chamber I) remains constant and the downstream pressure (chamber II) does not increase significantly from zero, the volume of chamber II and the rate-of-rise in pressure are a direct measure of the standard leak rate. Alternatively, the roles of the chambers can be reversed and a rate-of-fall in pressure can be measured. The standard leak rate, then, is measured under very specific conditions; however, if the mode of flow (laminar viscous, transition, molecular) is determined and remains unchanged with pressure excursion, the leak rate might be calculated by an integrated flow equation with pressure points more widely spaced for greater measurements accuracy. This latter, though, requires careful experimental investigation of the flow mechanism.

The actual gas handling system is depicted in Figure 20; standard symbols are used to indicated the components.[2] Chamber II and connecting lines have a volume of approximately 2l as measured by gas expansion techniques for an uncertainty of less than 0.2%; chamber I and lines have a volume of approximately 9l as measured to about the same uncertainty. The capacitance-diaphragm gauges (CD) connected to the chambers are differential sensing types with sensitivities of one part in 100,000. Reference arms are held at high vacuum. The low pressure instrument on chamber II is calibrated against a precision liquid nanometer[3] and linear ionization gauge[4] with pressure points generated within the system.[5] The high pressure instrument is calibrated against a reference barometer. A second vacuum system is used to provide the reference vacuum for the capacitance-diaphragm gauges and reference nanometers.

Capillary leaks in the range 10^{-6} to 1 atm·cm^3/s have been fabricated in glass, and entrance aperatures ranged from ∿1μm to ∿25μm in diameter. Specimens must be handled carefully to avoid contamination (dust, moisture).

Leak bodies have been measured repeatedly to determine measurements precision and leak stability. Dispersion within a measurement series has been about 2 1/2%, while repeatability over a 1 year period has been within ∿5%. Capillary leaks for this range generally evidence laminar flow[6], and expected uncertainty as provided by temperature and pressure variations is ∿1%. Additional imprecision is now due to operator manipulation and pressure readout procedures.

Flow analysis and stability measurements continue.

* 1 atm·cm^3/s = 0.1013 Pa·m^3/s.

** 1 std·atm. = 1.01325 x 10^5 Pa.

References

1. "Calibration of Helium Leak Detectors by Use of Secondary Standards," ASTM Designation F78-71, 1979 Annual book of ASTM Standards, Part 43, pp. 371-374.

2. Graphic Symbols in Vacuum Technology, Am. Vac. Soc. Standard 7.1 - 1966. J. Vac. Sci. Tech. 4, 139-142 (1967).

3. Micrometer U-Tube Manometers for Medium-Vacuum Measurement, A. M. Thomas and J. L. Cross, J. Vac. Sci. Tech 4, 1-5 (1967).

4. "The Measurement of Conductance to Free Molecular Flow by Substitution Procedures," S. Ruthberg, J. Vac. Sci. Tech. 9, 1457-1469 (1972).

5. "Calibration to High Precision in the Medium Vacuum Range with Stable Environments and Micromanometers," S. Ruthberg, J. Vac. Sci. Tech. 6, 401-412 (1969).

6. "Flow Through Micro Openings," W. H. Hedley et al., Final Report. U.S. Army Biological Center Contr. DA 18064-AMC-563(H). January 1968. Available from Defense Documentation Center, Alexandria, VA AD844907).
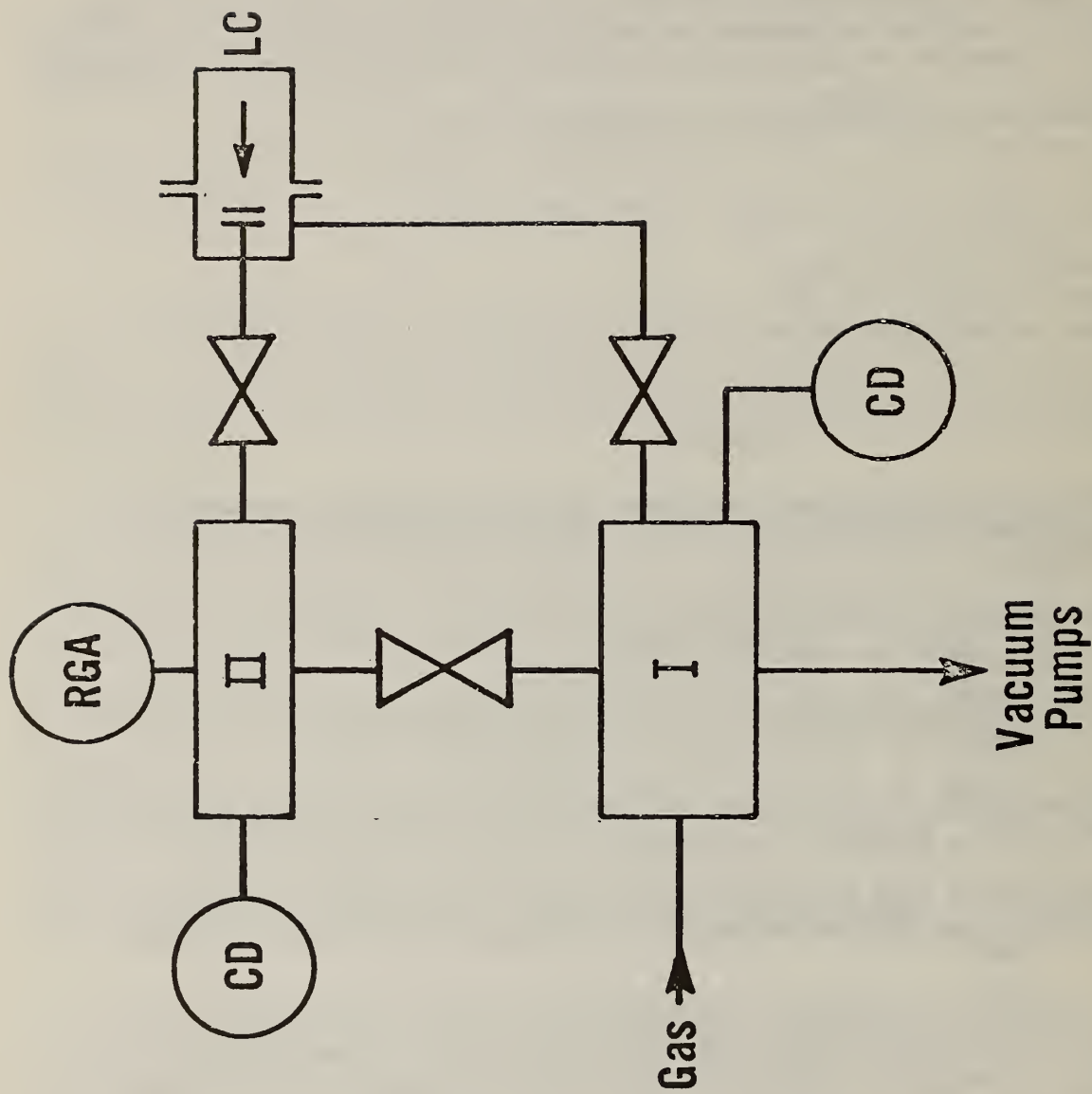
Fig. 19 Basic apparatus, rate-of-rise leak measurement. I, II-high vacuum chambers. LC-leak specimen holder chamber with vacuum connect. CD-capacitance-diaphragm gauges. RGA-residual gas analyzer. One standard atmosphere in I, pressure rate-of-rise in II.
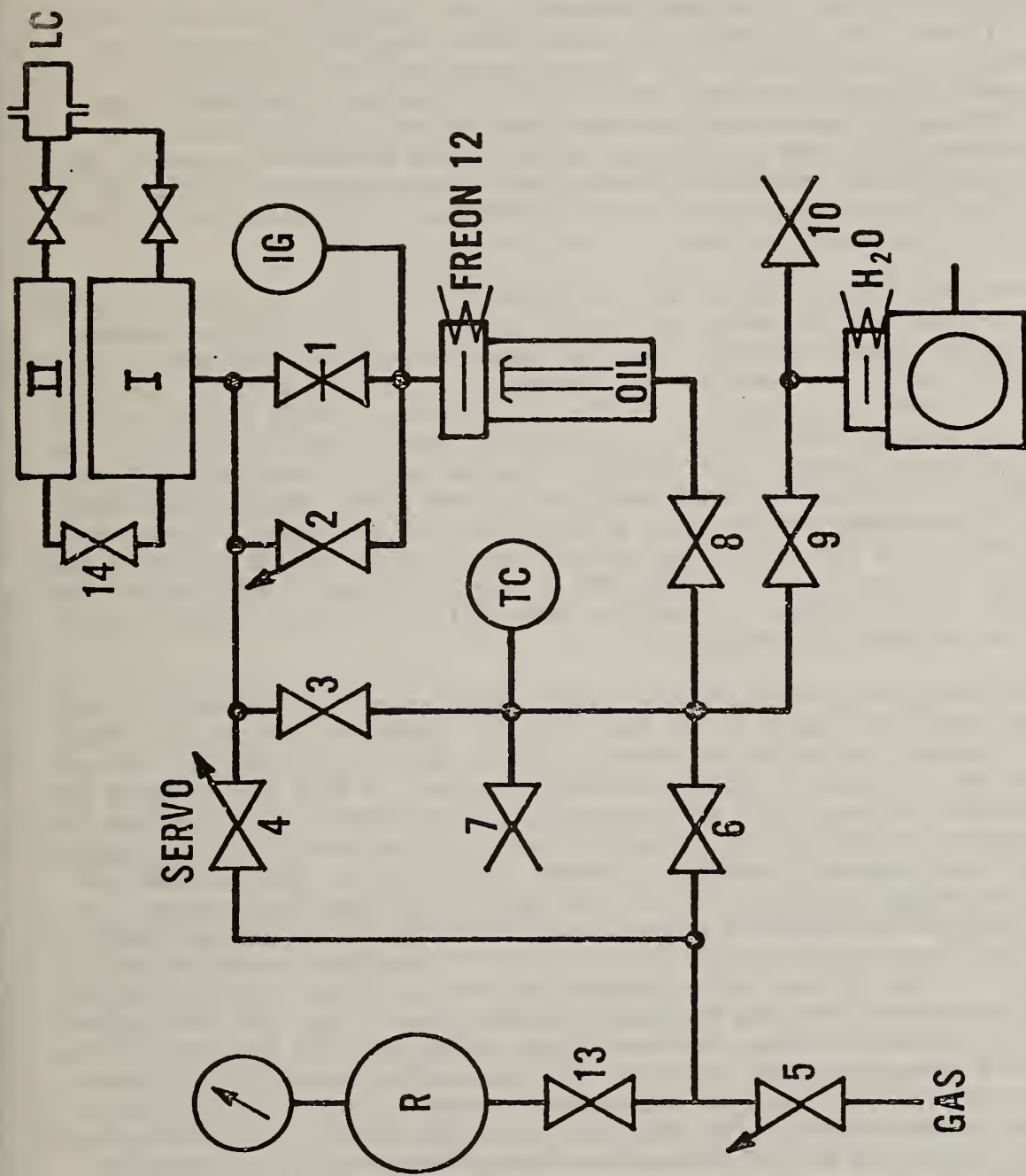
Fig. 20 Vacuum-gas control circuit.

20. Magnetic Measurements
   L. Swartzendruber
   Metallurgy Division
   National Measurement Laboratory

One of the most extensively used techniques in magnetic NDE is the magnetic particle method. The application of this method is currently guided by empirical rules for the amount of magnetization required to achieve the desired results. Also, there is no acceptable method for independently testing magnetic inks. The first steps in placing magnetic particle inspection on a more quantitative and reporducible basis are an understanding of how the leakage field from a defect is influenced by the defect geometry and level of magnetization reached by the material, and a detailed description of the influence of the leakage field on the formation of an indication by the magnetic ink.

We have previously investigated the leakage fields from a steel ring with artificial defects introduced by drilling a series of small holes at varying depths below the sample surface. The ring geometry used was the same as specified in MIL-E-6868E and in the new ASTM recommended practice for magnetic particle inspection. It was found that all residual and active leakage fields could be closely approximated using a linear dipole model provided that an apparent depth, less than the actual depth of the defect below the surface, and an equivalent dipole strength, greater than that predicted by the linear theory, were used. One of the disadvantages of the ring geometry was that the magnetization level actually achieved in the steel ring varied with the defect depth and could not be monitored. It was also found that the artificial defects specified for the ring were too close together in that the leakage field from one defect was distorted by its neighboring defects.

To overcome these difficulties a sample containing artifical defects with the geometry shown in Figure 21 was constructed. Using the pickup coil shown, the level of magnetization in the material can be monitored while the leakage fields from the artifical defects are being measured. A Hall effect probe was used to measure the tangential and perpendicular components of the leakage field at five different points on the hysterisis curve of the sample. These leakage fields were least squares fitted to a linear dipole model. Typical data and fits are illustrated in Figure 22. As for the case of the ring geometry, it was found that the residual and active leakage fields could be closely approximated using a linear dipole model with an apparent depth and an equivalent dipole strength. Both the equivalent depths and the equivalent dipole strengths were roughly the same as those found for the tool steel ring. An interesting feature of the results on the sample of Figure 21 is that the magnitude of the leakage field increases almost linearly with the applied magnetic field even after the material is driven into saturation. Further studies are planned on other defect geometries including very narrow cracks and slots of various depths in a sample similar to that of Figure 21. Using these results it should be possible to devise more valid tests for the quality of magnetic inks and to specify more precisely the level of magnetization required to detect defects of a given geometry.
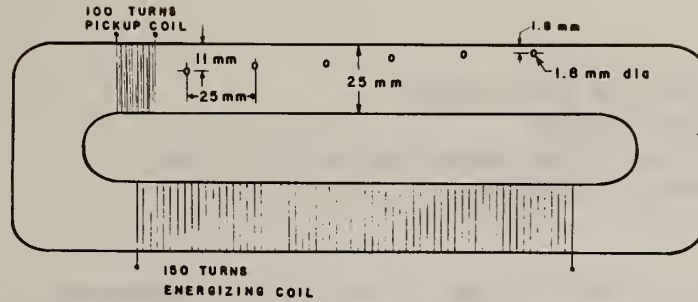
Fig. 21. Test yoke used for measuring leakage fields from
artificial defects. The entire yoke is 25 mm
wide. The ariticial defects are six holes drilled
as shown. The material is a low carbon steel. A
150 turn coil is used to magnetize the yoke and a
100 turn pickup coil is used to determine the
magnetization level reached inside the yoke.
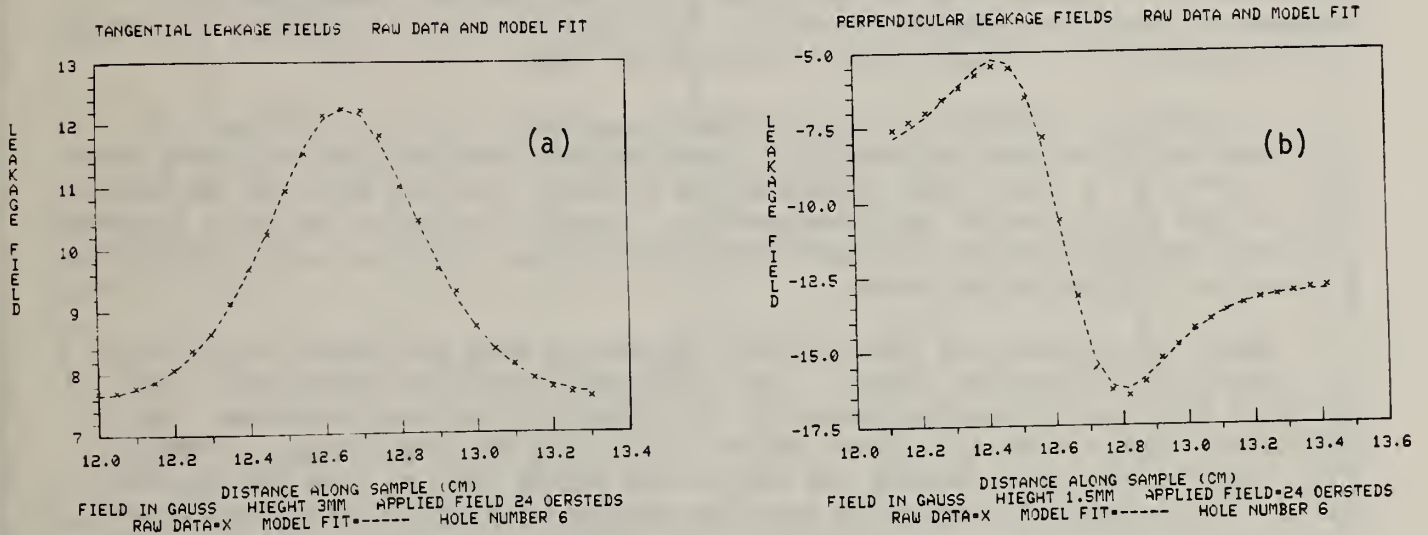
Fig. 22. Leakage fields measured from the yoke shown in
Figure 1 compared with the field calculated from
a magnetic dipole model. (a) Tangential field
with an applied field of 24 oersteds. (b) Per-
pendicular field with an applied field of 24 oersteds.
The crosses are data points and the dashed line is
a least squares fit to a linear dipole model.

21. Optical Nondestructive Evaluation
G. S. White and A. Feldman
Cermanics, Glass and Solid State Science Division
National Measurement Laboratory

Optical scattering from defects is an area of importance in Nondestructive Evaluation. It is the purpose of our research to determine whether quantitative data, such as defect dimensions, is obtainable from optical scattering data. For this purpose, we have been performing both measurements and model calculations of radiation scattered from shallow grooves in metallic surfaces and have compared theory with experiment.

In the experiments, chopped 10.6μm radiation from a 3 watt CO_2 laser was incident normal to a specimen containing a shallow rectangular groove. The specimens were prepared by scribing of grooves into an aluminum coating that had been evaporated onto glass optical flats. Two sets of specimens were used: one set of specimens was used as scribed; in the other set, the specimens were overcoated with an additional thin layer of aluminum. The groove dimensions in both specimen sets were nominally 10, 20 and 50μm wide by 0.5μm deep. Figure 23 shows the measured profile of a 50μm uncoated groove.

The use of 10.6μm has several advantages: the effect on scattering of surface microirregularities is minimized; the fabrication of well defined grooves of dimensions comparable to the wavelength is facilitated; the far field approximation in the model calculations can be used.

A schematic diagram of the measurement apparatus is shown in Figure 24. Scattered radiation was measured by a pyroelectric detector that was swung about the specimen in a plane that contained the incident beam and that was perpendicular to the groove in the specimen surface. Careful attention was paid to system alignment because certain alignment errors were shown to cause severe distortion of expected scattering patterns.

Model calculations of the expected scattering were performed on the basis of Fraunhofer diffraction theory. The following assumptions were made: the incident beam had a Gaussian intensity distribution; the beam width was significantly larger than the groove width; scattering was due to specular reflection from the specimen surface and the groove bottom but not from the groove walls. The resultant scattering function obtained was the diffraction pattern of a uniformly illuminated slit with the intensity uniformly modulated by a factor dependent on the depth of the groove. Figure 25 shows a comparison between experimentally determined scattering and an empirical fit to the data of a single slit diffraction pattern. The points denote the measured scattering intensity of a nominal 50μm wide uncoated groove as a function of scattering angle. The solid curve is the diffraction pattern of a 52μm wide slit. Agreement appears to be quite good. Comparable results have been obtained with some of the other grooves; however, with certain grooves, large discrepancies were observed with are attributed to groove irregularities.

Further work is planned to compare scattering from deep groove with theory and also to study the effect of polarization on the scattering function.
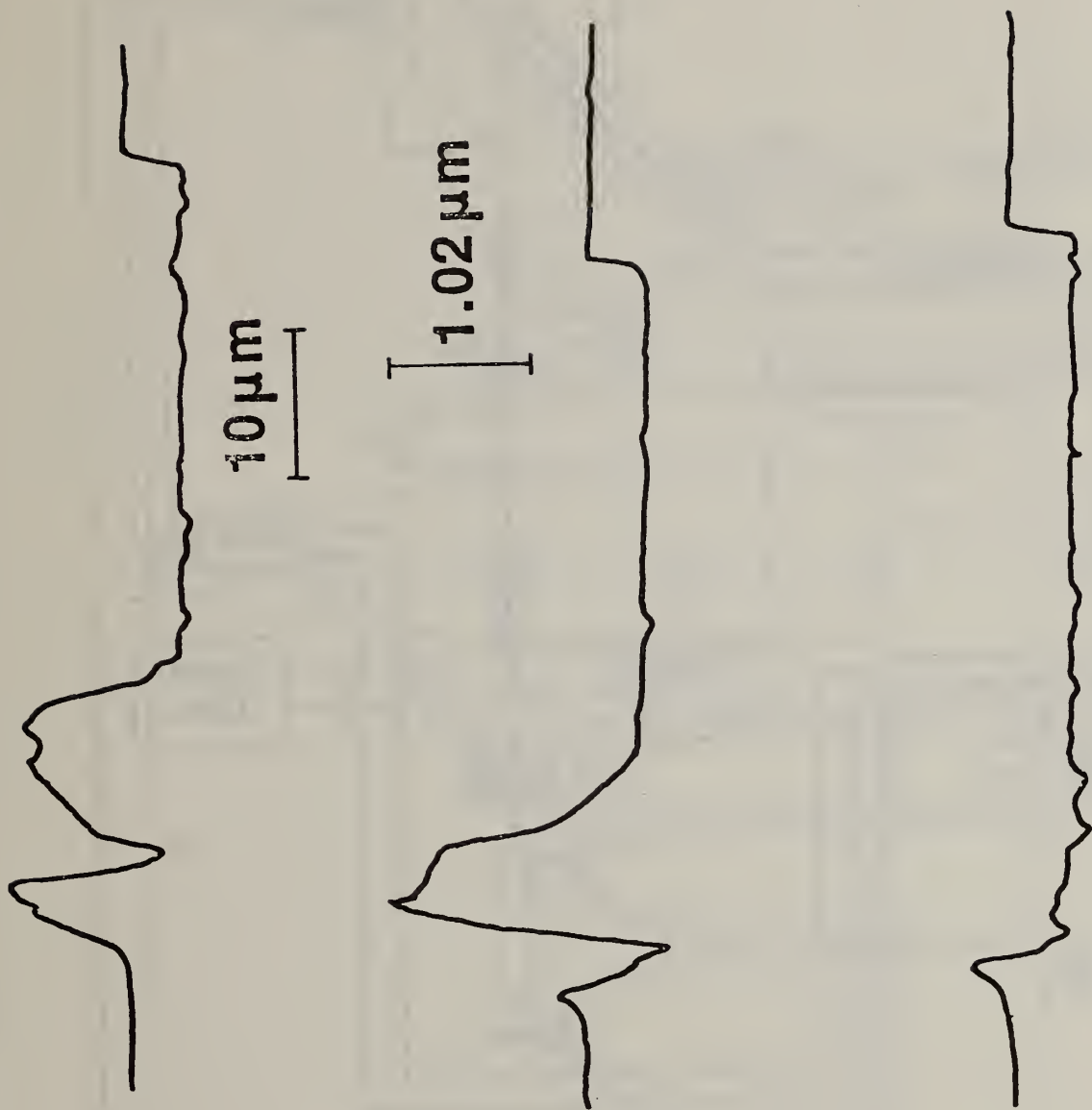
Figure 23. Upper, middle, and lower cross sections of uncoated 50μm groove measured by diamond stylus profilimeter.

10μm

1.02 μm
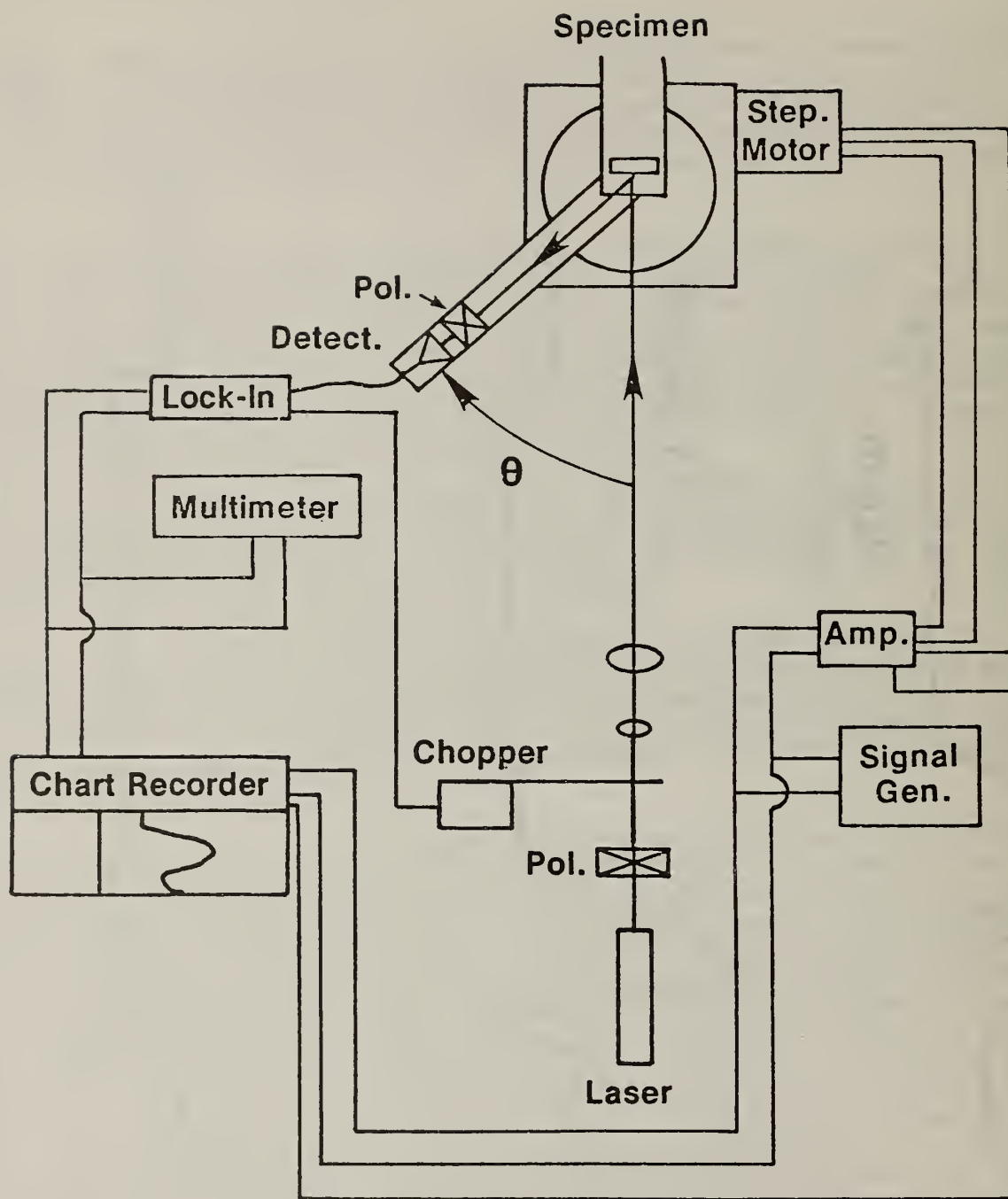
Figure 24. Schematic diagram of scattering apparatus.
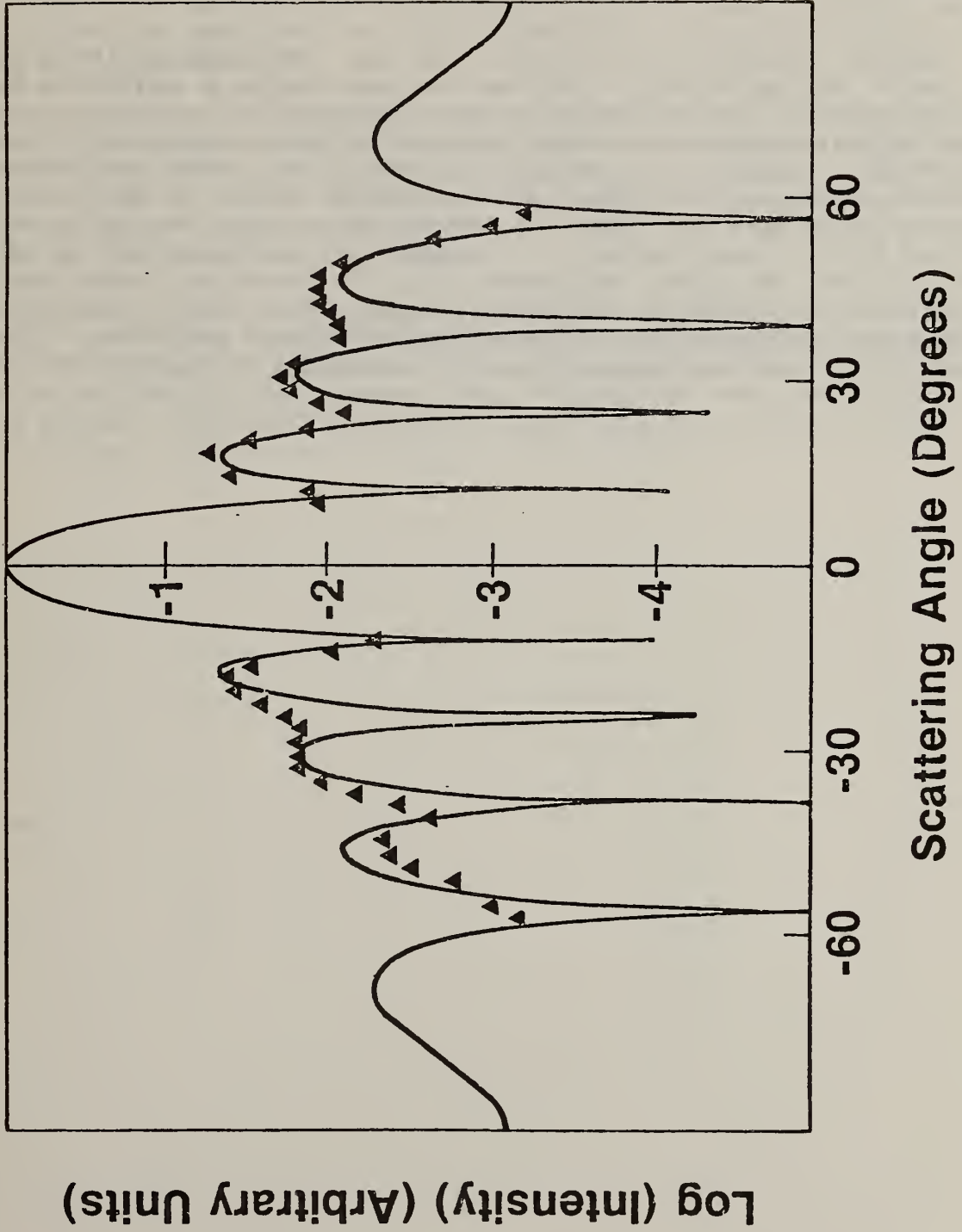
Figure 25. Logarithm of observed scattering (triangles) from uncoated 50μm wide specimen superimposed on the calculated logarithm of n (solid) ideal single slit diffraction pattern from a 52μm wide slit.

22. Quantitative Holographic NDE

C. M. Vest
University of Michigan

G. Birnbaum
Office of Nondestructive Evaluation
National Measurement Laboratory

Although holographic interferometry has been frequently applied to the solution of problems in NDE, it has thus far been used as a qualitative method of flaw detection. An experiment has been planned and is currently in progress to make an initial assessment of the potential of optical holography for quantitative NDE. To this end, a pressurized cylinder with several end plates containing different flat bottom holes has been designed. The deflection of these end plates when the cylinder is pressurized has been computed by the method of finite element analysis. Holographic interferograms will be taken of the distorted end plates and compared with the theoretical predictions. Further work may include the quantitative study of more complex geometries. Should optical holography be used more quantitatively in the future, it is felt that this experiment may help lay the development of appropriate standards.

23. Liquid Penetrant Test Blocks

J. Young and F. Ogburn
Ceramics, Glass and Solid State Science Division
National Measurement Laboratory

Liquid penetrants are frequently used to detect minute cracks in various metals. There is a need for test blocks with cracks of known widths that would be used to test the sensitivity of a liquid penetrant and the sensitivity of a penetrant test procedure.

A technique for fabricating a test block with isolated cracks has been developed. In principle, a nickel panel is plated with a layer of copper the thickness of which is the width of the desired crack. The copper is over plated with a thick layer of nickel. A polished cross section of the composite will reveal a thin copper line between two bands of nickel. When copper is etched out, a "crack" is formed; see Figure 26.

During the past year many penetrant test blocks have been prepared with crack widths of 0.2-2μm. Thirty of these have been sent to various individuals and groups for evaluation. In general, responses were favorable; many responses included suggestions for improvements. These suggestions were considered and many were adopted. The modified penetrant sensitivity crack plate will soon ben available as an SRM.

PLATED PENETRANT CRACK PLATE

Ni

Cu

0.1μm
0.5μm
2μm
4μm

20 cm

20 cm
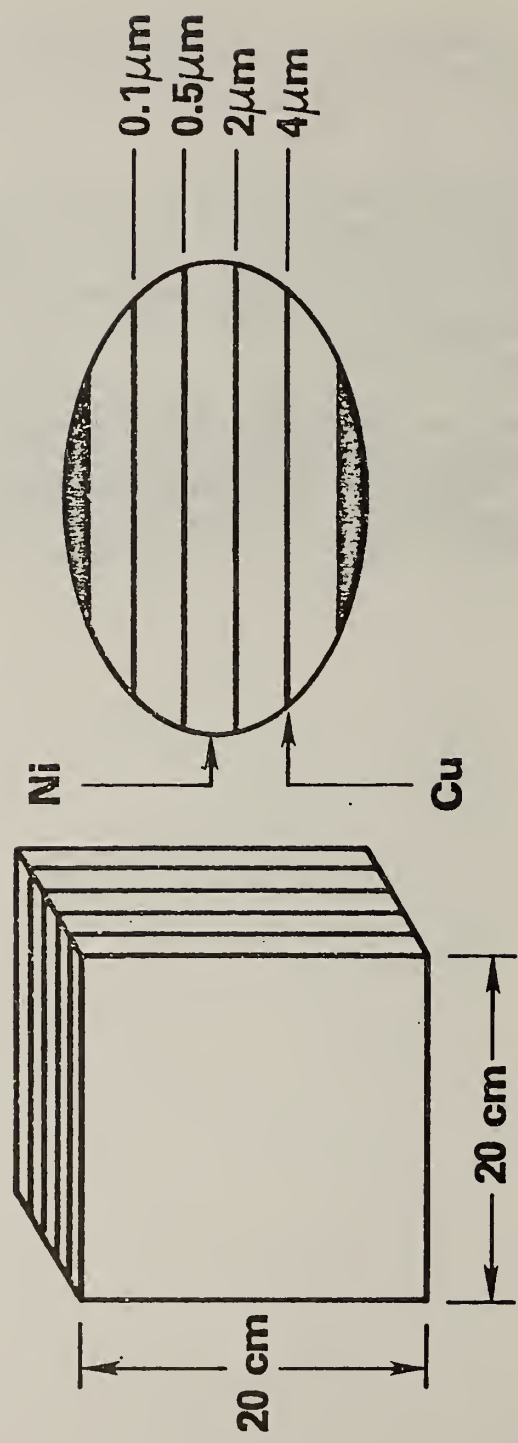
Figure 26. Diagram of penetrant sensitivity crack plate.

24. Doppler-Broadened Positron Annihilation Lineshape for Detection of
        Defects in Materials
     R. C. Reno and L. J. Swartzendruber
     Metallurgy Division
     National Measurement Laboratory

Positrons that annihilate in a metal produce gamma rays whose energy
distributions can be explained in terms of a Doppler shift caused by motion
of electrons. When defects are present in the metal, they attract and trap
positrons, and alter the Doppler shifts. A measurement of doppler-broadened
annihilation lineshapes thus gives information on the defect nature of materials.
Both the annihilation process and the method of detection leave the sample in-
tact, so the technique is extremely useful for the nondestructive evaluation
of materials.

Doppler-broadened lineshape measurements are performed by placing a
positron source in contact with the sample to be studied (see Fig. 27). Positrons
enter the sample, slow down to thermal energies, and then annihilate with elec-
trons. Each annihilation produces two gamma rays with a total energy equal to
the rest mass energy of the positron-electron pair (1022 keV). The distribution
of energy between the two gamma rays depends upon the electronic and defect
structure of the sample, and is measured with a high resolution solid state
detector-multichannel analyzer system. A lineshape parameter, S, is defined
which is a measure of the inverse width of the distribution.

The addition of a small number of defects to a metal will cause a signifi-
cant change in the lineshape parameter, and it is this sensitivity that is used
to observe changes in defect concentration and type. We have used this tech-
nique to study defects in cold worked titanium and, more recently, have begun
to study precipitation hardening in aluminum alloys. In the latter study, some
results of which are shown in Figure 28, we observe significant changes in S
parameter as microprecipitates form during ageing.
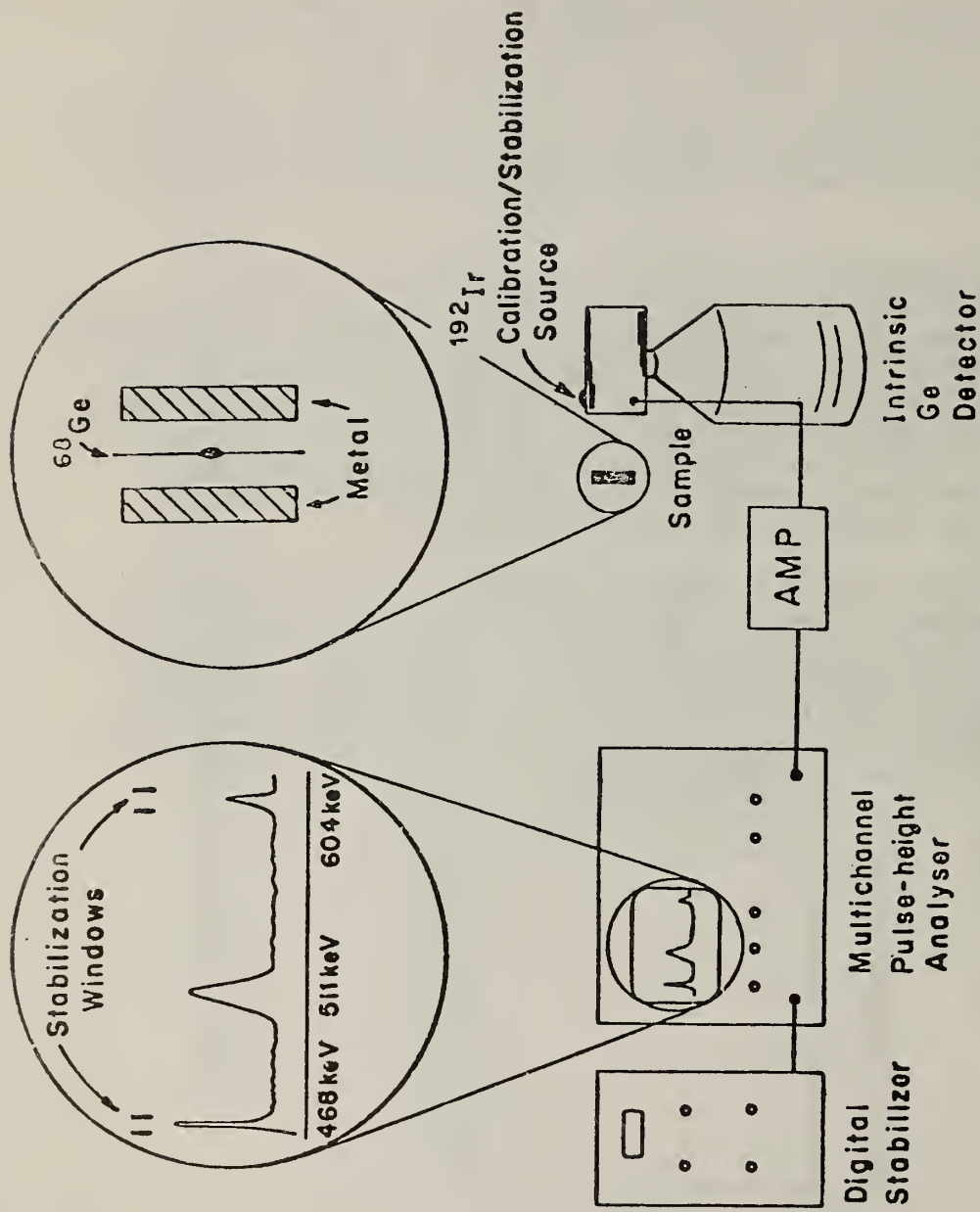
Figure 27.   Experimental Apparatus for Doppler-Broadened Lineshape Measurements.   The positron source is 25 microcuries of ^{68}Ge.   An ^{192}Ir source is used to calibrate the energy scale and maintain system stability.
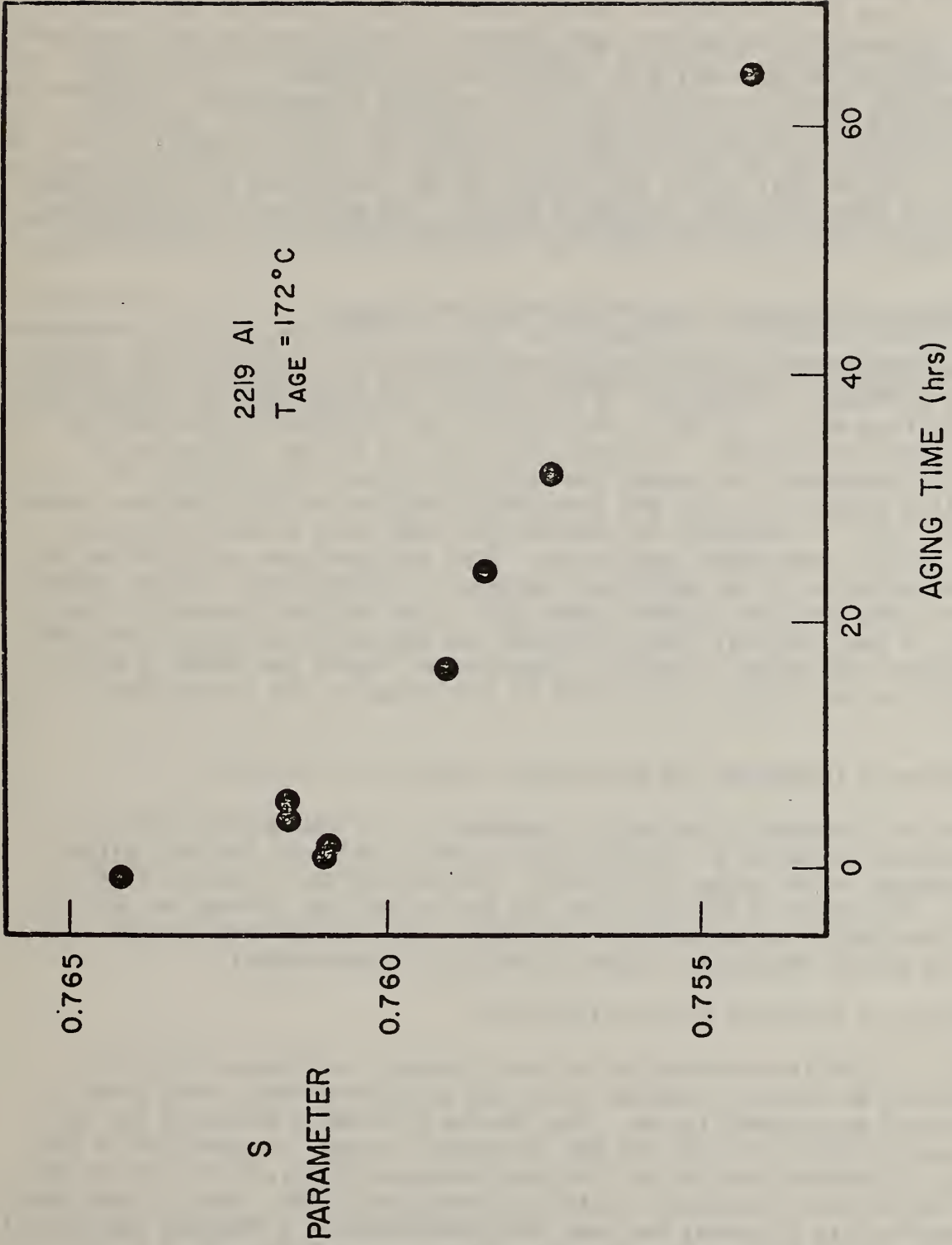
Figure 28. S Parameter Data for a 2219 Aluminum Alloy at Various States of Ageing.

25. Standards for Ultrasonic NDE
    D. G. Eitzen
    Mechanical Production Metrology Division
    National Engineering Laboratory

The detection and evaluation of defects using acoustic emission pulse/ echo ultrasonics relies heavily on comparative measurements. While these techniques have great potential, they are sensitive to measurement system characteristics and to the condition of the reference artifacts used. An effort to improve the reliability and uncertainty of these techniques is underway. Part of this effort has focused on the development of measurement services for transducers and reference blocks. The measurement services now available along with improvements, extensions and applications are listed below:

1. Ultrasonic Transducer Power Output Versus Frequency

Using a modified radiation pressure technique, the absolute total power output of ultrasonic transducers is measured versus frequency over any part of a range from about 1-20 MHz. The uncertainty is frequency dependent but is nominally about ± 5 percent. In addition to its use in the calibration of ultrasonic transducers for users, the system forms part of the basis for traceability between the Food and Drug Administration and NBS ultrasonic power standards. This is important for determining compliance of many ultrasonic products to FDA promulgated regulations. Work has been done on improving the vibration isolation of the radiation apparatus. Although the previous mounts had a very good isolation factor (about 50) at the working frequency of the apparatus, a new, inertial mounting system has been designed and constructed. The additional isolation is useful at lower power levels and seems to offer the best isolation factor of any table at the Bureau at the frequencies of interest.

2. Ultrasonic Transducer and System Power Output by Calorimetry

Using a ultrasonic calorimetric comparator, the time-averaged total absolute power output of a transducer or system is measured for any voltage input waveform in the range of 1-15 MHz. The uncertainty is approximately ± 7 percent. The operating procedure for the device has been changed so that the minimum sensitivity in now tens of microwatts, thus making many medical diagnostic and pulsed industrial systems accessible to measurement.

3. Ultrasonic Reference Block Calibration

Sets of ASTM flat-bottomed hole-type ultrasonic reference blocks are compared with an interim reference block and associated model using a well-characterized measurement system. The service provides a mechanism for comparing sets of blocks through the NBS ultrasonic system. In addition to the existing calibration service for aluminum reference blocks, a service for the calibration of steel reference blocks has been established. Also, a more meaningful uncertainty statement has been developed based on a thorough statistical analysis (with the help of the Statistical Engineering Division) of the ultrasonic measurements of reference blocks.

4.   By arrangement, carefully characterized ultrasonic source transducers and aluminum reference blocks can be made available for loan. These can provide on-site calibration with the user's system. Using the accurately measured ultrasonic source transducers, a user's power or frequency measurement system can be calibrated in-situ. Four of these source transducers were used in an international intercomparison of ultrasonic power measurement methods piloted by NBS. All data taking on the intercomparison has been completed. Measurements were made by seven laboratories in four countries. Analysis of this data is underway. The loaner aluminum ultrasonic reference blocks which have been carefully compared with the NBS interim reference standards. provide a means for users to compare their reference artifacts with those of NBS on their own ultrasonic system. A set of these loaner blocks is currently being used by Lockheed-Georgia to provide traceability between microprocessor controlled electronic test block and the response of the NBS interim standard blocks.

Additional work on ultrasonic measurement systems is in process. Digital measurements are being developed for the measurement of reference blocks. A more basic, better defined instrumentation system for block measurements is also being considered. Resumption of efforts to measure ultrasonic transducer fields in a solid media is also planned.

26. Ultrasonic Materials Characterization
   R. Mehrabian, S. Fick, R. B. Clough and J. A. Simmons
   Metallurgy Division
   National Measurement Laboratory

   This is a new activity using ultrasonic techniques for nondestructively
measuring microstructural material parameters. Ultrasonics as commonly used
in pulse echo or imaging systems detects macroscopic discontinuities such as
flaws or interfaces in material structures. However, the measurement of
ultrasonic attenuation and velocity changes of the study of the absorption
and transmission spectra of scattered ultrasonic waves provides a wealth of
detail on the mean microstructural properties of metallic materials. These
techniques have great potential for measuring texture, porosity, and multi-
phase distributions, as well as for studying the kinetics of phase transfor-
mations both by observing and inducing such transformations.

   Work in cooperation with Prof. R. Green of Johns Hopkins University has
been initiated on ultrasonic characterization for "soft spots" in aluminum
alloys. Detailed description of the overall program in this area is given in
a separate section entitled, "Nondestructive Evaluation of Nonuniformities in
2219 Aluminum Alloy Plate - Relationship to Processing." The first priority
of the effort in this task is to develop a reliable alternate NDE method for
detection of these soft spots. Velocity, attenuation, and ultrasonic scatter-
ing techniques are being employed and their reliability assessed.

   Currently, the relative merits of various developmental techniques for
measuring ultrasonic attenuation and velocity are being experimentally in-
vestigated. Since ultrasonic parameters are extremely sensitive to measure-
ment techniques, considerable effort has been devoted to the optimization of
procedural and equipment design. Methodologies under investigation include
the use of test fixtures incorporating design features allowing transducer-to-
specimen alignment independent of dimensional variations in the specimen. Test
fixtures employing long path and direct transducer-to-specimen contact in
liquid coupling media have been designed and constructed. Transducers capable
of high efficiency operation at the high frequencies necessary for adequate
sensitivity to precipitate development in a selected alloy have been designed
and fabricated. The use of conventional transducer designs at higher than
normal frequencies has also been investigated. Results obtained thus far in-
dicate that further developmental effort is necessary and justified. Longer
term studies are contemplated of the kinetics of the aging process itself lead-
ing to better specifications for such alloys in the future.

27. Ultrasonic Imaging
M. Linzer
Signal Processing and Imaging Group
Center for Materials Science
National Measurement Laboratory

     In the past year, emphasis was placed on various aspects of ultrasonic
imaging and computerized tomography. A theoretical and experimental analysis
of texture in ultrasonic imaging was carried out. Studies of cutting tech-
niques for transducer arrays and tomographic image reconstruction from lim-
ited projections were completed. Exact solutions were obtained for the first
time for three-dimensional reflectivity imaging using broad bandwidth pulses.
Inversion formulas were derived for three transmit-receiver apertures--plane,
cylindrical and spherical. Substantial progress was made in developing per-
turbation and iterative correction schemes for velocity tomography. The
theoretical and computer simulation phase of this activity is expected to be
completed during the first half of the next fiscal year and experimental
demonstration of the techniques in the second half.

28.   Nondestructive Evaluation of Composites
       H. M. Ledbetter and J. C. Moulder
       Fracture and Deformation Division
       Center for Materials Science
       National Measurement Laboratory

Elastic modulus and internal friction (damping) figure prominently in engineering design; they also provide basic information on the structure of a composite. Knowledge of the dynamic properties of composites allows the designer to prevent undesirable resonance, flutter, buckling, or other elastic instability. Despite their importance, few studies exist on the frequency dependences of the elastic constants and internal friction of composites. Most studies have been performed at frequencies ranging from 50 kHz to 10 MHz, owing to the ease of ultrasonic measurement techniques at these frequencies. Yet, the frequency spectrum of applied load of most concern to a designer ranges from dc to a few hundred hertz. Thus, there is considerable interest in measuring the elastic moduli and internal friction of composites at low frequencies (10^{-1} to 10^2 Hz).

Another impetus to study low-frequency elastic properties of composites arises from the possibility that such measurements may reveal low-level damage. Detection of low damage levels in composites is a serious, unsolved technological problem. Appropriate, reliable nondestructive methods do not exist. Previous studies in this laboratory failed to detect damage induced in graphite-epoxy by thermal cycling, mechanical fatigue, or tensile loading. These studies used a Young's-modulus mechanical-deformation mode at kilohertz frequencies. Low-frequency torsional-mode measurements should be especially sensitive to low damage levels in polymeric-matrix composites. Since torsion induces nearly zero strain along the torsion axis, the torsional modulus, T, of a uniaxial composite depends principally on the properties transverse to the fibers; it is less sensitive to the high-modulus fibers and more sensitive to the low-modulus matrix.

An apparatus was designed and built for low-frequency (0.5 to 10^2 Hz), forced-vibration determinations of torsional modulus, T, and the internal friction, Q^{-1}. The driving element consists essentially of a d'Arsonval galvanometer. The displacement sensor is a laser optical-level with phase-sensitive detection, capable of resolving strains of about 10^{-6}. One advantage of this type of apparatus is the number of alternative measurement techniques that may be used. By choosing the specimen geometry so that any mechanical resonances occur at frequencies far from the measuring frequency, a forced-vibration mode of operation may be used. In this mode of operation, the torsional modulus is determined from the ratio of applied force to observed displacement; internal friction is determined from the phase shift observed between the applied force and the resulting displacement. Alternatively, the internal friction may be determined in the forced-vibration mode of operation by displaying the applied force vs. displacement and integrating the area of the resulting hysteresis curve. The forced-vibration mode of operation also permits studying torsional modulus at a given frequency as a function of stress level or the torsional modulus at a given stress level as a function of frequency.

Another mode of operation may be obtained by choosing the specimen geometry to give a mechanical resonance at the freqeuncy of interest. In this forced-resonance mode of operation, the torsional modulus may be related to the resonance frequency, while the internal friction is obtained from the halfwidth of the resonance curve. Alternatively, internal friction may be measured in this mode of operation by observing the free decay of oscillations when the driving force is moved suddenly.

The apparatus has been used in both modes of operation to make preliminary measurements on three materials: ±45° boron-aluminum, glass-cloth/epoxy, and uniaxial graphite-epoxy. Metallic specimens of known modulus were used to calibrate the equipment. A representative resonance curve for a glass-cloth/epoxy specimen is shown in Fig. 29. Experiments are underway to study the possibility of detecting low damage levels induced by mechanical loading to 90% of the ultimate tensile strength.

Storage Modulus

Loss Modulus

FREQUENCY, Hz

10   30   50   70   90
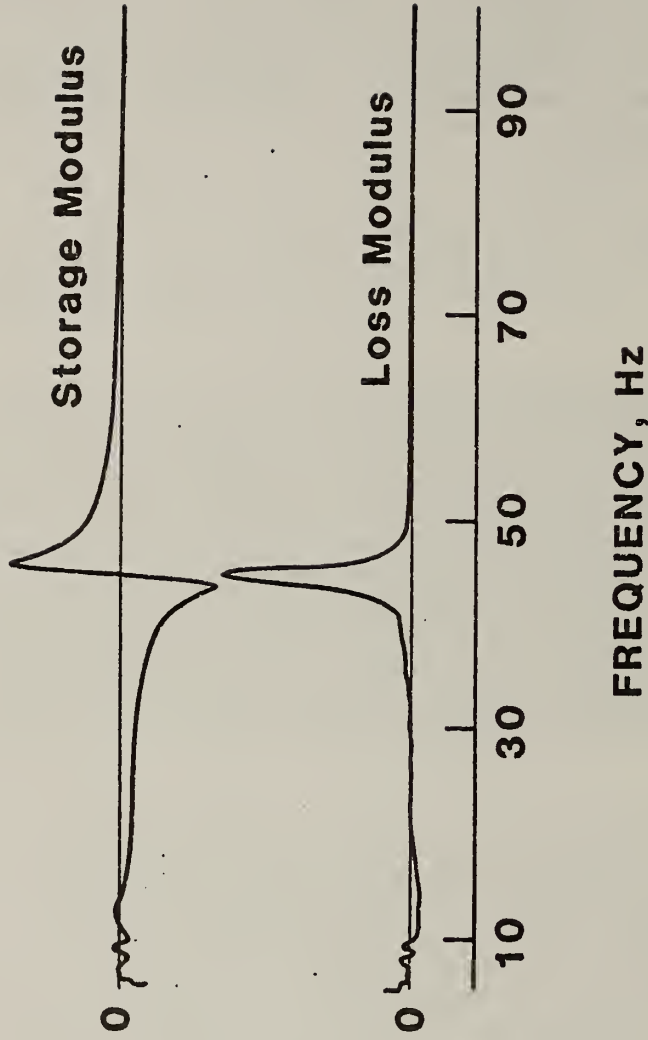
Fig. 29. Tracing of an x-y plot from a forced-vibration experiment. Upper curve is component of displacement, x_2, in phase with applied force. Lower curve is the component of displacement, x_1, 90° out of phase with applied force. The half width of the lower curve relates directly to internal friction, Q^{-1}. Except for scale factors, the total displacement curve $x^2 = x_1^2 + x_2^2$ is identical to the lower curve. The complex elastic stiffness is $K* = F_s/x$, where F_s is the spring force, which differs from the applied force, F_a, by a mass term, md^2x/dt^2.

29. Ultrasonic NDE Application Work
     D. Eitzen, G. Blessing, D. Chwirut, D. MacDonald and C. Tschiegg
     Mechanical Production Metrology Division
     National Engineering Laboratory

In addition to our core program on measurements research, we seek to maintain a level of selected applications work. Part of the benefit of this work is that it helps us maintain a fresh awareness of field measurements problems and needs. A brief outline of some of these small projects follows:

DOT Pipeline Weld Project (Phase 1)

The purpose of the project was to evaluate the possibility of using some ultrasonic technique for determining the depth of a crack in the weld region of gas pipeline. It was presumed that the flaw had been located and measured laterally by radiography. For the size of pipes of interest and for a model fracture criteria, flaws as small as 1 mm deep must be sized. The conclusions were that tip diffraction time-delay techniques hold the most promise (or possibly spectroscopic techniques). Very good results were obtained on moderately sized real and artificial defects. Real defects only 1 mm deep will still be a problem.

Well Characterized Fatigue Cracks for Ultrasonic and Eddy Current

For future studies the Air Force sought to obtain fatigue cracked aluminum and titanium. It is important that the profiles of the cracks be known with good precision. Specimens were fatigued using several loading programs. Crack profiles were measured nondestructively, using neutron radiography, ultrasonic C-scan, ultrasonic crack-tip line-delay methods, crack opening displacement (average length) and dye penetrant (surface length). The follow on work using the specimens for ultrasonic and eddy current studies has not been formulated.

Titanium Weld Inspection by Ultrasonics

The Naval Research Lab has asked us to assist them in determining whether it is possible to inspect titanium welds for gas contamination using ultrasonic techniques. Specifically, the work involves measuring the weld region elasticity of contaminated and non-contaminated samples by ultrasonics to determine whether the weld elasticity is a sensitive indicator of contamination. The results will be analyzed and reported to NRL and recommendations for further work will be made.

Technical Support for Reactor Inspection Guide

A Regulatory guide has been proposed for the volumetric inspection of nuclear reactor pressure vessel weldments. One of the tasks in this project is to provide technical support on issues such as ultrasonic transducer beam spread and scanning speed and evaluation of other positions taken with respect to the Regulatory Guide. The other task involves the evaluation of the effect of electronic distance amplitude correction (DAC) on the linearity of ultrasonic flaw detectors of the type used for reactor inspection. If there is a significant effect, a method of measuring the linearity while using the electronic DAC will be proposed.

30. Reliability of Ultrasonic Weld Inspection/NRC
   D. G. Eitzen
   Mechanical Production Metrology Division
   National Engineering Laboratory

In 1965 the Pressure Vessel Research Committee (PVRC) began an activity which is intended to determine the capability of the ultrasonic inspection method and of ultrasonic test procedures in evaluating thick section welds. (Reference 1 gives a good summary of this activity.) Cooperating participants prepared a variety of specimens with "intentional" flaws created by doping or modifying the welding process. Early in this activity some measurements were made using the various techniques. After this, some prescriptional solutions to some of the differences in procedures used by the different groups were adopted. Subsequently, data were taken on specimens 201 and 251J; the results for specimen 201 seem to have been the most published. The results of the ultrasonic evaluation of specimen 201, in retrospect, were relatively good, several teams apparently detecting seven to nine flaws out of ten. The flaws were small compared to ASME Section XI rejection criteria. After 201 and 251J were inspected, the PVRC prepared a procedure compatible with ASME Boiler and Pressure Vessel Code Section XI. This PVRC Section XI procedure was quite restrictive or prescriptional. To determine if the further restrictions lead to increased flaw evaluation reliability, trials were arranged using specimens 155, 202, and 203. An analysis comparing the data with the intended flaw locations produced _very_ disappointing results.* A further analysis employing a two-point coincidence method which only makes use of test data (not intended for actual flaw locations) was also performed[2] with somewhat more encouraging results.

The objective of this small study by the National Bureau of Standards for the U.S. Nuclear Regulatory Commission is to examine the efficacy of further analysis of the data on specimens 115, 202, and 203. More particularly, the work was to gain an understanding of the procedures, the data taken on the specimens and the subsequent statistical analysis, and to recommend whether it would be profitable to do further analysis of the data prior to specimen sectioning to determine actual flaw sizes and positions. If further analysis is indicated, a plan for the analysis was to be prepared.

The conclusions of the study were that, in the main, additional analysis of the data should await direct information about the specimen flaws, that additional analysis of the data would generally be most appropriate after metallographic sectioning of the specimens. This would permit standard approaches to a statistic based on a comparison of measured versus known flaw descriptions. In future analysis some attempt should be made to decompose the analysis into probability of detection and probability of proper evaluation of flaws. Also, the statistic used should be reevaluated; one is suggested that averages in a more predictable and more meaningful way. Some additional recommendations are made regarding additional work of this type. The descriptions of the full recommendation are contained in reference 3.

---

*It is emphasized that these results are preliminary, that radiographs indicate actual locations of flaws different than intended and that the results are relevant only with respect to a specific restrictive procedure, if relevent at all.

References

1. Pressure Vessel Research Committee Round Robin, Ultrasonic Inspection Results of Thick Section Weldments, A. Graber and O. Hedden, to appear as Welding Research Council Bulletin.

2. Analyses of the Ultrasonic Examination of PVRC Weld Specimens 155, 202, and 203 by Standard and Two-point Coincidence Methods, R. Buchanan, Interim Report to PVRC, August 1977.

3. Recommendations on Further Analysis of Data From PVRC Specimens 155, 202 and 203, D. G. Eitzen and C. Reeve, Report to the Office of Standards Development, U.S. Nuclear Regulatory Commision.

31. X-Radiographic Standards and Applications
    R. C. Placious and D. Polansky
    Radiation Physics Division
    Center for Radiation Research
    National Measurement Laboratory

I. Radiographic Standards

    1. Equivalent Penetrameter Sensitivity (EPS)

    The measurement of the quantity "EPS"[1] has been applied to evaluating image
quality response of industrial radiographic film.[2] This method standard and
test device were described in some detail in the 1979 annual report of the
"Office of Nondestructive Evaluation".[3] At that time it had not yet passed
final review by ASTM. This review is now complete and the standard has been
formally accepted by ASTM. Coordination of the drafting of the document, the
fabrication of the test device and administration of round robin feasibility
tests were done by NBS with Office of NDE support.

    Plans are now underway to make the test device available to users of the
standard through the NBS Office of Standard Reference Materials. At present
it appears that fabricating costs and expected demand do not make it attractive
enough for commercial production of the test device.

    2. EPS at Megavolt Energies

    The procedure discussed in (1) above applied to low energy x rays (200 kV).
The need has been expressed by many users for a similar system for high energy
x and γ rays (^{60}Co to 10 MeV). In response to these requests NBS has assumed
the responsibility of designing the test system and coordinating the round robin
tests as was done for the low energy standard. This work is being done in
cooperation with ASTM Committee E7.01 on "Radiographic Practice."

    Up to the present, two designs have been developed and tested. The image
quality indicators (IQI) used were fabricated and supplied by NBS to the par-
ticipating laboratories together with a prescribed protocol for testing. These
IQI were patterned after the one developed for the 200 kV standard. The results
to date indicate that measuring EPS in this way at megavolt energies is feasible
but as yet we have not achieved the degree of sensitivity needed for small
changes in EPS in the region where it normally changes rapidly. A third design
has now been made which we hope will overcome this problem. If it succeeds in
separating small changes in EPS the next step would be to develop a document
within ASTM for its use and arrange for a full scale test of the system.

    3. Unsharpness

    Our present goal is to develop a method for measuring unsharpness which
is based on a realistic estimate of the sensitivity of the eye to small changes
in image contrast. For further details see the attached report, "Recommendation
for Measuring Unsharpness in Radiography." Because of this possible new approach
to evaluating unsharpness we have requested a delay in the final recommendation
of a measurement procedure.

4.   Metal Screens

At this time we are developing a program for evaluating metal screens - particularly at high photon energies (megavolt region). Some of the experimental work for this program can be done with help from those laboratories cooperating with us in developing the EPS standard at high energies. Our goals in this work are:

a.   To evaluate the properties of metal screens - particularly as related to improved image quality.

b.   To accumulate available data for metal screens on relative speed or image quality either by measurement or literature search.

Relative to the primary goal (#1) image quality improvement can only be achieved by reducing the total unsharpness in the radiographic image and by minimizing x-ray scattering affects.

5.   Film Processing Standards
     Film Storage Standards

These are new areas of responsibility assigned to the film committee of ASTM E7.01 in the recent reorganization of that subcommittee. This responsibility therefore now descends on NBS which is providing the leadership for the film section. A task force has been launched with the request to provide an outline for drafting documents for these activities.

II.   Radiographic Applications

1.   Real Time Radiographic Inspection of Large Diameter (74 inch, 188 cm) Motors   (Outside Agency Sponsored, U.S. Navy)

D. Polansky is one of the principal consultants to the Navy for this project. He is required to design and supervise qualification tests for both the inspection procedures and the inspecting facilities. In work completed this year, it was recommended that real-time inspection be implemented and that it be regarded as the primary inspection for quality for the motor. This work has high national priority.

2.   Flaw Characterization by Radiography (Outside Agency Sponsored, Dept. of Transportation).

This project was initiated as part of an effort to develop a more scientific basis for flaw characterization in large pipeline welds. It began as a broadly based effort in both material studies and NDE. The radiographic phase of this work has been suspended at this time, per agreement with the sponsor. A final progress report will be transmitted to the sponsor and other interested readers. This report will address primarily the first objective of the work, that is, recommendations on the radiographic information needed in order to evaluate a flaw for which a waiver request has been made.

References

1. For a definition of EPS see ASTM Standard E-142-77, "Standard Method for Controlling Quality of Radiographic Testing," ASTM Book of Standards, Part 11, p. 273 (1979).

2. ASTM Standard E-746-80 (to be published).

3. "Annual Report 1979, Office of Nondestructive Evaluation," NBSIR 80-2007, p. 43.

32. Recommendation for Measuring Unsharpness in Radiography
   D. Polansky and R. Placious
   Radiation Physics Division
   Center for Radiation Research
   National Measurement Laboratory

The total unsharpness in radiography is a function of geometrical, screen, and motion unsharpness. Generally in industrial radiography, motion unsharpness equals zero and the screen unsharpness (when using metallic screens) is a fraction of the geometrical unsharpness. The result is that a straightforward calculation of the geometrical unsharpness as published in the Annual Book of ASTM Standards, Part 11, results in a number that has been representative of the total unsharpness of the radiograph.

The recent increase in the use of real time radiography and fluorescent screens in industrial radiography has required that the total unsharpness be evaluated. The analytical expression of the total unsharpness

$$U_T = (U_g^n + U_m^n + U_s^n)^{1/n} \tag{1}$$

has been recently investigated by several authors with the opinion that the value of n is most probably between 1.5 and 2.0.[1] In radiographic systems where the unsharpness is individually measured or calculated, the value chosen for the exponent obviously determines the total unsharpness value. At the present time we have no specific recommendation as to the specific value to be chosen for the exponent n.

A schematic representation of the unsharpness in a radiographic system is obtained when a densitometric trace is made of the radiographic image of the edge of a step object. The trace is the familiar S shaped curve. It is the value of unsharpness determined from this curve that characterizes the system. In general there is no standard way of measuring this unsharpness. Some authors have used the X intercepts found by the line through the points .16 $(D_{max} - D_{min})$ intersecting the horizontal lines of D_{max} and D_{min}.[2] Harms and Zeilinger in their work suggested several arbitrary definitions of unsharpness for the practicing radiographer. Their suggestion was that if the optical density variation near the asymptotes is of particular interest then by choosing a convenient value for $S(X_1\alpha)$ and $S(X_2\alpha)$ to define X_1 and X_2. One can say that:

$$U = \frac{X_2 - X_1}{S(X_2\alpha) - S(X_1\alpha)}$$

This suggestion seems to warrant further consideration. The effect of unsharpness is to reduce image contrast and therefore the detection of small low contrast anomalies. If the asymptotes of the S curve do not approach the D_{max} or D_{min} value rapidly, the edge is said to be blurred. We therefore, suggest measuring the X_1 and/or X_2 point at the asymptote as determined by an arbitrarily chosen ΔD of .04 from the maximum and/or minimum. The choice of a ΔD of .04 to determine the X value offers two advantages: (a) this density represents a brightness change of 9.6% and has a high order of reliability of visual detection and (b) the microdensitometer has a capability of resolving density differences of .02 so that reasonably accurate points can be measured from the densitometer traces. What we propose is to use this value of X to indicate unsharpness or perhaps a resolution index. This value will be compared with the value of unsharpness as determined by Klasens or an integration of the curve to ensure that the data are consistent with these methods. If such an approach is practical then the method will relate the unsharpness number to

resolution $\dfrac{\Delta D}{\Delta X}$ and may be termed a visibility index.

References

1. A. A. Harms and Z. Zeilinger, "A New Formulation of Total Unsharpness in Radiography," Phys. Med. Biol., 22 (1977).

2. H. A. Klasens, Measurement and Calculation of Unsharpness Combinations in X-Ray Photography, Philip Research Reports (1946).

33. X-Ray Residual Stress Evaluation In The Interior of Industrial Materials

M. Kuriyama, W. J. Boettinger, and C. J. Bechtoldt
Metallurgy Division
Center for Materials Science
National Measurement Laboratory

R. C. Placious
Radiation Physics Division
Center for Radiation Physics
National Measurement Laboratory

Improved quality control of industrial materials and early detection of flaws in these components require quantitative information concerning the stress distribution near cracks and residual stress distributions after different types of cold working and heat treating or under various conditions of load. These demands naturally lead to the necessity of measuring residual strains in the interior of materials. Among many nondestructive techniques for the measurement of residual stresses, the x-ray diffraction technique, called Bragg diffractometry, excels in its accuracy. Yet this technique is incapable of detecting stresses in the interior of bulk materials.

More than two years ago, we proposed[1] an entirely different approach to the x-ray evaluation of residual strains (or stresses) although it uses the principles of x-ray diffraction. This approach uses energy dispersive spectroscopy, where an energy dispersive solid state detector is employed with a well-collimated high energy beam of photons. Last year (NDE Annual Report 1979, p. 66), we proved,[2] using ordinary laboratory x-ray sources and thin materials, that the desired resolution and detectability can be achieved for the determination of residual stresses if this technique is employed simultaneously with the curve fitting technique. The objective of this year's activity it to demonstrate this capability using an industrial radiographic x-ray source with radiation up to 200 kev and commercial steel and aluminum plates up to 1 cm (or a half inch) and 3 cm (or one and half inch) thick, respectively. If the feasibility of this technique is proved for use outside the laboratory, the mapping of a residual stress distribution inside an industrial material can be performed with relative ease on site.

To achieve this methodology, the following three major principles are involved:

a. Well-defined diffraction energy peaks should be obtained at an energy range of about 100 kev. These high energy photons can penetrate through relatively thick material, so that the diffraction peaks obtained by these high energy photons guarantee to deliver the stress information within a bulk material.

b. These diffraction energy peaks should have a Gaussian profile so that the curve fitting technique can be used for the determination of the centroid (or peak) positions, and

c.   The measurement accuracy of lattice constants or their variations (hence, residual stresses) should be increased by a factor of 100, compared with the resolution limit of solid state detectors, by use of curve fitting. The relationship between the improvement factor (that is, the accuracy of determined strains) and counting statistics should be investigated.

All of these principles have been confirmed with thin materials using low energy photons. The use of high energy photons creates scattering problems and background problems which directly affect the accuracy of our measurements. We have succeeded in controlling these problems. The results are shown in the following:

a.   As shown in Figure 30, diffraction energy peaks are clearly separated with significant intensities. This spectrum was obtained from a commercial steel plate (AISI-C1015-SAE1015) 3/8 inch thick. In this case, the scattering angle was set at $2\Theta = 5.7°$ with the incident divergence 3 mrad (0.17°=10 min.) and the receiving divergence much less than 3 mrad, so that the diffraction peaks can be obtained through the entire thicknesss of the sample at a given point of the sample surface. The spatial size of the beam on the sample is less than 1.5×1.5 mm^2. The diffraction peaks are indexed as shown in Fig 30. Note that the well-defined (211), (220), and (310) appears in the energy range between 90 kev and 150 kev in this transmission geometry. This result indicates that the previously mentioned principle (a) is completely satisfied.

b.   Figure 31 shows an example of the observed spectral profile, say (110), which has been fitted by a Gaussian curve with a linear background. A perfect Gaussian fitting demonstrated here certainly indicates a great promise in the precision determination of centroid (or peak positions for each observed energy peak. Hence, principle (b) has also been confirmed experimentally for high energy photons.

c.   We are now in the process of proving principle (c). And further efforts are being made to increase the scattering angle without loss of resultant intensities in peaks, so that one can really determine stresses within small volumes inside materials.

References

1.   M. Kuriyama, W. J. Boettinger, and H. E. Burdette, ASNT National Fall Conference, October 1979, Denver, CO, p. 49 (1978).

2.   M. Kuriyama, W. J. Boettinger, and H. E. Burdette, Proceeding of Symposium on Accuracy in Powder Diffraction, NBS Special Publ. 567, p. 479 (1980).
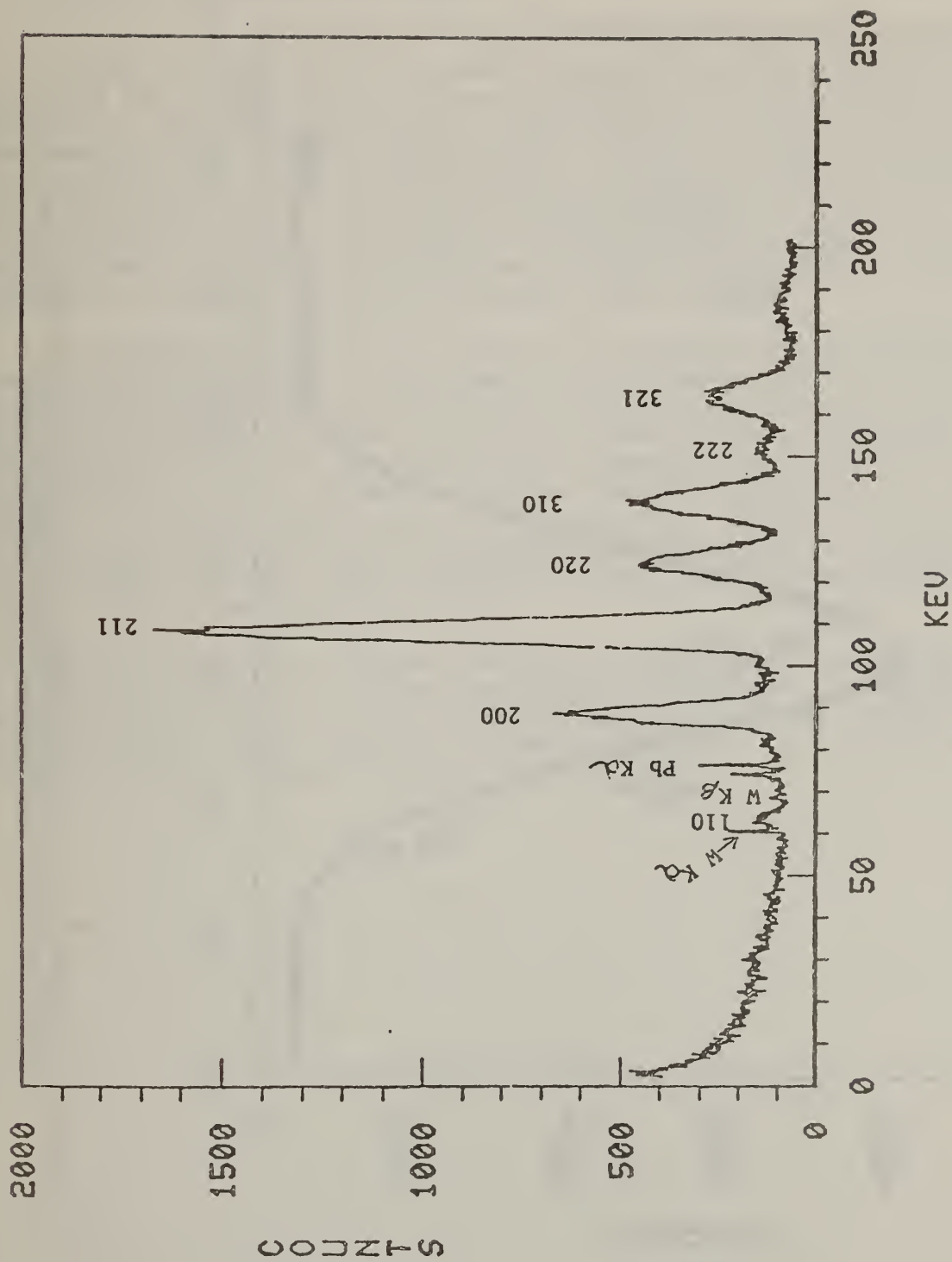
Figure 30. A Bragg diffraction energy spectrum obtained from a commercial AISI-C1015-SAE1015 steel plate 3/8 inch thick. The scattering angle is 5.7° ensuring a transmission geometry through the entire thickness of the sample.
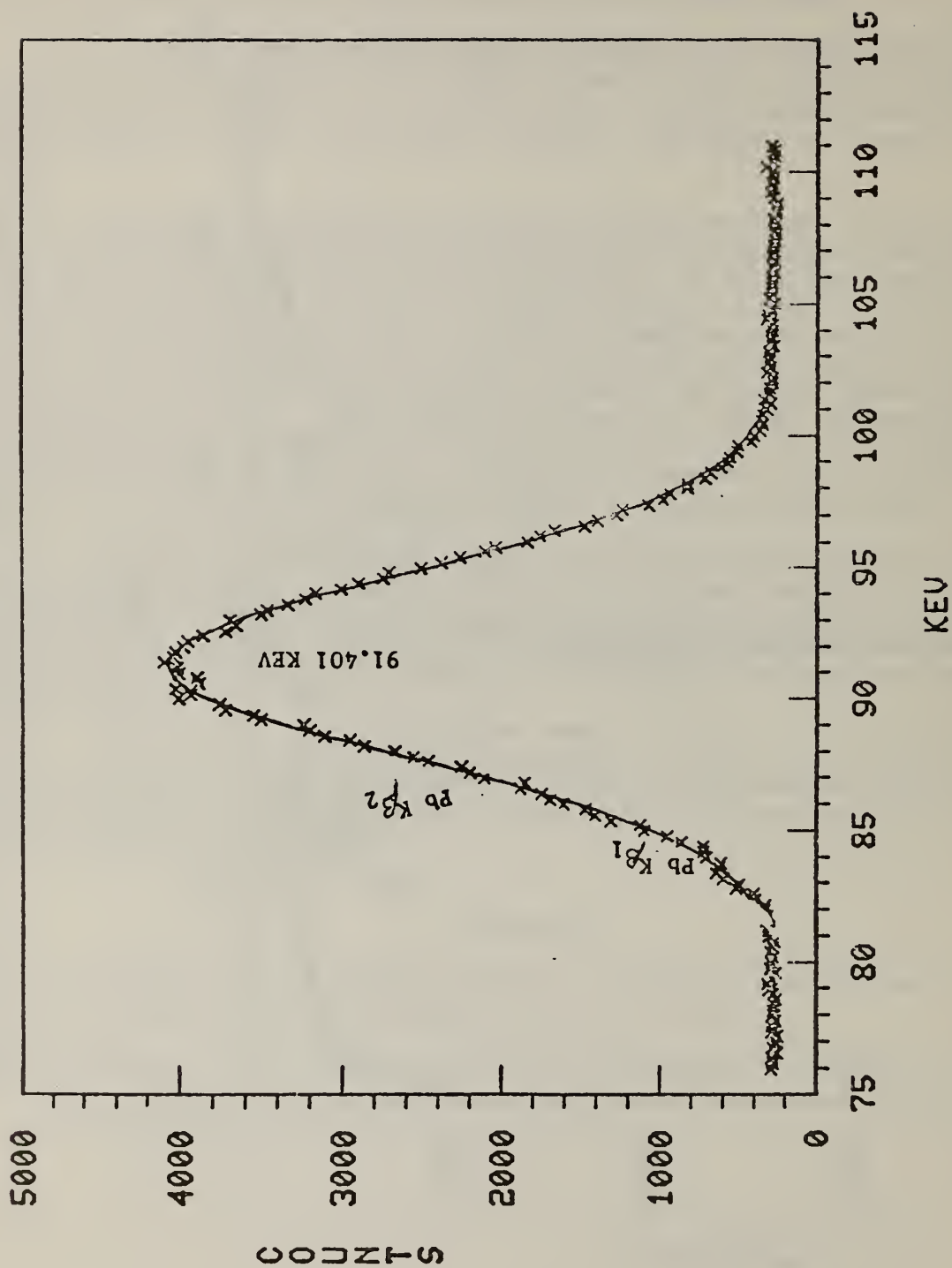
Figure 31. An example of the observed diffraction profile, (110), from a steel plate 1/2 inch thick fitted with a Gaussian curve with linear background.

34. Accelerator-Based Radiography
J. W. Behrens, R. A. Schrack and C. D. Bowman
Nuclear Radiation Division
Center for Radiation Research
National Measurement Laboratory

Efforts continue for improvement of resonance neutron nondestructive assay and for implementation of these methods using small accelerators suitable for an industrial environment. A two dimensional detector has been developed and tested with 1 mm resolution. This detector was developed in collaboration with the Oak Ridge National Laboratory. Taking into account the greater surface area and greater detector thickness, an increase in performance compared to the 1-D detector of a factor 50 is achieved. This gain may be taken in improved statistical accuracy or reduced source intensity. The detector is shown in Figure 32 with its cover removed.

Design effort has begun on a new type of detector which promises to make possible low energy neutron spectrometry without neutron time of flight. The detector combines the properties of materials which capture neutrons with a probability inversely proportional to the neutron velocity with neutron interaction position sensitivity. The detector inherently has a high efficiency. If successful, the large separation between source and detector for neutron time-of-flight measurements would not be necessary. Neutron sources might thereby be used with more than two orders of magnitude greater efficiency. High accuracy resonance neutron radiography might then even be possible with isotopic decay sources such as ^{252}Cf.

Resonance neutron radiography appears to have several useful applications in nuclear safeguards, in reactor fuel burn-up measurements, and in assay for water storage. It offers high selectivity also for many heavy metals including precious metals. With further development, application to the more common fabrication metals appears likely.

Figure 32. Two dimensional position sensitive neutron detector
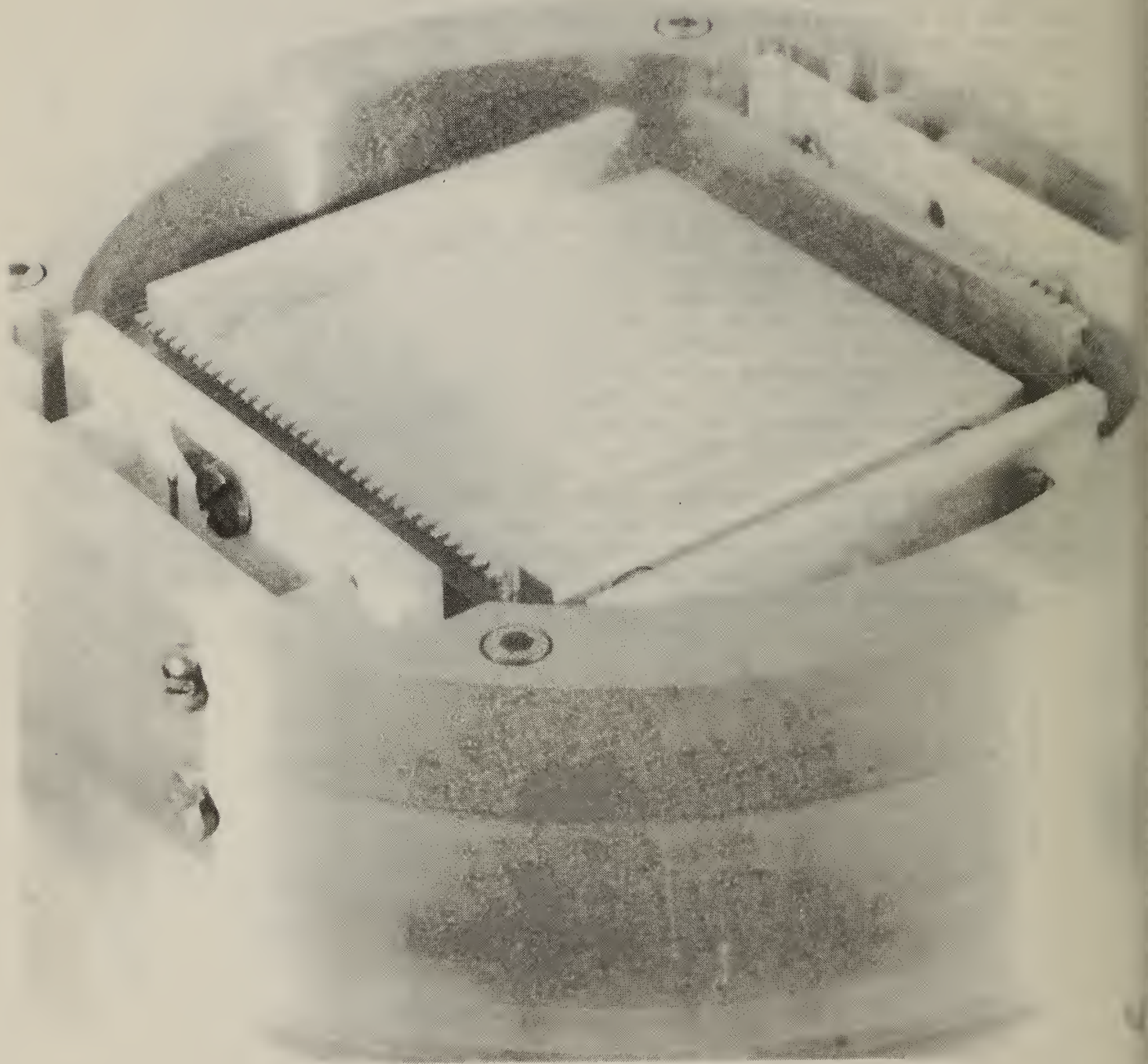
35. Measurement of the L/D Ratio For Neutron Radiography
     W. L. Parker and D. A. Garrett
     Reactor Radiation Division
     Center for Materials Science
     National Measurement Laboratory

The last report of this work[1] describes a method for determining the L/D ratio for a neutron radiographic facility from microdensitometric measurements made of the shadow images of a series of small, identical, and parallel linear obstacles placed at uniformly increasing distances from the image plane. Also described were the test objects used--one borrowed from Aerotest Operations and one built at the National Bureau of Standards.

The report also defines the important parameters: L and h--the distances of the source and obstacle from the image plane, respectively, and D = 2R and d_o --the widths of the source and the obstacle, respectively.

The methods consists of approximating the microdensitometer tracings by trapezoids and measuring the widths of the base (w_d) and the top (w_c) of the trapezoid. When w_d and w_c are plotted vs. h, the resulting plots should be approximately straight lines from whose slopes the value of L/D can be determined.

Work this year has been largely concerned with the theoretical treatment of the images to be expected when the source is circular instead of linear, as was assumed in the earlier treatment.

1. Theory

The detailed analysis will be published elsewhere and only the results are given here.

One of the most important derived parameters is the value of h for which the umbra goes to zero, b; as was shown previously[1] it is given by

$$b = Ld_o/D. \qquad (1)$$

For a parallel linear source and linear obstacle the shadow patterns will be symmetrical trapezoids whose height will be constant as long as h < b with w_d increasing and w_c decreasing as h increases until the pattern becomes a triangle when h = b. For h > b, the pattern is again a trapezoid whose height decreases, while w_d and w_c both increase as h increases. The area of the trapezoid should remain constant.

For the case of a circular source and linear obstacle when h < b the pattern will have a constant central region and will approximate a trapezoid with rounded corners. When h > b, there is no constant region, and the patterns deviate more and more from a trapezoid as h increases.

Figures 33a and 33b are calculated shadow patterns from the same parameters (L/D = 68.8, h = 0.25, 0.75, 1.25,..., 4.25 inches) for the linear source-- parallel linear obstacle and the circular source--linear obstacle, respectively. Figure 33c is a reproduction of microdensitometer tracings from a radiograph taken with the same parameters. The agreement of figures 33b and 33c is excellent although, if the two figures are superimposed, there are some slight discrepancies.

The slopes of the plots for w_d and w_c are found by fitting the data by linear regression to equations of the form

$$w = a_0 + a_1 h(1-h/L)^{-1}.$$ (2)

The slope values: a_{1d}, a_{1c} and a_{1c+} are defined in the last report.[1] The average slope is defined as follows:

$$a_{1av} = (2a_{1d} + a_{1c-} + a_{1c+})/4$$ (3)

The theoretical value of a_{1av} is MD/L, where M is the linear magnification of the microdensitometer.

It follows then, that

$$(L/D)_{exp} = M/a_{1av} \qquad \text{Linear-linear} \quad (4)$$

where (L/D)exp represents the value of L/D obtained by this method.

The case of a circular source and linear obstacle is different. As is evident from figure 33b, the patterns are approximately trapezoidal only for quite small values of h. Furthermore, when h > b there is no region of constant illumination. It is assumed that the measurement line when h < b is drawn through the "half-power point" with the slope of the shadow pattern at that point, and that the intersections of this line with the top and bottom of the trapezoid determine w_d and w_c. When this is done, it is found that $a_{1av} = M(\pi/4)D/L$ and

$$(L/D)_{exp} = \pi M/4a_{1av} \qquad \text{Circular-Linear} \quad (5)$$

When b < h < 2b, the plot of w_d va $h(1-h/L)^{-1}$ is still very close to a straight line. It can be shown that a_{1d} for this range will differ from that for h < b by only a few percent. Since measurement errors are normally of this order of magnitude, we use a value of a_{1d} obtained for measurements for 0 < h < 2b. Values of w_c for h > b are not used and $a_{1av} = (a_{1d} + a_{1c-})/2$.

94

It is apparent that the effect of going to a circular source, at least when h < b, has been to replace D by $\pi D/4$. In other words, the normalized patterns for a circular source will approximate those for a linear source whose width is $(\pi/4)D$. This agrees very well with the experimental results.

The method described here which leads to equation (4) or (5) will be called the NBS method of determining L/D.

The NU method developed by the Aerotest Operations group uses only w_c. Linear regression is used to find an expression such as equation (2) for $w_c = 0$. The resulting value of h shall be called b_{exp}. It is found that the resulting values of L/D are

$$(L/D)_{NU} = b_{exp}/d_o \qquad \text{Linear-Linear} \qquad (6)$$

$$(L/D)_{NU} = \pi b_{exp}/4d_o. \qquad \text{Circular-Linear} \qquad (7)$$

2. Experimental Results

The NBS method of determining L/D has now been used at the NBS 10 MW Research Reactor and at three non-reactor-based facilities. The range of L/D measured is from 12 to 170.

Figure 34 shows the results of measurements from twelve radiographs taken at the NBS facility of the NBS test object described in the last report.[1] The size of the circles indicates the standard error. The straight lines were obtained by linear regression to fit the equation

$$(L/D)_{exp} = L_o/D + L'/D. \qquad (8)$$

L' is measured from the face (biological shield) of the reactor and L_o, the distance of the source behind the reactor face is measured to be 32 inches.

The values of L_o and D resulting are within the standard error of what would be expected. Although a_{1d} and a_{1c} may differ by as much as twenty percent of their average, the NBS method appears to be correct for whatever artifacts are producing the discrepancy.

Similar results have been obtained from the radiographs taken at the non-reactor-based facilities, thereby increasing confidence in the validity of the method.

The values of $(L/D)_{exp}$ derived from a set of radiographs taken with the same parameters as those for another set, but with a 0.070 inch lead sheet between the test object and the cassette, agree with those derived from the normal set to within the standard error with the fluctuations being random. Accordingly it is felt that the results are not affected by capture gamma rays from the obstacles or background gamma rays from the reactor.

The vaules of $(L/D)_{NU}$ obtained from equation (6) or (7) agree generally to within 10 percent with the values of $(L/D)_{exp}$ obtained from equation (4) or (5); but the internal consistency of the results from the NU methods does not seem to be as good as that from the NBS method.

The NBS method is preferred to the NU method for two reasons: first, it uses more of the available data. In fact, for small values of L/D, the number of measurements of w_d used will be at least twice the number of measurements of w_c used. Second, the NU method uses the value of d_o, which may not be known to the desired accuracy, while the NBS method depends only on the fact that all the obstacles have the same width.

References

1.   W. L. Parker and D. A. Garrett, NBS Tech. Note No. 1117 (ed. F. J. Shorten) 1980.
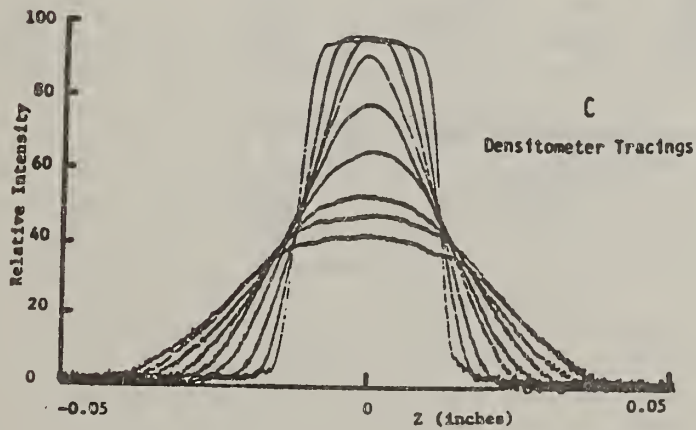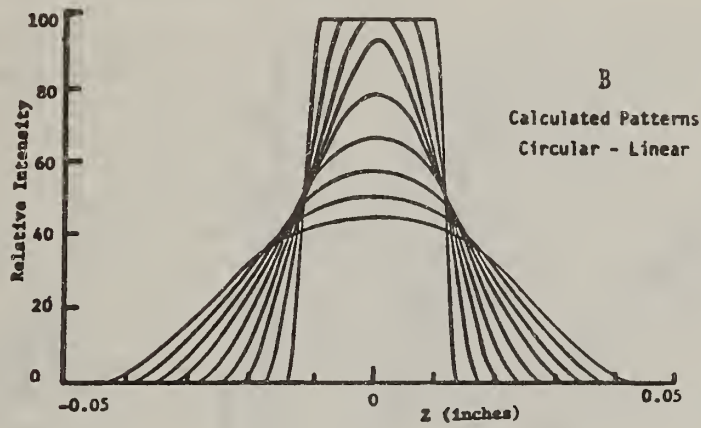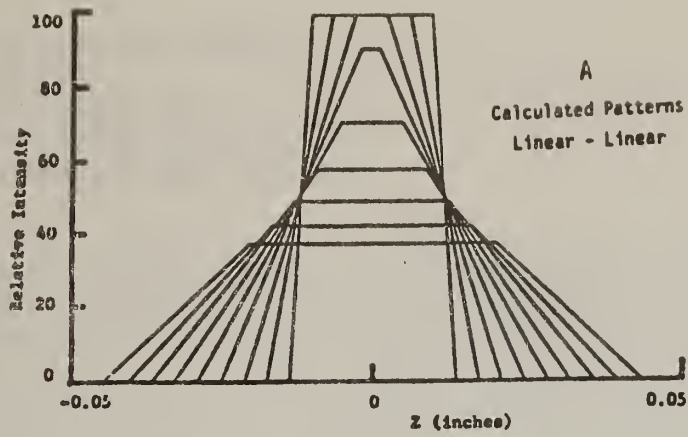
Figure 33.   Shadow patterns: (A) calculated for Linear-Linear
             Case, (B) Calculated for Circular-Linear Case,
             (C) Densitometer Tracings.   See text for parameters.
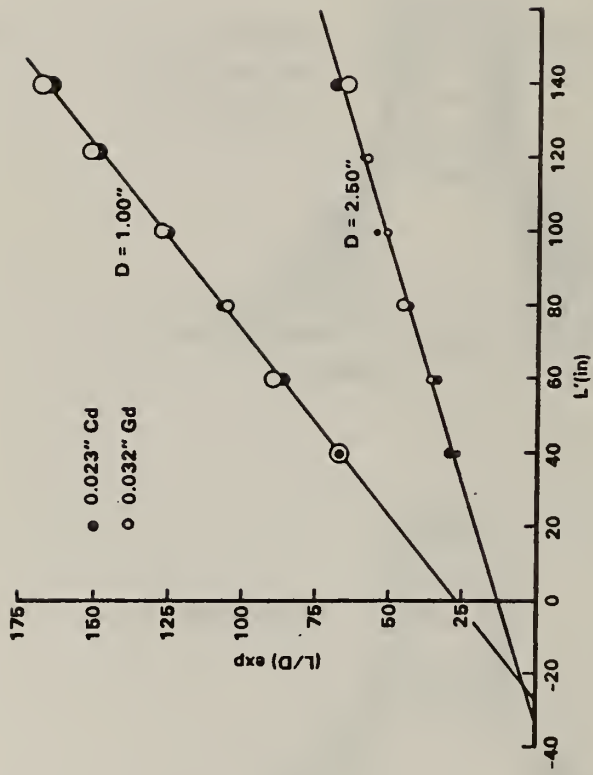
Figure 34. Values of $(L/D)_{exp}$ obtained from radiographs of NBS test object.

36. Wear Condition Monitoring
   A. W. Ruff
   Metallurgy Division
   Center for Materials Science
   National Measurement Laboratory

This project involves the use of two techniques to nondestructively determine and monitor the wear condition in operating machinery. One technique recovers and characterizes lubricating fluids and the wear debris particles in the fluids. The other technique applies acoustic emission detection methods to wearing components in order to monitor the development of fatigue cracks associated with the wear contacts. The wear debris technique has been used for several years in numerous programs in the DOD to monitor such systems as turbine engine bearings, helicopter transmissions, and various pump systems. The acoustic emission wear monitoring technique is new and at present is being studied only under laboratory conditions.

Wear debris recovery and analysis is used in both military and civilian systems for wear monitoring. Basically, the lubricating fluid is sampled periodically and the wear particles are removed by magnetic recovery methods, e.g., Ferrography, or by ultrafiltration. Chemical analysis of the oil is also done routinely. It has been found in many studies that while chemical oil analysis can detect small wear particles successfully, it is not a reliable method for particles larger than a few micrometers in size. On the other hand, wear debris methods are particularly efficient at recovering particles greater than 1 μm in size. Thus, the two methods complement each other and are jointly used in many condition monitoring systems. The more serious modes of wear frequently involve the generation of relatively large wear debris particles, greater than 5 μm for example. Therefore, it is important to capture and examine all the larger wear particles in any wear monitoring program. Magnetic recovery methods are proving to be quite satisfactory in this regard.

We are carrying out laboratory studies of the production of wear debris particles under different conditions of load, speed, metallurgy and environment. The particles are recovered using Ferrography and analyzed to relate the wear mode and worn surface with the particle characteristics. Further improvements in the system of identifying types of wear particles are needed and are being worked on. We plan to apply quantitative microscope methods next year to this problem. We are participating in an international activity on wear debris analysis for system condition monitoring with the TTCP (Technical Cooperation Program, Action Group 7) group. Members represent Australia, England, New Zealand, Canada and several DOD groups in the United States. This group has carried out interlaboratory comparisons on wear debris collections and plans more activities of this type. There is considerable interest in standardizing wear debris analysis. We have had preliminary discussions on the idea of providing samples of reproducible reference wear particles and it seems feasible to do this. Work next year in this project will apply more effort to this topic. In that connection, a conference at the University of Maryland in September will discuss particulate characterization methods and standards. We hope that some new, useful

concepts will emerge from this meeting. The NBS Office of Standard Reference Materials is cooperating with our group on the characterization and possible standardization of abrasive particles. We believe similar methods can be applied to metal wear particles.

The second nondestructive method being developed in this project concerns acoustic emission monitoring of wear processes. We have assembled an instrumented system (with considerable consultation from NBS colleagues, Drs. Clough and Hsu) for this purpose consisting of a broad band AE preamplifier and amplifier with gain adjustable from 60 db to 100 db. A conventional piezoelectric transducer is used with the system. The amplified signals are fed to a video tape recorder. We have characterized the frequency response of this system over the band of interest (100 kHz to 1 MHz) and have studied the dynamic range and transient response of the system and they seem acceptable. Our experimental approach will be to tape record events during controlled wear experiments. Those tapes will then be replayed into the Metallurgy Division's AE signal processing system including analog/digital conversion and computer processing so that significant events can be identified. The wear experiments will be carried out on a computer-controlled block/ring wear system that has been modified for locating the acoustic transducer on the block specimen in the epicenter position. The blocks will be fabricated and fatigued to contain a distribution of preexisting cracks. We plan to preload the specimens and carry out wear on them so as to properly stress the cracks in the wear-affected volume of the block. Growth of the cracks will then occur and be recorded by the system. At the conclusion of the test, the specimen blocks will be sectioned and examined metallographically to determine crack location, size, and other relevant details. The wear experiments at first will emphasize the fatigue or delamination modes so that we have the best chance for success in detection. Specimen materials will involve carbon and tool steels at first for which there is a good body of data on acoustic emission from cracks.

37. Safety Factors and Mathematical Modeling
     J. T. Fong
     Mathematical Analysis Division
     Center for Applied Mathematics

Traditionally speaking, engineers adopt a numerical value known as safety factor to convey their experience and judgment in estimating the uncertainties of a physical quantity such as loads, moduli, yield strengths, etc. Safety factors also appear in design codes and operational guidelines for engineering components and structures, and are usually arrived at by committee actions based on knowledge of the best available experts in the field. The values assigned by these experts reflect both their experience and their perception of the prevailing quality of engineering work. The possibility of a crude verification of those values based on field performance data is seldom realized.

To shed some light on this extremely complex problem using the general tools of mathematical modeling, a strategy was introduced during FY78 in response to the request by NBS Office of NDE. The technical work will be subdivided into three phases, each one lasting approximately 3 to 4 years depending on the level of support:

Phase I   -   Development of a Mathematical Model with Special
                Applications to the Utilization of NDE Data.

Phase II   -   Pilot Testing of the Proposed Model with Controlled
                Experiments on NDE Measurement and Performance.

Phase III -   Verification of an Updated Version of the Model with
                Real-Time NDE Measurement and Field Performance Data.

During all three phases, it is essential that the project investigators keep close contact with the appropriate technical communities in order to achieve credible and relevant results.[1] A total of six tasks were designed to accomplish the objectives of Phase I:

Task 1.1 Data Acquisition and Initial Screening

Task 1.2 Data Analysis and Sampling Theory

Task 1.3 Safety Factors and Fatigue Life Modeling

Task 1.4 Fatigue Life Modeling and NDE of Fatigue Damage

Task 1.5 NDE of Fatigue Damage and Safety Factors

Task 1.6 Conference Proceedings and Articles of General Interest

The first two tasks dealt with the processing of raw data before an interpretative model can be seriously developed. Tasks 1.3 through 1.5 were designed to elevate the importance of NDE into the traditional concept of fatigue life preditions. Finally, task 1.6 resulted from an active participation of project investigators in technical conferences sponsored by ASTM, ASME, and ASNT.[2]

During FY79, considerable progress was made in each of the six tasks with visible output from Tasks 1.1, 1.3 and 1.6. The principal mathematical result that was published under task 1.3 was a formula for the estimate of a safety factor which took into account sample, size, allowable risk, and a modification of the sample variance based on engineering judgment.[3]

During FY80, four mathematical results were accomplished under tasks 1.1, 1.2, 1.3 and 1.5. A brief description of each is given below:

<u>Task 1.1</u> Mandel's Structure Index[G] Algorithm and Screening of NDE Data

Using the method of singular value decomposition (SVD) of a rectangular array of data, Mandel[5,6] introduced a new analysis of variance model for a general class of data such that the eigenvalues of the analysis can be used to define a structure number for a given array as an indication of its suitability for curve fitting. At Mandel's suggestion, a Monte Carlo study of the same array using random normal deviates to generate another structure number is performed to calculate a structure index which can be used qualitatively to assess the noise level of the given array. For example, if the structure index (ratio of structure number of real array to that of random array) is from 1 to 5, the real array is too noisy to yield any useful information. On the other hand, if the structure index is 1,000 to one million, the array is said to have a strong structure, and further analysis of data can proceed. A documentation of this work is in progress and will be completed in FY81.

<u>Task 1.2</u> Three-paramater Characterization of a Regression Line for
Comparing Experimental Data from Several Laboratories

A simple yet quantitative approach to assess interlaboratory fatigue crack growth rate data is proposed. Seven sets of da/dN vs. ΔK data from six laboratories on nominally the same material and loading conditions in a cooperative test program sponsored by the Society of Automotive Engineers are analyzed to illustrate the approach. Each set of data is subjected to a standard first-order linear regression analysis based on the method of least squares. Three characteristics of the regress line, namely, the location of the "center" of the data, the slope, and the vertical half-width of the confidence band (for some specified level of confidence), are used to define a composite measure of the closeness of one regression line to another. A graphical representation of the results of the six laboratories is given in Fig. 35. The work is being published by ASTM in a forthcoming STP.

<u>Task 1.3</u> Four-Component Decomposition of Safety Factors for Fatigue
Life Design

In a paper delivered to a Critical Issue Symposium of ASME at San Francisco in August 1980, it was proposed that four categories of uncertainties could be identified and subsequently estimated in modeling the service life of a structure or component. The four categories were:

a. <u>Measurement Science and Statistics.</u> This category includes measurement errors and uncertainties on all aspects of testing and data gathering. In particular, sampling errors are included in this category.

b. <u>Materials Science and Modeling</u>. This category includes variabilities due to inherent material inhomogenieties as well as the uncertainties associated with the empirical models of numerous mechanisms at the microstructural level.

c. <u>Scaling</u>. This category includes all uncertainties due to scaling effect in structural geometry and load spectra between real and laboratory configurations.

d. <u>Human Factors</u>. It was emphasized at the conference that the 4-way decomposition is necessarily of a vectoral nature, i.e., the safety margins for the four components cannot in general be added to arrive at an overall estimate on account of the interactive nature of the four components. See Fig. 36.

<u>Task 1.5</u> Mandel's Approach of Variance Decomposition and an Estimate of the Safety Factor for the Alaska Pipeline Girth Weld Defect Size

In a paper delivered at a Conference on the Mechanics of Nondestructive Testing held at the VPI & State University, Blacksburg, VA, in September 1980, an algorithm for estimating the safety factor for defect sizes based on several readings of the radiographs of those defects was given. The algorithm was based on a 1977 paper authored by Mandel[7] where a variance decomposition algorithm was introduced to analyze interlaboratory data. A numerical example for estimating the safety factor of the length of a weld defect was presented using data from the Alaska pipeline project. The documentation of this work is in progress and will be completed in FY81.

Future Directions

So far, we have accomplished five mathematical results distributed as follows:

	<u>Task 1.1</u>	<u>Task 1.2</u>	<u>Task 1.3</u>	<u>Task 1.4</u>	<u>Task 1.5</u>
FY79			yes		
FY80	yes	yes	yes		yes

The key result has appeared under Task 1.5 where a safety factor for defect dimensioning can now be estimated. We consider this result the principal contribution of Phase I for this modeling project. FY81 will be spent mostly on documenting the results developed during FY80.

Where do we go from here? I believe it is not premature to discuss several directions for the implementation of the Second and Third Phases of this project. In particular, there are three logical extensions of Phase I in planning for Phase II work:

Task 2.1 Computer-Aided NDE Data Screening and Analysis

This is a logical extension of tasks 1.1 and 1.2.

Task 2.2 NDE Measurement and Fatigue Mechanism Research

This is a logical extension of tasks 1.3 and 1.4.

Task 2.3 Human Factor Estimate for NDE Measurement

Again, this is a natural extension of task 1.5 using the variance decomposition algorithm of Mandel to separate machine-induced uncertainty from that due to human factors.

References

1.   In May 1978, J. Fong accepted an invitation to serve ASTM as chairman of its subcommittee E9.01 on fatigue research (130 members), and in Jan. 1979, he became the chairman of the Materials and Fabrication Committee (over 100 members) of the ASME Pressure Vessel and Piping Division (4000 primary and 7000 secondary members).

2.   Most of these conferences were co-sponsored by NBS in collaboration with EPRI, DoT, NRC, PVRC, MPC, SwRI, and other prominent engineering-oriented institutions.

3.   See Fong, J. T., Nucl. Eng. & Design, 51 (1978) 45-54.

4.   Private communication as a result of a lecture given by Dr. J. Mandel on Jan. 16, 1980 at a mathematical modeling colloquium sponsored by the Center for Applied Mathematics, NBS.

5.   Mandel, J., "The Partitioning of Interaction in Analysis of Variance," J. Res., NBS, Vol. 73B, No. 4, pp. 309-328 (1969).

6.   Mandel, J., "A New Analysis of Variance Model for Non-Additive Data," Technometrics, Vol. 13, No. 1, pp. 1-18 (1971).

7.   Mandel, J., "The Analysis of Interlaboratory Test Data," ASTM Standardization News, Vol. 5, No. 3, pp. 17-20 (1977).
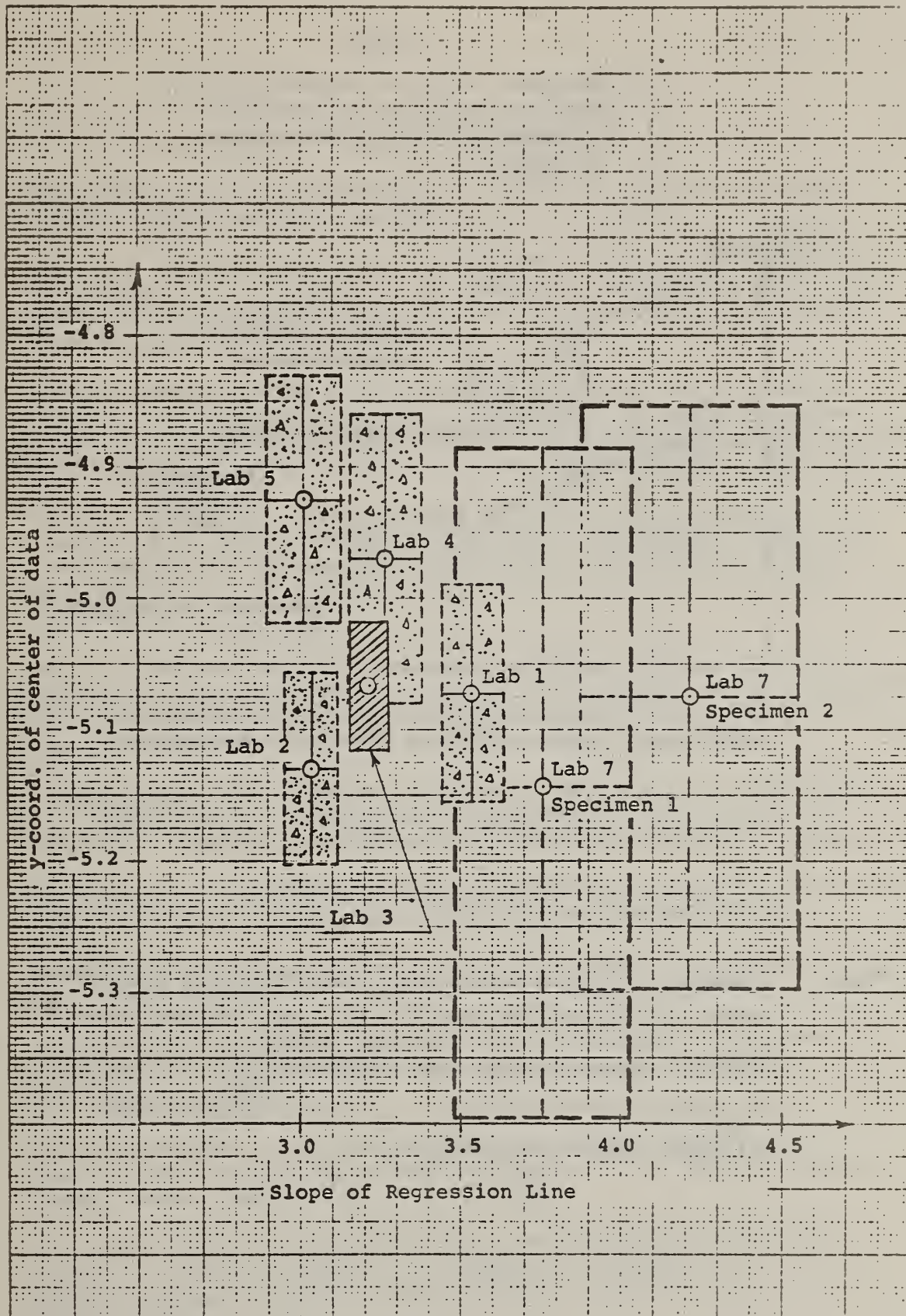
Fig. 35 Comparison of the Characteristics of Some Fatigue Crack Growth
Data from Six Laboratories with 95% Confidence Limits (Data
Obtained for Man-Ten steel with R = 0.1, P_{max} = 1.60, 5 Hz.)
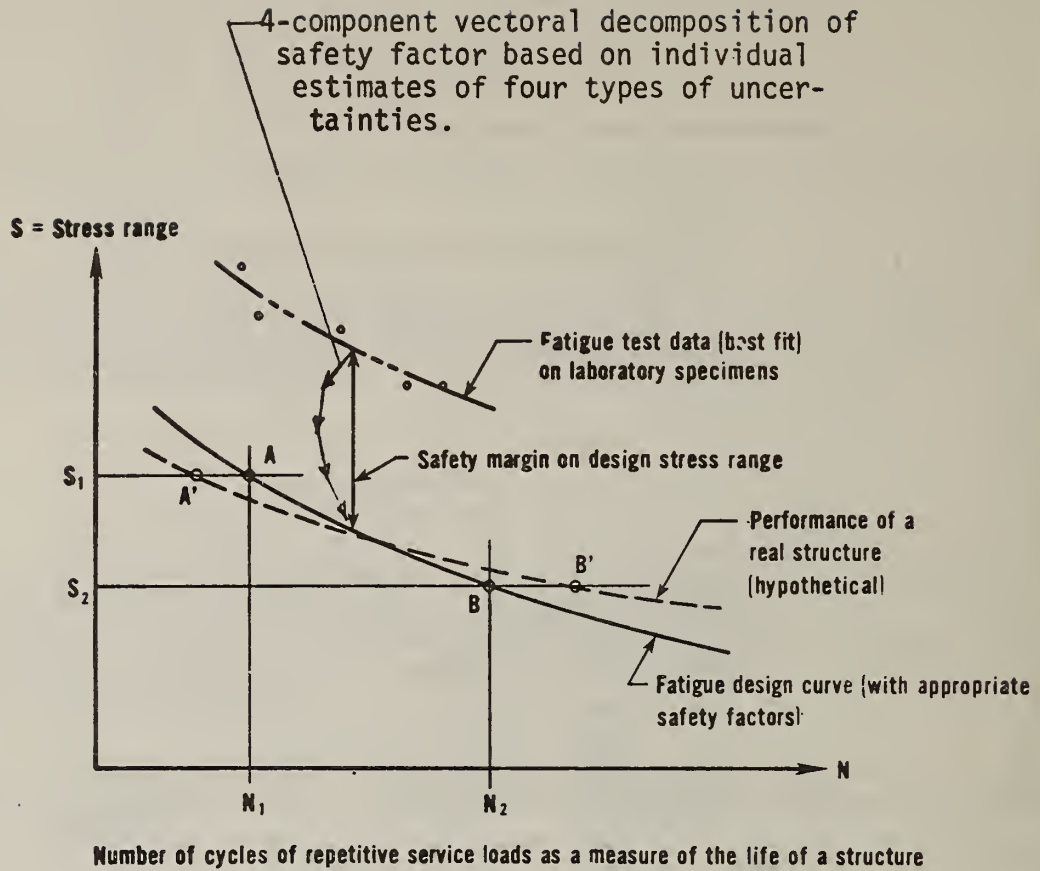
Fig. 36   A Schematic Fatigue Design Curve Indicating the Role of Safety Factors and the Need for Its 4-Way Decomposition.

The four components are: (a) Measurement Uncertainties. (b) Modeling Uncertainties. (c) Scaling Uncertainties. (d) Human Factor Uncertainties.

Appendix

A. Publications, September 1979 to October 1980

1. "The Sounds of Failure, Developments in Acoustic Emission Research,"
   M. Baum, Dimensions, May/June 1980.

2. "Resonance Neutron Radiography For Nondestructive Evaluation and Assay
   Applications," J. W. Behrens, R. A. Schrack, A. D. Carlson and C. D.
   Bowman, NBS Special Tech. Publ. 594, pp. 436-439, National Bureau of
   Standards (Sept. 1980).

3. "Recent Progress in Eddy Current Testing for Nuclear Applications,"
   H. Berger, G. Birnbaum and G. Free, Proceedings of Symposium on New
   Methods for NDE and Their Applications in the Nuclear Industry, Deutsche
   Gesellschaft fur Zerstorungsfreie Prufung, Berlin (1979), pp. 99-106.

4. "Neutron Laminagraphy for Inspection of Nuclear Fuel Subassemblies,"
   H. Berger, N. P. Lapinski and K. J. Reimann, Proceedings of Symposium
   on New Methods for NDE and Their Applications in the Nuclear Industry,
   Deutsche Gesellschaft fur Zerstorungsfreie Prufung, Berlin (1979),
   pp. 275-282.

5. "National and International Standards for NDT: To Achieve Improved
   Repeatability and Measures Related to Performance," H. Berger, Proceedings
   of the Ninth World Conference on Non-Destructive Testing, Melbourne,
   Australia, November 1979.

6. "A Comparison of NDT Standards in the U.S. and U.S.S.R.," H. Berger,
   V. A. Koukhar, and A. A. Maksimov, Proceedings of the Ninth World
   Conference on Non-Destructive Testing, Melbourne, Australia, November 1979.

7. "Annual Report 1979, Office of Nondestructive Evaluation," H. Berger and
   L. Mordfin, NBSIR 80-2007, National Bureau of Standards (1980).

8. "Nondestructive Testing in the 1980's," H. Berger, Metal Progress, 118,
   No. 3, 33-37 (1980).

9. "Nondestructive Testing of Railroad Rail," H. Berger, Transportation
   Research Record 744, pp. 22-26, National Academy of Sciences,
   Washington, DC (1980).

10. "Three Dimensional Radiography," H. Berger and W. A. Ellingson,
    Research Techniques in Nondestructive Testing, R. S. Sharpe, editor,
    Academic Press, London, Vol. 4, 1-38 (1980).

11. "Ultrasonic Diffraction Technique for Characterization of Fatigue
    Cracks," S. Golan, L. Adler, K. V. Cook, R. K. Nanstad and T. K.
    Bolland, Journal of Nondestructive Evaluation, Vol. 1, No. 1, 11-20
    (March 1980).

12. "An Appraisal of Current and Future Needs in Ultrasonic NDE Standards," G. Birnbaum and D. G. Eitzen, a report to DARPA, NBSIR 79-1907 (Oct. 1979).

13. "Energy Dispersive XRF Composition Profiling Using Crystal Collimated Incident Radiation," W. J. Boettinger, H. E. Burdette and M. Kuriyama, Advances in X-ray Analysis, 23, 209-217 (1980).

14. "A Simple Technique for Visualizing Transmitted or Reflected Sound Fields," D. J. Chwirut, Materials Evaluation 37, No. 13, pp. 29-32 (1979).

15. "Anisotropic Elastic Constants of a Fiber-Reinforced Boron-Aluminum Composite," S. K. Datta, H. M. Ledbetter, Mechanics of Nondestructive Testing, W. W. Stinchcomb, editor, pp. 215-230, Plenum Press, New York (1980).

16. "Nondestructive Evaluation Program: Progress in 1979," D. G. Eitzen and J. Quinn, EPRI NP-1234-SR, Special Report (December 1979).

17. "Ultrasonic Nondestructive Evaluation," D. G. Eitzen, PMTE Update 1, No. 3 (December 1979).

18. "Critical Materials and Fabrication Issues for Pressure Vessels, Piping, Pumps, and Valves," J. T. Fong, R. C. Dobbyn and L. Mordfin, editors, NBS Special Publication 588 (June 1980).

19. "Sizing of Cracks With Scattered Ultrasonic Waves," S. Golan, Ultrasonic Materials Characterization, NBS SP-596, National Bureau of Standards (1980).

20. "Neutron Diffraction and Small-Angle Scattering as Nondestructive Probes of the Microstructure of Materials," C. J. Glinka, H. J. Prask and C. S. Choi, in Mechanics of Nondestructive Testing, W. W. Stinchcomb, editor, pp. 143-164, Plenum Press, New York (1980).

21. "Elastic-Constant Variability in Stainless-Steel 304," H. M. Ledbetter, N. V. Frederick and M. W. Austin, J. Appl. Phys. 51, 305-309 (Jan. 1980).

22. "Orthotropic Elastic Stiffnesses of a Boron-Aluminum Composite," H. M. Ledbetter, J. Appl. Phys. 50, 8247-8248 (Dec. 1979).

23. "Anomalous Low-Temperature Elastic-Constant Behavior in Fe-13Cr-19Mn," H. M. Ledbetter, Metall. Trans. 11A, 543-544 (Mar. 1980).

24. "Room-Temperature Elastic Constants and Low-Temperature Sound Velocities for Six Nitrogen-Alloyed Austenitic Stainless Steels," H. M. Ledbetter, Metall. Trans. 11A, 1067-1069 (June 1980).

25. "Correlation Between Superconducting-Transition Temperature and the Cuachy Discrepancy in Body-Centered-Cubic Transition Metals, H. M. Ledbetter, Phys. Lett. 77A, 359-361 (June 1980).

26. "X-ray Residual Stress Evaluation by an Energy Dispersive System," M. Kuriyama, W. J. Boettinger and H. E. Burdette, Proc. of Symposium on Accuracy in Powder Diffraction, NBS Spec. Pub. 567, pp. 479-487 (1980).

27. "Evaluation of Ultrasound Echo Amplitude Measurements for Assessment of Bond Integrity in Zirconium Alloy Samples," M. Linzer, J. G. Abbott and S. I. Parks, Report to Westinghouse Atomic Power Laboratory, West Mifflin, PA, DOE Contract No. EY-76-C-11-0014 (1980).

28. "Program and Abstracts, Fifth International Symposium on Ultrasonic Imaging and Tissue Characterization and Second International Symposium on Ultrasonic Materials Characterization," M. Linzer and H. Berger, editors, National Bureau of Standards, June 1980.

29. "NDE Publications: 1978," L. Mordfin, NBSIR 80-2080 (1980).

30. "Reliability of Nondestructive Evaluation," L. Mordfin, published in NBS SP-588, Critical Materials and Fabrication Issues for Pressure Vessels, Piping, Pumps, and Valves (June 1980).

31. "Further Development and Clinical Evaluation of the Expanding - Aperture Annular Array System," S. I. Parks, M. Linzer and T. H. Shawker, Ultrasonic Imaging 1, pp. 378-383 (1979).

32. "Positron Annihilation Study of Defects in Titanium," R. C. Reno, L. J. Swartzendruber and L. H. Bennett, NDT International, 224 (1979).

33. "Debris Analysis of Erosive and Abrasive Wear," A. W. Ruff, Proceedings of the International Conference of Fundamentals of Tribology, MIT Press (1980).

34. "Studies of Microscopic Aspects of Wear Processes in Metals," A. W. Ruff and P. J. Blau, NBS Report 80-2058 (1980).

35. "The Characterization and Calibration of Ultrasonic Transducers Used in NDT and Materials Testing," W. Sachse and N. Hsu, Ultrasonic Materials Characterization, NBS SP-596, National Bureau of Standards (1980).

36. "Ultrasonic Transducers for Materials Testing and Their Characterization," W. Sachse and N. Hsu, Physical Acoustics, Vol. 4 (1979).

37. "Amplitude Analysis of Pancreatic B-Scans: A Clinical Evaluation of Cystic Fibrosis," T. A. Shawker, S. I. Parks, M. Linzer, B. Jones, L. A. Lester, and V. A. Hubbard, Ultrasonic Imaging, 2, pp. 55-66 (1980).

38. "Internal Friction and Sodium Transport in Beta Alumina," J. H. Simmons, A. D. Franklin, K. F. Young, and M. Linzer, J. Amer. Ceram. Soc. 63, pp. 78-83 (1980).

39. "Eddy Currents in a Conducting Cylinder with a Crack," R. D. Spal and A. H. Kahn, J. Appl. Phys., 50, 6135 (1979).

40. "A Study of Deformantion and Fracture Processes in a Low-Alloy Steel by Acoustic Emission of Transient Analysis," H. N. G. Wadley and C. B. Schruby, Acta Met., 27, pp. 613-625 (1979).

41. "Inservice Data Reporting Standards for Engineering Reliability and Risk Analysis," J. T. Fong, Nuclear Engineering and Design 60, pp. 159-161 (1980).

B. NDE Meetings at NBS

The NDE program has been active in sponsoring NDE meetings, both symposia and workshops. The purposes behind this significant meeting activity include (1) drawing attention of the the industrial community to NDE, (2) providing a good record of the state-of-the-art, (3) providing a forum for information exchange, (4) helping our NBS staff meet individuals active in NDE and learning the status of current work in the field, and (5) providing a mechanism for NDE people to discuss their NDE standard needs.

During this past year, NBS sponsored the Second International Symposium on Ultrasonic Materials Characterization. The meeting, held in cooperation with American Society for Nondestructive Testing (ASNT), was held at NBS on June 4 to 6, 1980. There was a one-day overlap of this NDE meeting with the Fifth International Symposium on Ultrasonic Imaging and Tissue Characterization (June 1 to 4, 1980) to encourage interactions between ultrasonic specialists from the medical and industrial communities.

An NDE course was held at NBS on April 15 to 17, 1980. The course, Fundamentals of Nondestructive Testing, was sponsored by the local sections of the American Society for Metals and the ASNT.

C. NBS Seminars on NDE

A list of NBS-NDE Seminars held during the past year is given in Table 4. Notices of the seminars are distributed broadly in the Washington area. Visitors are welcome and often attend.

1979-1980 NBS-NDE Seminars

Speaker	Date	Topic
Sam Golan National Bureau of Standards	Sept. 11, 1979	Ultrasonic Diffraction Technique for Characterization of Cracks
B. Auld Ginzton Laboratory Stanford University	Nov. 9, 1979	Principles of Eddy Currents Testing
Frank G. Becher Olympus Corp. of America	Jan. 17, 1980	An Analysis of The Optical Factors in the Total Internal Visual Inspection System
Michael J. Buckley DARPA	April 8, 1980	DARPA-NDE Research Programs and Future Plans
John K. Aman E. I. duPont de Nemours & Co., Inc.	May 7, 1980	Image Quality Variables in Radiographic NDT
Alex Vary NASA	May 20, 1980	Advanced Ultrasonic Materials Characterization at Lewis Research Center
R. C. Reno Univ. of Maryland Baltimore County, and National Bureau of Standards	June 10, 1980	Positron Annihilation in Metals
Don Alger University of Missouri	July 17, 1980	Diagnostics of Neutron Beams
Jackson C. S. Yang University of Maryland	Aug. 5, 1980	Application of the Random Decrement Technique For The Measurement of Damping and Detection of Structural Deterioration
T. J. Jessop The Welding Institute	Sept. 25, 1980	Sizing and Characterization of Weld Defects by Ultrasonics

D.   Awards

There were several recognitions of NBS-NDE people during the past year. Awards include the following:

Industrial Research, IR-100 Award

NBS was recognized with an IR-100 Award for the second consecutive year for an NDE-oriented development. This award recognized Dr. Nelson N. Hsu, Mechanical Production Metrology Division, for his development of an acoustic emission simulator.

The AE simulator is essentially a precision mechanical pencil with pre- cision "lead", a holding fixture with a loading screw attached to a load cell and a peak hold circuit with a digital force readout. To generate a simulated AE event, the pencil lead is forced against a structure until the pencil lead breaks. The breaking pencil lead generates a point force step function un- loading at the surface of the structure. Since the shape of the input load (a step function) is known, a single number, the force step height, determines the input. The load cell can be calibrated on an absolute basis so that the whole simulator provides an absolute input for the calibration of AE systems and subsystems.

The Harry Diamond Award, IEEE

Martin Greenspan has been selected to receive the Institute of Electrical and Electronics Engineers Harry Diamond Award for 1980. Greenspan, retired from NBS in 1976 but still consults with the Center for Mechanical Engineering and Process Technology. Greenspan was honored for many contributions in acous- tics and elasticity over a long period of time. One of the areas in which Greenspan's contributions were cited was NDE, particularly for the concepts that led to the calibration methods for acoustic emission transducers.

E.   Talks and Appearances by NDE Office Personnel

1.   "Verification of Liquid Penetrant Examination Systems," L. Mordfin, ASME
       Boiler & Pressure Vessel Subcommittee V, Subgroup on Surface Examination,
       New York City, NY, October 31, 1979.

2.   "National and International Standards for NDT: To Achieve Improved
       Repeatability and Measures Related to Performance," H. Berger, Plenary
       Lecture at the Ninth World Conference on NDT, Melbourne, Australia,
       November 19, 1979.

3.   "A Comparison of NDT Standards in the U.S. and the U.S.S.R.," H. Berger
       et al, paper presented at the Ninth World Conference on NDT, November 21,
       1979.

4.   "Nondestructive Testing of Railroad Rail," H. Berger 59th Annual Meeting
       of the Transportation Research Board, Washington, DC, January 21, 1980.

5.   "NDE Standards for Nuclear Power Systems: An NBS Perspective," L. Mordfin,
       Third International Conference on Nondestructive Evaluation in the Nuclear
       Industry, Salt Lake City, UT, February 12, 1980.

6.   "Review of the NBS Program in NDE," H. Berger, Nondestructive Testing
       Committee, American Iron and Steel Institute, Pittsburgh, PA,
       February 13, 1980.

7.   "NBS Program in Nondestructive Evalation," H. Berger, Physics Department
       Seminar, Martin Marietta Laboratories, Baltimore, MD, March 17, 1980.

8.   "Measurement of Residual Stresses: Problems and Opportunities,"
       L. Mordfin, American Society for Metals Conference on Residual Stress
       for Designers and Metallurgists, Chicago, IL, April 10, 1980.

9.   "The NBS Program in NDE," H. Berger, Army Materials and Mechanics
       Research Center, Boston, MA, April 29, 1980.

10.   "What is NBS Doing in NDE?," H. Berger, Mohawk Valley Section ASNT,
       Schenectady, NY, May 8, 1980.

11.   "Introduction and Welcome, H. Berger, Second International Symposium on
       Ultrasonic Materials Characterization," NBS, Washington, DC, June 4, 1980.

12.   "NDE Standards Program at the National Bureau of Standards," G. Birnbaum,
       Pennsylvania North Central Section of the ASNT, Williamsport, PA,
       June 10, 1980.

13.   "Acoustic Emission Definition and Deformation Fracture of Metals,"
       H. Wadley, Acoustic Emission Working Group of Materials Research
       Council, DARPA, LaJolla, CA, June 18, 1980.

14.   "Reliability of Nondestructive Evaluation," L. Mordfin, American Society
       of Mechanical Engineers Symposium on Critical Materials and Fabrication
       Issues, San Francisco, CA, August 14, 1980.

15. "Acoustic Emission Definition and Deformation Fracture of Metals,"
    H. Wadley, IBM, Yorktown Heights, NY, August 20, 1980.

16. "The Role of Calibration in Nondestructive Evaluation," H. Berger,
    National Conference of Standards Laboratories, NBS, September 22, 1980.

17. "Acoustic Emission Definition and Deformation Fracture of Metals,"
    H. Wadley, Canadian Atomic Energy Authority, Chalk River, Ontario,
    Canada, September 24, 1980.

U.S. DEPT. OF COMM. BIBLIOGRAPHIC DATA SHEET	1. PUBLICATION OR REPORT NO. NBSIR 80-2162	2. Gov't. Accession No.	3. Recipient's Accession No.

4. TITLE AND SUBTITLE	5. Publication Date
Technical Activities of the Office of Nondestructive Evaluation	
	6. Performing Organization Code

7. AUTHOR(S) H. Berger and L. Mordfin	8. Performing Organ. Report No.

9. PERFORMING ORGANIZATION NAME AND ADDRESS	10. Project/Task/Work Unit No.
NATIONAL BUREAU OF STANDARDS DEPARTMENT OF COMMERCE WASHINGTON, DC 20234	11. Contract/Grant No.

12. SPONSORING ORGANIZATION NAME AND COMPLETE ADDRESS *(Street, City, State, ZIP)*	13. Type of Report & Period Covered
	14. Sponsoring Agency Code

15. SUPPLEMENTARY NOTES

☐ Document describes a computer program; SF-185, FIPS Software Summary, is attached.

16. ABSTRACT *(A 200-word or less factual summary of most significant information. If document includes a significant bibliography or literature survey, mention it here.)*

A review of nondestructive evaluation programs at NBS, for FY1980 is presented in this annual report.

17. KEY WORDS *(six to twelve entries; alphabetical order; capitalize only the first letter of the first key word unless a proper name; separated by semicolons)*

Acoustic emission; eddy currents; imaging; leakage testing; magnetics; material parameters; nondestructive evaluation; optics; penetrants; radiography; and ultrasonics.

18. AVAILABILITY ☐ Unlimited	19. SECURITY CLASS (THIS REPORT)	21. NO. OF PRINTED PAGES
☐ For Official Distribution. Do Not Release to NTIS	UNCLASSIFIED	116
☐ Order From Sup. of Doc., U.S. Government Printing Office, Washington, DC 20402, SD Stock No. SN003-003-	20. SECURITY CLASS (THIS PAGE)	22. Price
☒ Order From National Technical Information Service (NTIS), Springfield, VA. 22161	UNCLASSIFIED	$9.00

USCOMM-DC